

**IMPROVING RUNOFF PREDICTION BY DATA
ASSIMILATION IN HBV HYDROLOGICAL
MODEL FOR UPPER EUPHRATES BASIN**
Master of Science Thesis

Bulut AKKOL

Eskişehir, 2016

**IMPROVING RUNOFF PREDICTION BY DATA ASSIMILATION
IN HBV HYDROLOGICAL MODEL FOR UPPER EUPHRATES BASIN**

Bulut AKKOL

MASTER OF SCIENCE THESIS

**Department of Civil Engineering
Supervisor: Assoc. Prof. Dr. Aynur ŐENSOY ŐORMAN**

**EskiŐehir
Anadolu University
Graduate of School of Sciences
July, 2016**

This thesis is partially supported by TŪBİTAK project number 113Y075

FINAL APPROVAL FOR THESIS

This thesis titled “Improving Runoff Prediction by Data Assimilation in HBV Hydrological Model for Upper Euphrates Basin” has been prepared and submitted by Bulut AKKOL in partial fulfillment of the requirements in “Anadolu University Directive on Graduate Education and Examination” for the Degree of Master of Science in Civil Engineering Department has been examined and approved on 22/07/2016.

Committee Members

Signature

Member (Supervisor) Doç.Dr. AYNUR ŞENSOY ŞORMAN

Member Yard.Doç.Dr. TUĞRUL YILMAZ

Member Yard.Doç.Dr. ALİ ARDA ŞORMAN

.....
Date

.....
Director

Graduate School of Sciences

ABSTRACT

IMPROVING RUNOFF PREDICTION BY DATA ASSIMILATION IN HBV HYDROLOGICAL MODEL FOR UPPER EUPHRATES BASIN

Bulut AKKOL

**Department of Civil Engineering
Anadolu University, Graduate of School of Sciences, July, 2016**

Supervisor: Assoc. Prof. Dr. Aynur ŞENSOY ŞORMAN

Advancing technology and increasing world population are valid reasons for using natural resources effectively. The necessity of efficient water resources management highlights the hydrology science. Improvements in modelling and forecasting studies contribute to optimal operation of hydraulic structures, decreased risk of flooding and drought and increased hydropower generation.

In this study, Karasu Basin, which is a headwater of Euphrates River, is selected as a pilot region. Firstly, HBV hydrological model is calibrated and validated for the years 2002-2008 and 2009-2013 respectively and daily runoff values are forecasted for 2015. Data Assimilation (DA) technique, which is commonly used in atmosphere, meteorology and hydrology science in the last decade, is used to improve the forecast results. One of the 4-Dimensional variational (4D-VAR) methods, Moving Horizon Estimation (MHE) is selected among the variety of data assimilation algorithms. HBV model, which is integrated into Delft-FEWS platform, is configured to run with MHE. The model inputs and states are assigned as objective function variables utilized in DA application. Recently improved satellite technology products of MODIS and MSG-SEVIRI snow covered area and SSMI/S snow water equivalent are used in DA after preprocessing. Model initial states are updated by DA application and then short and medium range (2 to 9 days lead time) runoff forecasting is done for 2009-2013 water years with perfect forecast data sets. In addition, during 2015 water year snowmelt period, real time runoff forecasting is conducted using Numerical Weather Prediction and data assimilation approach. The results show that DA applications provide significant improvement on the performance of streamflow forecasts. Moreover, utilization of satellite snow products in DA applications increase the consistency of forecasted internal model variables compared to the observed snow data.

Since the study includes up-to-date satellite snow products through a data assimilation method in real time forecasting which results in improved lead time runoff forecast accuracy, this could be considered as a pioneer application for operational hydrology in Turkey.

Keywords: Data Assimilation, HBV Model, Runoff Forecasting, Satellite Snow Product,
Upper Euphrates Basin

ÖZET

YUKARI FIRAT HAVZASINDA HBV HİDROLOJİK MODELİNDE VERİ ASİMİLASYONU İLE AKIM TAHMİNLERİNİN İYİLEŞTİRİLMESİ

Bulut AKKOL

İnşaat Mühendisliği Anabilim Dalı

Anadolu Üniversitesi, Fen Bilimleri Enstitüsü, Temmuz, 2016

Danışman: Doç. Dr. Aynur ŞENSOY ŞORMAN

Gelişen teknoloji ve artan dünya nüfusu, doğal kaynakların kullanımının daha verimli hale gelmesi için geçerli sebepler oluşturmaktadır. Su kaynaklarının etkin yönetimine duyulan ihtiyaç hidroloji biliminin öne çıkması sağlamıştır. Modelleme ve tahmin çalışmalarındaki iyileştirmeler su yapılarının optimum işletilmesine, taşkın ve kuraklık risklerini azaltmaya ve hidroelektrik enerji üretiminin artmasına katkı sağlamaktadır.

Bu çalışmada, Yukarı Fırat Havzasında bulunan Karasu Havzası pilot bölge olarak seçilmiştir. HBV hidrolojik modeli 2002-2008 ve 2009-2013 yılları için sırasıyla kalibre edilmiş ve doğrulanmıştır ve günlük akım verileri tahmin edilmiştir. Tahmin sisteminin iyileştirilmesi için son on yıldır atmosfer, meteoroloji ve hidroloji alanlarında yaygın bir kullanımı olan Veri Assimilasyonu (VA) tekniği kullanılmıştır. Çeşitli veri asimilasyonu algoritmaları arasından 4-boyutlu değişken (4D-VAR) metodlarından birisi olan Moving Horizon Estimation (MHE) yöntemi seçilmiştir. Delft-FEWS platformuna uyarlanan HBV modeli, MHE ile beraber çalışacak şekilde düzenlenmiştir. Model girdileri ve durum değişkenleri VA'da kullanılan amaç fonksiyonunun değişkenleri olarak atanmıştır. Son zamanlarda gelişen uydu teknolojilerinin ürünlerinden MODIS, MSG-SEVIRI karla kaplı alan ve SSMI/S kar su eşdeğeri verileri, ön işlemden geçirilerek VA uygulamasında kullanılmıştır. Veri asimilasyonu ile başlangıç koşulları güncellenerek, 2009-2013 su yılları için mükemmel tahmin veri seti ile kısa ve orta dönemli (2 den 9 güne kadar) tahminler yapılmıştır. Ayrıca, 2015 su yılı erime döneminde, Sayısal Hava Tahmin verileri kullanılarak ve veri asimilasyonu uygulanarak gerçek zamanlı akım tahmini yapılmıştır. Sonuçlara göre, VA tekniği akım tahmini çalışmalarında önemli iyileştirmeler sağlamıştır. Ayrıca, uydu ürünlerinin kullanıldığı VA çalışmaları, içsel model kar değişkenleri tahminlerinin kar gözlem verilerine uyumluluğunu da arttırmıştır.

Bu çalışma gerçek zamanlı akım tahmininde güncel kar uydu ürünleri kullanılarak veri asimilasyonunu içermesi ve ileriye dönük tahmin sonuçlarını iyileştirmesi nedenleriyle Türkiye'deki operasyonel hidroloji alanında öncü bir çalışmadır.

Anahtar Kelimeler: Veri Asimilasyonu, HBV, Akım Tahmini, Uydu Kar Ürünleri, Yukarı Fırat Havzası

To my family...

ACKNOWLEDGEMENT

Foremost, I would like to express my sincere gratitude to my advisor Dr. Aynur ŞENSOY ŞORMAN and Dr. Ali Arda ŞORMAN for their continuous support of my MSc thesis, for their patience, motivation, enthusiasm, and immense knowledge. Their guidance helped me all the time in research and writing of this thesis. I could not have imagined having better advisors and mentors for my study and my life.

My sincere thanks also go to my colleagues and friends, Cihan ÇOŞKUN, M. Cansaran ERTAŞ and Gökçen UYSAL for offering me a good teamwork and a good friendship.

I would also like to acknowledge Dr. Tuğrul YILMAZ from Middle East Technical University as the third reader of this thesis, and I am gratefully indebted to him for his valuable comments on the thesis.

Besides, I would like specially to thank my girlfriend Elif SARAÇOĞLU for her endless patience and everlasting support.

Finally, I must express my very profound gratitude to my parents, my grandfather and grandmother for providing me with unfailing support and continuous encouragement throughout my years of study and through the process of researching and writing this thesis. This accomplishment would not have been possible without them. Thank you.

Bulut AKKOL

August 2016

**STATEMENT OF COMPLIANCE WITH ETHICAL PRINCIPLES
AND RULES**

I hereby truthfully declare that this thesis is an original work prepared by me; that I have behaved in accordance with the scientific ethical principles and rules throughout the stages of preparation, data collection, analysis and presentation of my work; that I have cited the sources of all the data and information that could be obtained within the scope of this study, and include these sources in the references section; and that this study has been scanned for plagiarism with “scientific plagiarism detection program” used by Anadolu University, and that “it does not have any plagiarism” whatsoever. I also declare that, if a case contrary to my declaration is detected in my work at any time, I hereby express my consent to all the ethical and legal consequences that are involved.

Bulut AKKOL

TABLE OF CONTENTS

| | <u>Page</u> |
|--|-------------|
| TITLE PAGE | i |
| FINAL APPROVAL FOR THESIS | ii |
| ABSTRACT | iii |
| ÖZET | iv |
| DEDICATION | v |
| ACKNOWLEDGEMENT | vi |
| STATEMENT OF COMPLIANCE WITH ETHICAL PRINCIPLES AND RULES | vii |
| TABLE OF CONTENTS | viii |
| LIST OF FIGURES | x |
| LIST OF TABLES | xii |
| ABBREVIATIONS AND SYMBOLS | xiii |
| 1. INTRODUCTION | 1 |
| 1.1. General | 1 |
| 1.2. Scope of the Study | 1 |
| 1.3. Thesis Outline | 3 |
| 2. LITERATURE | 4 |
| 2.1. Previous Studies in the Pilot Area | 4 |
| 2.2. Satellite Snow Products | 5 |
| 2.3 Hydrological Modelling and Forecasting | 7 |
| 2.4 Data Assimilation | 9 |
| 3. STUDY AREA & DATA | 12 |
| 3.1. Study Area | 12 |
| 3.2. Hydro-meteorological Data | 19 |
| 3.3. Satellite Snow Data | 25 |
| 4. METHODOLOGY | 31 |
| 4.1. Hydrological Modelling | 31 |
| 4.1.1. Precipitation routine | 33 |
| 4.1.2. Soil routine | 33 |
| 4.1.3. Runoff response routine | 34 |
| 4.2. Flood Early Warning System (Delft-FEWS) | 37 |

| | |
|--|----|
| 4.3. Integration of Delft-FEWS and HBV | 39 |
| 4.4. Data Assimilation (DA) | 40 |
| 4.4.1. Purpose of Data Assimilation | 41 |
| 4.4.2. Methods of Data Assimilation | 42 |
| 4.4.3. Moving Horizon Estimation (MHE) | 44 |
| 4.5. Ensemble Verification System (EVS) | 45 |
| 5. DATA ASSIMILATION & MODELLING | 48 |
| 5.1. Pre-Processing of Snow Products | 48 |
| 5.1.1. MSG-SEVIRI (H10) snow covered area | 48 |
| 5.1.2. SSMI/S (H13) snow water equivalent | 51 |
| 5.1.3. MODIS snow covered area | 52 |
| 5.2. Calibration and Validation of HBV Model in Karasu Basin | 54 |
| 5.3. Data Assimilation Configuration | 57 |
| 5.4. Number of Iteration in DA Procedure | 59 |
| 5.5. Results and Assessments | 61 |
| 5.5.1. First experiment | 62 |
| 5.5.2. Second experiment | 65 |
| 5.5.2.1. DA application including SCA (H10 and MODIS) ... | 65 |
| 5.5.2.2 DA application including SWE | 71 |
| 5.5.3. Real-Time DA application | 74 |
| 5.5.3.1. Real-Time DA application with observed data | 74 |
| 5.5.3.2 Real-Time DA application with WRF | 77 |
| 6. CONCLUSION | 80 |
| REFERENCES | 83 |
| CV | |

LIST OF FIGURES

| | <u>Page</u> |
|--|-------------|
| 3.1. Outlet and river network of Karasu Basin | 13 |
| 3.2. Hydrograph of Karasu Basin for different years | 14 |
| 3.3. Elevation zones of Karasu Basin | 16 |
| 3.4. Hypsometric curve of Karasu Basin | 16 |
| 3.5. Land use map of Karasu Basin | 17 |
| 3.6. Aspect map of Karasu Basin | 18 |
| 3.7. Slope map of Karasu Basin | 19 |
| 3.8. AWOS stations in and around Karasu Basin | 20 |
| 3.9. Total annual precipitation over Turkey | 21 |
| 3.10. Total annual precipitation for Erzurum (1860 m) | 22 |
| 3.11. Monthly mean precipitation for Erzurum AWOS (1758 m) | 23 |
| 3.12. Comparison of monthly average temperature for Turkey and Erzurum AWOS | 24 |
| 3.13. The interface of DK program | 25 |
| 3.14. View of MSG-SEVIRI (H10) product at 31-12-2012 | 28 |
| 3.15. View of SSMI/S (H13) product at 26-03-2012 | 29 |
| 3.16. View of MODIS snow cover product at 31-12-2012 | 30 |
| 4.1. General flow chart of HBV model | 31 |
| 4.2. Schematization of HBV model | 32 |
| 4.3. Workflow of flood risk management | 37 |
| 4.4. Schematic interaction between the General Adapter and an external module in FEWS | 40 |
| 4.5. Interface of EVS program | 46 |
| 4.6. File format and order as EVS input format | 47 |
| 4.7. File view for importing values in EVS | 47 |
| 5.1. Import Module for H10 | 49 |
| 5.2. Workflow to start H10 import module | 49 |
| 5.3. (a). MSG-SEVIRI (H10) Original Image | 50 |
| 5.3. (b). Clipped MSG-SEVIRI (H10) Product with Reference to Karasu Basin | 50 |
| 5.4. SCA values derived from MSG-SEVIRI (H10) | 51 |

| | |
|---|----|
| 5.5. SWE values derived from SSMI/S (H13) | 52 |
| 5.6. Flowchart of filtering daily MODIS data | 53 |
| 5.7. Observed and modelled runoff of Karasu Basin, calibration period | 56 |
| 5.8. Observed and modelled runoff of Karasu Basin, validation period | 57 |
| 5.9. Objective function value versus iteration number | 60 |
| 5.10. Lead time performance of DA on discharge using state variables | 64 |
| 5.11. First lead time runoff values using DA, 2011 water year | 64 |
| 5.12. Lead time performance of DA on discharge using MODIS | 66 |
| 5.13. Lead time performance of DA on SCA using MODIS | 66 |
| 5.14. Lead time performance of DA on discharge using H10 | 67 |
| 5.15. Lead time performance of DA on SCA using H10 | 68 |
| 5.16. Lead time performance of DA on discharge using snow products and P_T | 69 |
| 5.17. Lead time performance of DA on SCA using snow products and P_T ... | 70 |
| 5.18. First lead time runoff values using DA based on SCA, 2011 water year . | 70 |
| 5.19. First lead time SCA values using DA based on SCA, 2011 water year ... | 71 |
| 5.20. Lead time performance of DA on discharge using H13_Int and P_T | 72 |
| 5.21. First lead time runoff values using DA based on SWE, 2011 water year | 73 |
| 5.22. First lead time SWE values as a result of SWE based DA, 2011 water year | 73 |
| 5.23. Performance analysis of DA on discharge, 2015 water year | 75 |
| 5.24. Performance analysis of DA on SCA, 2015 water year | 76 |
| 5.25. Comparison of discharge in Karasu Basin for 2015 water year | 76 |
| 5.26. Comparison of SCA in Karasu Basin for 2015 water year | 77 |
| 5.27. Comparison of discharge in Karasu Basin with WRF data for 2015 water year | 78 |
| 5.28. Comparison of SCA in Karasu Basin with WRF data for 2015 water year | 79 |

LIST OF TABLES

| | <u>Page</u> |
|--|--------------------|
| 3.1. Elevation Range of Karasu Basin | 15 |
| 4.1. Parameters of HBV model and default interval of their values | 36 |
| 5.1 Performance indicators and their assessment | 55 |
| 5.2. Calibrated model parameters of HBV | 55 |
| 5.3. Performance statistics for the calibration period | 56 |
| 5.4. Performance statistics for the validation period | 57 |
| 5.5. Terms in the objective function | 58 |
| 5.6. Number of iterations and their properties | 60 |
| 5.7. Optimization variables with their bound constraints | 62 |
| 5.8. RMSE according to SCA for forecasting period | 69 |
| 5.9. RMSE according to discharge for forecasting period | 69 |
| 5.10. Lead time performance of DA using WRF with respect to discharge | 79 |
| 5.11. Lead time performance of DA using WRF with respect to SCA | 79 |

ABBREVIATIONS AND SYMBOLS

| | |
|-------------------|--|
| 4D-VAR | : Four Dimensional Variational |
| AMSR-E | : Advanced Microwave Scanning Radiometer-Earth Observing System |
| ASCII | : American Standard Code for Information Interchange |
| CSV | : Comma Separated Values |
| DA | : Data Assimilation |
| DEM | : Digital Elevation Map |
| DK | : Detrended Kriging |
| DPT | : Government Planning Organization |
| DSI | : General Directory of Hydraulic Works |
| EA | : Environment Agency |
| EFFS | : European Flood Forecasting System |
| EKF | : Extended Kalman Filtering |
| EnKF | : Ensemble Kalman Filtering |
| EOS | : Earth Observation System |
| EPS | : Ensemble Prediction System |
| EVS | : Ensemble Verification System |
| EUMETSAT | : European Organization for the Exploitation Meteorological Satellites |
| FEWS | : Flood Early Warning System |
| GIS | : Geographical Information System |
| GRIB | : General Regularly Distributed Information in Binary form |
| HBV | : Hydrologiska Byrans Vattenbalansavdelning |
| HDF | : Hierarchical Data Format |
| H-SAF | : Satellite Application Facilities on Support to Operational Hydrology and Water Management |
| HTML | : HyperText Markup Language |
| IDW | : Inverse Distance Weighted |
| KF | : Kalman Filter |
| LZ | : Lower Zone |
| METEOSAT | : European Geostationary Meteorological Satellites |
| MHE | : Moving Horizon Estimation |
| MM5 | : Mesoscale Model 5 |
| MODIS | : Moderate Resolution Imaging Spectroradiometer |
| MSG-SEVIRI | : Meteosat Second Generation-Spinning Enhanced Visible and Infrared Imager |
| NASA | : National Aeronautics and Space Administration |
| NATO | : The North Atlantic Treaty Organization |
| NFFS | : National Flood Forecasting System |
| NWP | : Numerical Weather Prediction |
| P | : Precipitation |
| RTC | : Real Time Control |
| Q | : Discharge |
| SCA | : Snow Covered Area |
| SDC | : Snow Depletion Curve |
| SM | : Soil Moisture |

| | |
|--------------|--|
| SRM | : Snowmelt Runoff Model |
| SRTM | : Shuttle Radar Topographic Mission |
| SSM/I | : Special Sensor Microwave Imager |
| SWE | : Snow Water Equivalent |
| T | : Temperature |
| TSMS | : The Turkish State Meteorological Service |
| UZ | : Upper Zone |
| WMO | : World Meteorological Organization |
| WRF | : Weather Research Forecast |
| XML | : Extensible Markup Language |

1. INTRODUCTION

1.1. General

Enhancing the efficiency and protecting the natural resources are vital aims for human being with regard to increasing human needs. The problems of global warming, ecocide, flood and drought highlight the importance of hydrology science with the increase in population. Developing technologies in hydrological science not only enables more reliable hydrological models to minimize the risk of flooding and drought, but also improves operation of reservoir systems efficient.

Although Turkey is covered by sea in three borders, it is a mountainous country according to its mean elevation as 1130 m. The snowmelt runoff is a major contribution of streamflow especially in the mountainous eastern part of Turkey, since the precipitation commonly falls as snow during winter seasons. Karasu and Murat are the two major tributaries of Euphrates River, which is one of the longest and important rivers in southwest Asia. Karasu Basin, located at the headwater of Euphrates River in Turkey, is selected as a pilot basin for this study. Euphrates Basin is not only important for Turkey but also it is a major water resource for the riparian countries before it reaches the Persian Gulf. In addition, there are large dam reservoirs located in the downstream of the pilot basin. Thus, improving the runoff prediction in this headwater add-value to our capability to manage water resources in the sense of flood mitigation and hydropower generation.

Considering the importance of short and long-term operation of reservoirs downstream, modeling and runoff forecasting studies have been carried out for a long while; therefore, a pioneer study on data assimilation to improve streamflow forecasts using a hydrologic model is the main goal of this study. The critical part before the application of a hydrologic model on snow-dominated basins is to get observed and forecast data in sufficient quantity and quality. Since both data and models cause uncertainties in applications, data assimilation techniques are developed to decrease the uncertainty and to improve streamflow forecasts.

1.2. Scope of the Study

Hydrologic model is one of the key elements for a consistent forecast. Since initial state conditions play relatively significant roll on the performance of a forecast, if the representation of these conditions is not accurate enough, skill of the hydrological model would not be high to make true forecasts. Thus, to overcome this problem

Data Assimilation (DA) technique is applied to Karasu Basin to improve initial states and lead time forecast performance.

In literature, variety of hydrologic models is applied according to the characteristics of the basins and the data quality. HBV hydrological model integrated in the Delft-FEWS platform is used in this study.

There are several DA techniques defined in literature both for atmospheric and hydrological science. Moving Horizon Estimation (MHE), which is a variational four-dimensional (4D-VAR) DA (including the time component), is selected for this application. The study includes DA applications under three experiments. First, direct state updating without a new observation, second, state updating with satellite snow products, finally, real time forecasting with Numerical Weather Prediction data

In addition, to improve the originality of this study, Moving Horizon Estimation DA is used with an integration of satellite snow products. Main objective is to improve the forecast robustness by including observed satellite data into a conceptual model. These satellite products are areal snow cover extends of Moderate Resolution Imaging Spectroradiometer (MODIS) and Meteosat Second Generation-SEVIRI (H10) (<http://hsaf.meteoam.it>), and snow water equivalent product of Special Sensor Microwave Imager/Sounder (SSM/I) (H13). To understand the effect of DA with and without satellite data products on the forecast skills, performance indicators are used in comparison of the results against observed snow covered area, snow water equivalent and streamflow.

Since, short-term runoff forecasting studies based on Numerical Weather Predictions are limited in Turkey, another scope of the study is to use DA with short-term deterministic weather prediction data that is integrated with the hydrological model. Therefore, the study attempts to be one of the leading applications in the operational hydrology area in Turkey.

The overall objective is to enhance the operation of large reservoirs located in the downstream of Euphrates Basin by improving the real time runoff forecasting skill of a conceptual hydrological model. 4D-VAR DA technique, MHE, is applied through the selected hydrological model, which is integrated by NWP data for a snow dominated mountainous basin by updating the state conditions using observed in situ and satellite snow data.

1.3. Thesis Outline

Thesis starts with literature research, which consists of four parts. First, the previous studies carried out in the pilot basin are defined, and then a brief literature review on the satellite snow products used in this study is provided. Finally, a literature search on the conceptual hydrological model and DA methods are provided.

Study area described with all dimensions is given in Chapter 3. Then the data used in the hydrological model as input are explained.

HBV hydrologic model, Delft-FEWS platform, the integration of Delft-FEWS and HBV model and data assimilation procedure are explained with details in Chapter 4.

All the pre-processes are described and the application results are given with the necessary assessment and discussions in Chapter 5.

Chapter 6 is the conclusion of the thesis. Overall evaluation of the study is provided and future recommendations are presented for further studies and improvements.

2. LITERATURE

In this chapter of the thesis, first the previous applications in the pilot area are highlighted. Then, the literature on satellite products, hydrological modelling and data assimilation are reviewed.

2.1. Previous Studies in the Pilot Area

Snow studies and snowmelt modelling is challenging at mountainous regions with high elevations. On the other hand, hydrologic applications are based on hydro-meteorological data. Since the measurement network was generally located only in city or suburban centers in Turkey, the first step was to improve the number and quality of measuring network especially at mountainous Eastern Anatolia through various projects.

First Automated Snow-Meteorological Observation Stations were installed with NATO SfS and METU Research Fund Projects (Kaya, 1999; Uzunođlu, 1999; Őensoy, 2000; Tekeli, 2000; BeŐer, 2002). With the help of collected data, first modeling studies were carried out. These studies were followed by projects that were supported by Government Planning Organization (DPT). Protocols and collaborations were made with two major government agencies of General Directorate of State Hydraulic Works (DSI) and Turkish State Meteorological Service (TSMS) within the scope of these projects. These helped to extend the measurement network and improve the quality of stations with additional sensors.

Committed thesis studies (Őensoy, 2005; Tekeli, 2005; Őorman, 2005) involve not only model application but also collecting raw data, real time data transfer, analysis, runoff estimates with models. As a results of these studies, conceptual, energy and mass balance models were applied. In addition to this, river isotope samples were analyzed in Karasu Basin within the scope of Anadolu University Scientific Research Projects. One day lead time deterministic forecasts were made with Meso-scale Model Version 5 (MM5) data at 2012 with a TŐBŐTAK project (108Y161).

The study area is also well known by contribution to satellite technology and their validations. Especially many studies on validation of Moderate Resolution Imaging Spectroradiometer (MODIS) snow cover area and albedo products (Tekeli et al., 2005a and Tekeli et al., 2006) were conducted. Karasu Basin is a pilot basin in Satellite Application Facility on Support to Operational Hydrology and Water Management (H-SAF) which is supported by European Organization for the Exploitation of

Meteorological Satellites (EUMETSAT). The new projects in Anadolu University are a follow up H-SAF projects, which support improvement and development on this area.

Diverse BAP Projects aim that cloud filtering method is applied on combined satellite images at mountainous Eastern Anatolia Region and the results are validated by ground observations. Also snowmelt streamflow is modelled by artificial neural network (ANN) at the same region. Snow probability maps for upper and central Euphrates Basin is targeted to be used in hydrological modeling. Nevertheless, TÜBİTAK project (113Y075) which evolved to COST action ES1404 (http://www.cost.eu/COST_Actions/essem/ES1404) operational hydrologic forecast system is aimed to be improved by Ensemble Prediction System (EPS) and satellite data at mountainous Euphrates and Seyhan Basins.

Many studies were conducted with Karasu Basin in last decade. Snow Cover Area (SCA), which is the 500 m resolution product of MODIS, was compared with ground observations (Tekeli et al., 2005b). HBV model with the input data from MM5 was used by Şorman et al. (2009) for forecasting streamflow prediction. Albostan et al. (2010) investigated seasonal index for low flows at Murat River. At the study of Şen et al. (2011), effect of temperature changes at Euphrates and Tigris Basins and early snowmelt on flow timing was researched by using central time method. An atmosphere-hydrology model with daily time step was improved for Central Euphrates Basin and especially the flood of 2004 was investigated. In another application, 4 different scenarios were tested by using dynamic water profit model at Euphrates and Tigris Basins (Ohara et al., 2011). Şensoy and Uysal (2012) conducted forecast studies with numerical weather forecast data (MM5) for one-day lead time at Karasu Basin. Also in the same study, snow depletion curves (SDC) were created by MODIS satellite images and 4 different methods were developed to forecast SDCs. After all, Snowmelt Runoff Model (SRM) was used to forecast streamflow for one-day lead time.

2.2. Satellite Snow Products

With improving technology in satellite instruments and their computational process algorithm, the ability to obtain data from space is increasing both quantitatively and qualitatively. This abundance of satellite products are created by different institutes and initiatives. One of the well-known snow cover product is produced by Moderate Resolution Imaging Spectroradiometer (MODIS). The main objective for this satellite

product is enhancing to understand the Earth dynamics and processes on lower atmosphere. This knowledge plays a fundamental roll on considering the actual states of Snow cover area (SCA). Another initiative is the EUMETSAT H-SAF project generating products related with precipitation, soil moisture and snow. One of the main goals of this project is the development and validation of these new products and their evaluation in operational use. Snow recognition product of MSG-SEVIRI (H10) and Snow Water Equivalent (SWE) product of SSMI/S (H13) are the two main snow products produced in this project.

SCA is an important hydrological input for simulating and forecasting the amount of water from snowmelt. The importance of SCA was further accentuated with the studies performed by various researchers to develop and apply runoff models (WMO, 1986; WMO, 1992; Etchevers et al., 2002). Regional to global scale satellite-derived estimation of snow cover area became available daily. Remotely sensed SCA information has been used successfully in snowmelt and runoff models; the runoff prediction studies incorporate SCA as a major and sensitive input into operational models that relate snow distributions to snowmelt runoff generation or as a means of updating hydrologic model snowpack simulations and checking the internal validity of snowmelt runoff model (Tekeli et al., 2005a; Andreadis and Lettenmaier, 2006; Clark et al., 2006; Dressler et al., 2006; Kolberg and Gottschalk, 2006; Kolberg et al., 2006; Udnaeset al., 2007; Parajka and Blöschl, 2008, Şorman et al. 2009, Immerzeel et al., 2009, Tahir et al., 2011, Şensoy and Uysal, 2012, Kult et al., 2014, Cornwell et al., 2016). Remotely sensed snow water equivalent (SWE) has also been used in hydrological modelling (Derksen et al., 2003; Andreadis and Lettenmaier, 2006; Pulliainen, 2006; Hall and Riggs, 2007; Dong et al., 2007; Molotch, 2009; Clark et al., 2011; Bavera et al., 2012; Dziubanski and Franz, 2016).

Snow detection product, MSG-SEVIRI (H10), with VIS/IR radiometer is a rather new product with some validation studies and/or usage in operational hydrology. Validation results of H10 snow product are provided in (Sürer and Akyürek, 2012; Çoskun, 2016). In addition, the evaluation of the H10 into a hydrologic model has been tested by Şensoy et al., (2014).

Among the variety of satellites, MODIS (Moderate Resolution Imaging Spectroradiometer), with visible/near-IR satellite sensors of Terra and Aqua, provides already compiled Snow Cover Area (SCA) products since early 2000s. Numerous global

and regional studies have been conducted on validation of MODIS snow data to identify snow mapping accuracy (Maurer et al. 2003; Tekeli et al. 2005a; Riggs et al., 2006; Hall and Riggs, 2007; Parajka and Blöschl, 2008; Wang et al. 2009; Huang et al., 2011; Raleigh et al., 2013; Arsenault et al., 2014; Crawford, 2015). MODIS data have been successfully applied in snowmelt modeling (Parajka and Blöschl, 2008; Li and Williams, 2008; Şensoy and Uysal, 2012; Franz and Karsten, 2013; Day, 2013; Duethmann et al., 2014; He et al., 2014; Finger et al., 2015) or in hydro-climatological and topographic research of snow cover variations (Singh et al., 2003; Wang and Xie, 2009; Tong et al., 2009; Jain et al., 2010; Forsythe et al., 2012; Tang et al., 2013; Gescoïn, 2015; Cornwell et al., 2016). Moreover, various researchers attempted to apply different algorithms to eliminate cloud coverage of MODIS products (Parajka and Blöschl, 2008; Gafurov and Bárdossy, 2009; Parajka et al., 2010; Gao, et al., 2010; Da Ronco and De Michele, 2013; Krajčič et al., 2014; Morriss et al., 2016).

H13 product (Snow Water Equivalent by MicroWave radiometry) is based on the SSMI/S being flown on EOS-Aqua. There is no abundance of study related with SSMI/S (H13), but SWE product are generated by using different algorithm from satellite product (Şorman and Beşer, 2013), some property analysis (Struzik, 2014) and a hydrological implementation (Montero et al., 2016) has been studied.

2.3 Hydrological Modelling and Forecasting

The complex hydrological modeling was represented by computers using simply mathematical equations in the 1960s by Crawford and Linsley (1966) with The Stanford Watershed Model. World Meteorological Organization (WMO) made comparison of different hydrological models in 1975 (WMO, 1975), comparison of snow models in 1986 (WMO, 1986) and comparison of real-time models in 1992 (WMO, 1992). There is no such model whose sound is better than the others, because each model has its own powerful sides. Thus, selection of a model is varying with basin features, purpose of usage and input data.

Temperature index method is very commonly used in conceptual hydrological models to predict snowmelt. This method is recommended by WMO to determine streamflow prediction at the mountainous region (WMO, 1986). SRM (Martinec, 1975; Martinec et al., 1998) and HBV (Bergström, 1976; SMHI, 1996) are used for forecasting streamflow especially at mountainous regions via temperature index method. In this

study, HBV hydrologic model is selected considering the heritage of its applications in the pilot basin for the last decade. Therefore, the literature review will be given on this model.

Johansson et al. (2001) made a streamflow prediction as giving 5 days precipitation and temperature data to the HBV, which is calibrated with runoff and observations of SCA, at Sweden at a mountainous region in the scope of HydAlp project. It is determined that more accurate streamflow predictions results were handled in the short-term forecast. At the project of Jónsdóttir and Þórarinnsson (2004), forecast data were used as input into HBV model. They made an inference that using numerical weather forecasting data (MM5) was helpful for planning water resources. At another similar study, numerical weather forecasting data (MM5) was used as input into HBV model in Germany by Kunstmann and Stadler (2005).

Brown et al. (2008) mentioned that due to insufficient hydro meteorological data at the upper level of basin, verification of the model can only be done with discharge data; yet snow covered area (SCA) could be another data to determine the performance of the model. In addition, hydrological simulations were more accurate by using both SCA and discharge of the basin. Şorman et al. (2009) also made a similar study including multi-purpose calibration, which has two objectives snow cover area by MODIS and discharge data, moreover MM5 forecast data were used at the streamflow prediction.

Modelling of periodical snow potential was made at upper Euphrates basin by using SRM model by Gözel (2011). In the study by Yamankurt (2010), cloud filtering was applied on MODIS products and the SCA results were compared with the output of HBV model.

Flood forecasting and modelling came into prominence at Europe especially after the flood in 2002. In this scope, flood forecasting, including snowmelt, was made for 57 basins where the elevation range is varying between 200-3800 m using HBV model at Austria and South Germany by Nester et al. (2012). Zelelew and Alfredsen (2013) focused on calibration period on conceptual hydrological models and they made a sensitivity analysis for 15 model parameters with the methods of “Sobol’s variance-based sensitivity analysis (VBSA)” and “Generalized sensitivity analysis (GSA)”

HBV hydrologic model is used in several different studies including sensitivity and uncertainty analysis (Abebe et al., 2010; Zelelew and Alfredsen, 2013; Fan et al.,

2015), data assimilation for flood forecasting purpose in fully distributed HBV model (Weerts et al., 2010; Rakovec et al., 2012) and DA for forecasting in HBV model (Lü et al., 2015; Montero et al., 2016).

2.4 Data Assimilation

Scientists try to understand the complexity of Earth with theoretical equations and experiment over the beginning of human life. The information of these researches and studies accumulated to the human knowledge century by century. Solving the secret of nature is one of the main aim for human being. Weather or climate could be the most important element of nature.

Data assimilation is an analysis technique in which the observed information is accumulated into the model state by taking advantage of consistency constraints with laws of time evolution and physical properties (Bouttier and Courtier, 1999).

Ideally, a system that optimally combines snow information from both remote sensing and modelling predictions and at the same time accounts for the limitations of each should provide estimates that are superior to those derived from either models or remote sensing alone (McLaughlin, 1995). Data Assimilation techniques helps to integrate these information.

The first numerical attempt to comprehend the weather forecasting relies on the beginning of 20th century. Lewis Fry Richardson, who was an English mathematician, meteorologist and pioneered modern mathematical technique of weather forecasting, used modified Bjerkenes's primitive equations to produce 6-hour forecast for the state of atmosphere at two points in central Europe by hand calculations (Kalnay, 2003).

Gandin (1963), who took a step forward on improvement of data assimilation, introduced one of the first and robust data assimilation techniques called optimal interpolation. This technique is well known by filling blanks in sparse time series data.

In literature, Charney et al. (1969) first recommended merging current and past data in an explicit dynamical model, by using model's prognostic equations to provide time continuity and dynamic coupling amongst the fields. Data assimilation method was further improved from this approach.

Meteorologists have elementarily used the data assimilation techniques to improve operational weather forecasting for many years (Daley, 1991). In Oceanography,

Data assimilation can take important role for enhancing ocean dynamic predictions (Bennett and Thorburn, 1992).

Cumulative knowledge on data assimilation at oceanography and meteorology let the kick off the data assimilation applications in the area of hydrology. Kostov and Jackson (1993) have inferred that if the hydrological model is convenient to take remote sensing data as input, both hydrological model output and proper remote sensing data can be used to keep simulation results on track through data assimilation.

Soil moisture is one of the key element of Earth science and it has an important effect on data assimilation in the history of hydrology science. Thermal infrared derived near surface soil moisture content was assimilated whenever the data were available; the results of annual runoff values are improved by DA approach (Ottlé and Vidal-Madjar, 1994).

Screen-level measurement of relative humidity and temperature was examined in terms of improving estimation of land surface flux by (Bouttier et al., 1993; Viterbo and Beljaars, 1995).

The recent development is now related on several different disciplines with sophisticated methods and equations. The algorithms become exceedingly specific from simple rule-based to advanced smoothing. The implementation of these algorithms consist of the one, two, three and four dimensional variational algorithms (1D, 2D, 3D, and 4D-VAR, e.g., Seo et al., 2003, 2009; Valstar et al., 2004), extended or ensemble Kalman Filtering (EKF,EnKF)(Moradkhani et al., 2005b; Clark and Slater, 2006;Weerts and El Serafy, 2006; Shamir et al., 2010), particular filtering (Weerts and El Serafy, 2006; Matgen et al., 2010; Moradkhani et al, 2012), hybrid EnKF or 4D-VAR approaches (Zhang et al., 2009), and other Bayesian approaches (Reggiani and Weerts, 2008; Todini, 2008; Reggiani et al., 2009).

In-situ observation is the oldest technique to get the information of any type of data directly from point measurements. Many of the hydrological applications assimilated these observations (e.g. discharge, soil moisture and snowpack) into a model to enhance forecasting of streamflow and other variables of model outputs (Seo et al., 2003, 2009; Vrugt et al., 2005; Weerts and El Serafy, 2006; Clark et al., 2008; Komma et al., 2008; Moradkhani and Sorooshian, 2009; Thirel et al., 2010).

With developing satellite technology, plenty of data from satellites are available to be used in hydrological applications. These products as soil moisture (Pauwels et al., 2001; De Lannoy et al., 2007; Yirdaw et al., 2008; Crow and Ryu, 2009; Kumar et al., 2009; Brocca et al., 2010; Peters-Lidard et al., 2011; Liu et al., 2012), and snow cover area and/or snow water equivalent (Rodell and Houser, 2004; Lee et al., 2005; Andreadis and Lettenmaier, 2006; Zaitchik et al., 2008; Durand et al., 2008; Kolberg and Gottschalk, 2010; Kuchment et al., 2010; DeChant and Moradkhani, 2011; De Lannoy et al., 2012) are taking into account for data assimilation as input to force.

The hydrological model aiming to use DA can vary from physically based land surface models (Albergel et al., 2008; Nagarajan et al., 2011), to distributed hydrologic models (Clark et al., 2008; Rakovec et al., 2012) and conceptual rainfall-runoff models (Aubert et al., 2003; Seo et al., 2003, 2009; Moradkhani et al., 2005a, b; Weerts and El Serafy, 2006).

While the major DA applications are related with hydrological model state updating, some researches apply DA on model state and model parameter simultaneously (Moradkhani et al., 2005b; Vrugt et al., 2005; Franssen and Kinzelbach, 2008; Lü et al., 2010; Leisenring and Moradkhani, 2011; Nie et al., 2011; Vrugt et al., 2013; Corato et al., 2014; Schumacher et al., 2016).

One of the DA technique Moving Horizon Estimation (MHE) using 4DVAR is known by the help of Model Prediction Control applications (Allgöwer et al., 1999). Then, comparison of MHE with different DA methods is studied by Haseltine and Rawlings (2005). In hydrology, Montero et al. (2016) use the MHE to evaluate satellite products within the DA procedure.

This study is the first step for integrating a prototype of the data assimilation test bed with selected available components according to the specified pilot area. Moreover, this generic test bed involves the satellite products used through DA procedure to improve the forecast performance. The preliminary results of this thesis study are presented in Montero et al. (2016)

3. STUDY AREA & DATA

3.1. Study Area

Turkish geographical regions are divided into seven sub regions, and one of them is Eastern Anatolia Region, which is 21% of Turkey with respect to the surface area as 164,000 km². Even it has a large area; the population is relatively low because of tough winter conditions. Several important streams, with the names Euphrates, Tigris, Aras and Kura are located in this region.

Mesopotamia region, home to several civilizations, owns Euphrates and Tigris Rivers, which play vital role for irrigation and energy production. These two rivers with their significant potential flow rate have a unique importance for Turkey. Euphrates has major tributaries as Murat, Karasu, Peri and Munzur. On the other hand, Tigris's major tributaries are Batman, Botan, Habur and Greater Zap.

Euphrates, which is the longest river in the Southern West Asia, has potential flow of 35.6 billion m³/month. Its total length is 2700 km and 1236 km of it is in the border of Turkey (Aytemiz and Kodaman, 2006). Keban, Karakaya, Atatürk, Birecik and Karkamış are outstanding large reservoirs located on Euphrates River. These dams have a huge storage capacity, so water resources management is relatively important in these regions.

Upper Euphrates (Karasu) Basin, which is a headwater of Euphrates River Basin, has been selected for this study. The main reason for this selection is that Karasu Basin is one of the important highly snow dominant basin at Upper Euphrates River. Even though it is a prominent basin, it can be described as data scarce region according to the observation network. Moreover, important cities in Karasu Basin assist to reach the stations and support the data accessibility. Furthermore, the heritage of previous projects and existing infrastructure encourages the studies in this region and basin.

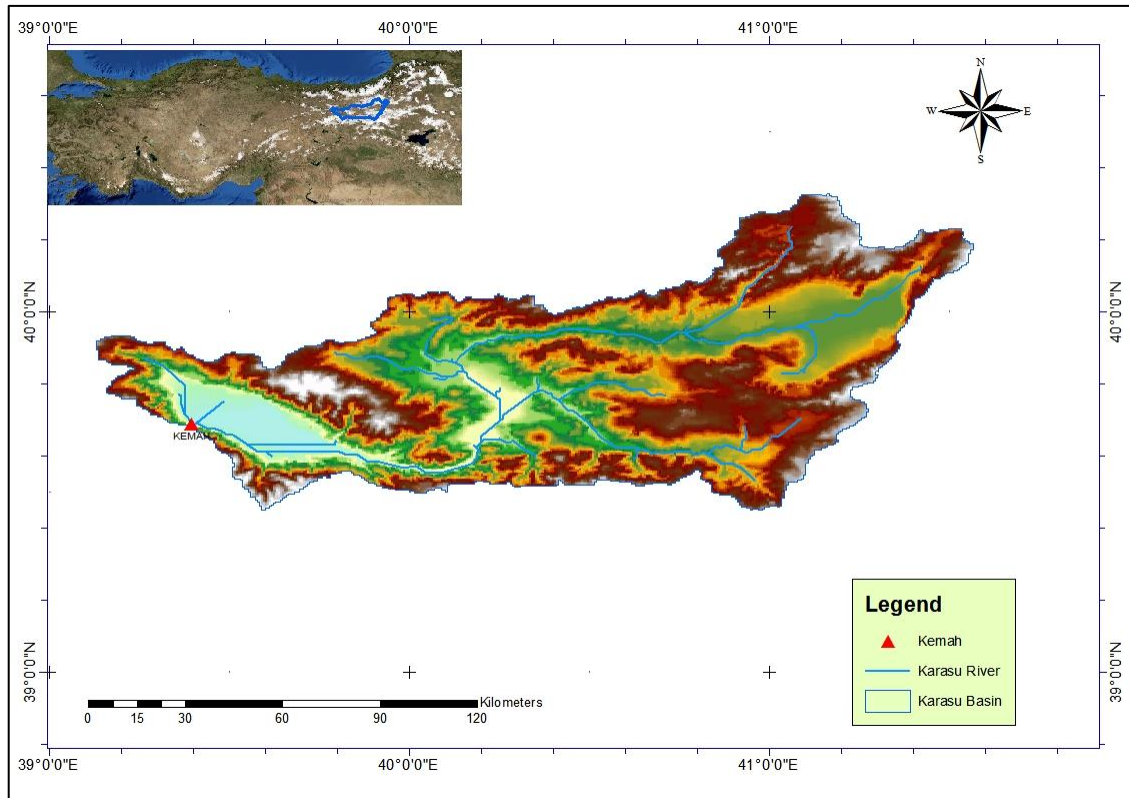


Figure 3.1. *Outlet and river network of Karasu Basin.*

Karasu Basin is located between 39° 50' N latitude and 40° 20' E longitude (Figure 3.1). Its area is 10,275 km² and its elevational range is between 1125 m to 3500 m. Its mean elevation is 1983 m and its mean slope is 20%. In addition, according to the land use maps, it consists of pasture (35%), agricultural area (31.5%), bare ground (27.5%) and water (1%).

Outlet of Karasu basin is controlled by a streamflow station (E21A019 – Kemah) which is operated by General Directorate of State Hydraulic Works. Long-term stream flow measurement shows that 60-70% of total yearly flow arises during spring and early summer (Kaya, 1999; Tekeli, 2005).

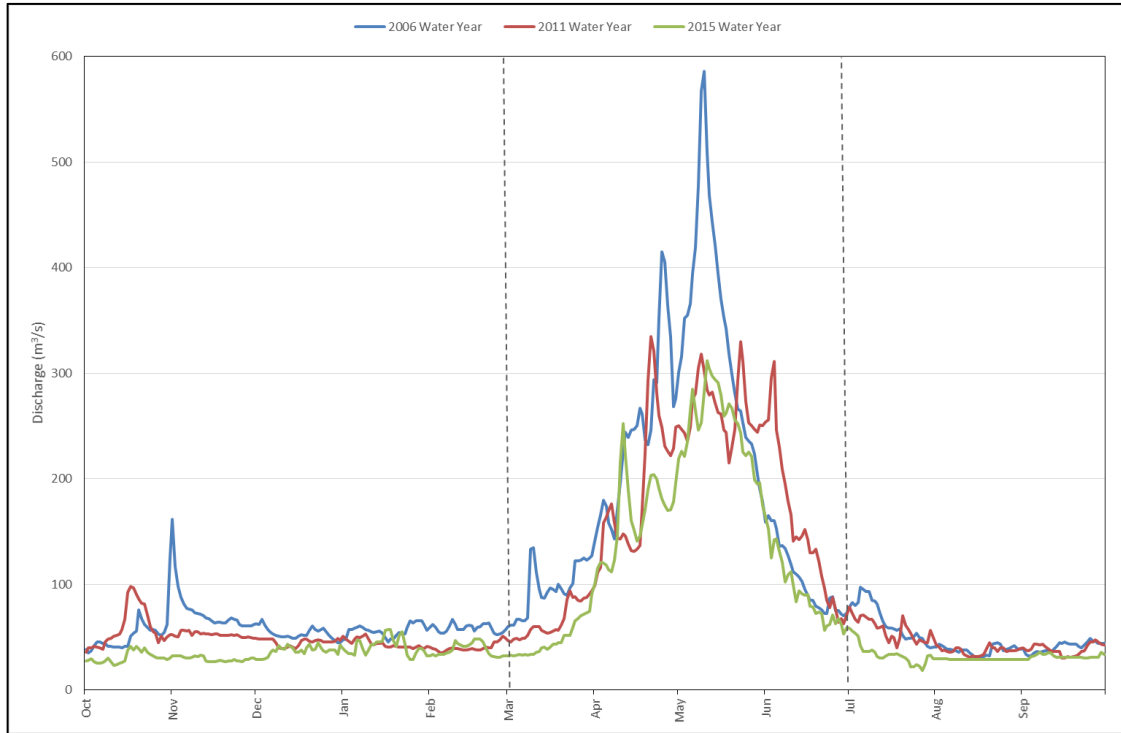


Figure 3.2. *Hydrograph of Karasu Basin for different years.*

2006, 2011 and 2015 water years, which are representing calibration, validation and forecasting periods respectively, are shown in Figure 3.2 with the sample hydrographs of Karasu Basin. As it could be interpreted from Figure 3.2, snowmelt runoff generally starts at the beginning of March and ends in July in that period.

In order to understand the characteristic properties of Karasu Basin, Geographical Information System (GIS) techniques have been used. To get the information by using GIS, Digital Elevation Model (DEM) was downloaded from Shuttle Radar Topography Mission (SRTM) at “<http://srtm.csi.cgiar.org/SELECTION/inputCoord.asp>” website, which generates high resolution digital topographic database. Because of the location of Karasu Basin, four tiles have been selected to download, and then all four was merged to create the watershed where the spatial resolution is 90 m.

With the help of ArcGIS 10.4 program (<http://www.esri.com/software/arcgis>), area, elevation zones, aspect and slope of the basin are calculated and visualized as a map. Area is a physical variable for nearly any hydrologic model as well as HBV hydrologic model, so firstly the area of Karasu Basin has been calculated. Then elevation zones are created as equal percentage areas. In this study, Karasu has been divided into 10 equal area, the reasons for this is the representation of the basin more precisely in calculations

and sound calculations of Snow Covered Area (SCA) of the basin. Because SCA is derived from SWE, a smooth SCA curve can be generated with a number of elevation zones. Moreover, this semi-distributed modelling approach uses the computational advantage of fully distributed applications. Nonetheless, it is not as course as lump model.

After Karasu Basin is divided into 10 zones, each representing 10% of the area, elevation ranges and mean elevation values are provided in Table 3.1. Figure 3.3 shows the elevational zone map. According to hypsometric elevation curve, the mean elevation of Karasu Basin is found as 1983 meters (Figure 3.4).

The values in Table 3.1 are used in HBV model to configure zonal characteristics. Understanding the contribution of each zone and respective output of discharge, SCA, SWE and soil moisture (SM) is also possible.

Table 3.1. Elevation range of Karasu Basin.

| Zone | Elevation Range [m a.s.l.] | Area [km²] | Area [%] | Mean Elevation [m] |
|-------------|---------------------------------------|----------------------------------|---------------------|-------------------------------|
| Zone1 | 1125-1485 | 1027.5 | 10 | 1315 |
| Zone2 | 1486-1678 | 1027.5 | 10 | 1587 |
| Zone3 | 1679-1781 | 1027.5 | 10 | 1740 |
| Zone4 | 1782-1873 | 1027.5 | 10 | 1827 |
| Zone5 | 1874-1981 | 1027.5 | 10 | 1926 |
| Zone6 | 1982-2103 | 1027.5 | 10 | 2041 |
| Zone7 | 2104-2218 | 1027.5 | 10 | 2159 |
| Zone8 | 2219-2346 | 1027.5 | 10 | 2281 |
| Zone9 | 2347-2537 | 1027.5 | 10 | 2434 |
| Zone10 | 2538-3500 | 1027.5 | 10 | 2733 |

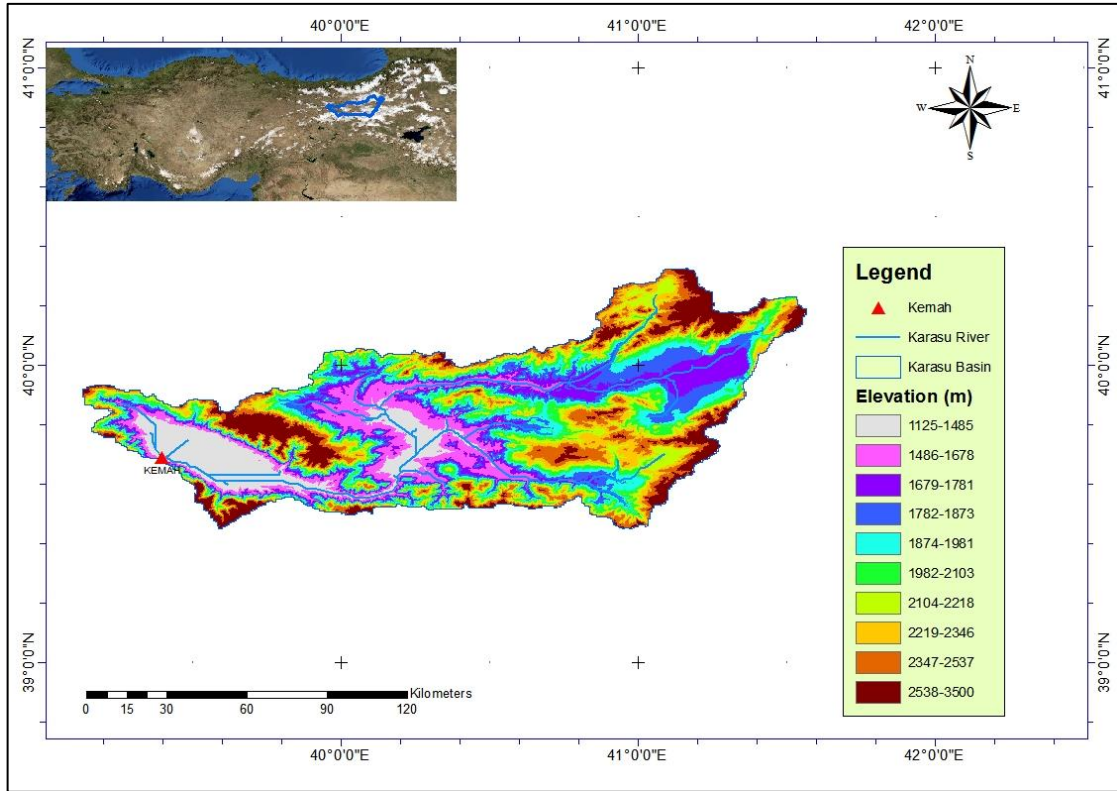


Figure 3.3. *Elevation zones of Karasu Basin.*

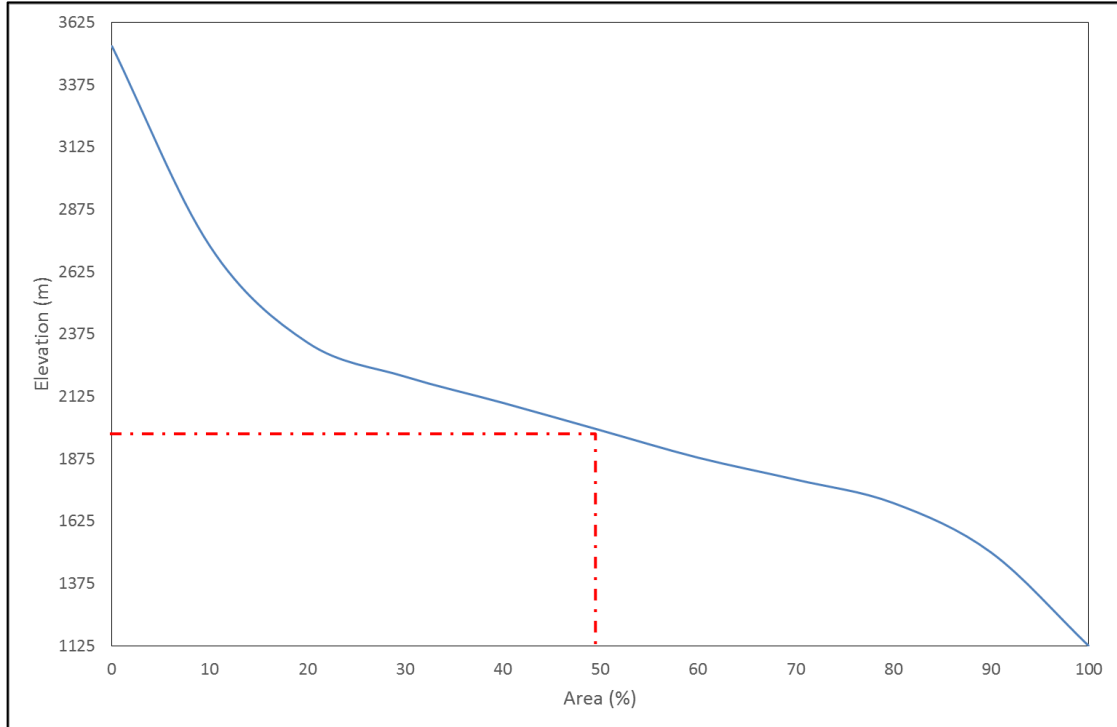


Figure 3.4. *Hypsometric curve of Karasu Basin.*

After downloading and processing the data archived in <http://www.eea.europa.eu/data-and-maps/data/corine-land-cover-2006-raster-3> web site, Figure 3.5 is prepared for land cover. The majority of total area consists of agricultural, grassland and little or no vegetation. Relatively small amount of urban area, which includes Erzurum and Erzincan cities, is not so effective on hydrological modelling since it constitutes only 2% of impervious area. With the minor contribution of forest area (3.61%), the whole area of Karasu Basin is considered as bare ground.

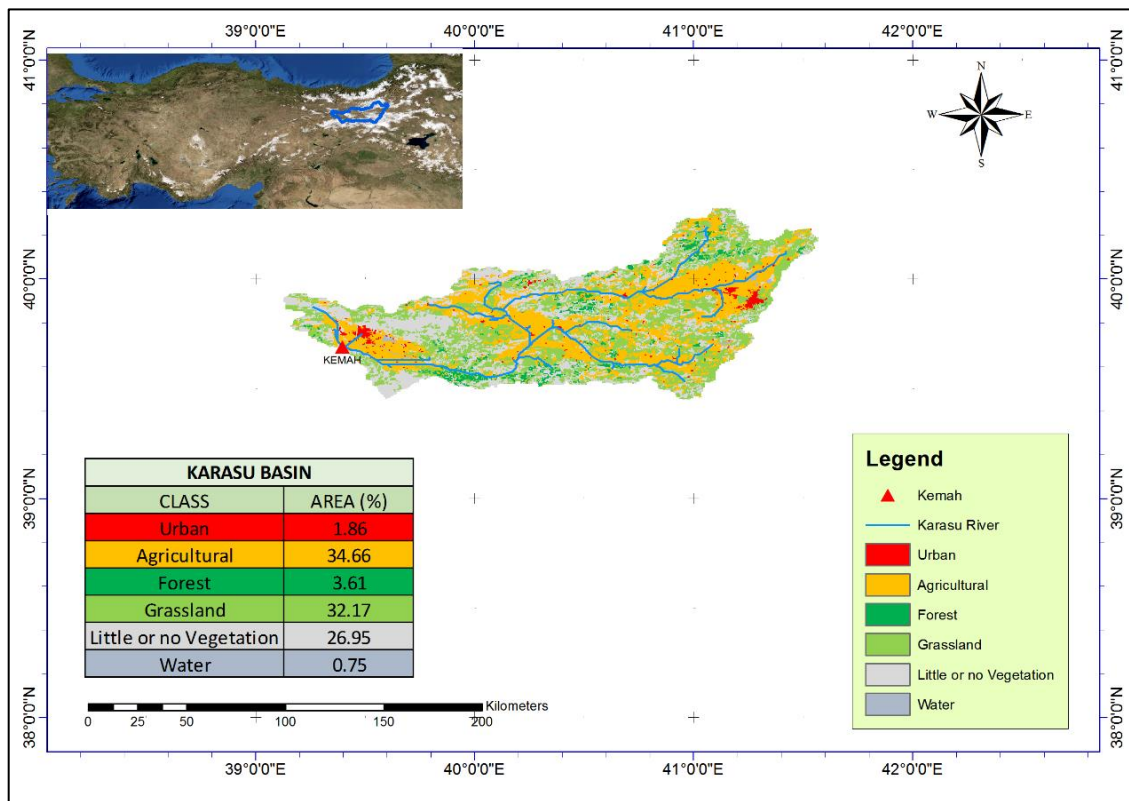


Figure 3.5. Land use map of Karasu Basin
Source: <http://www.eea.europa.eu/>

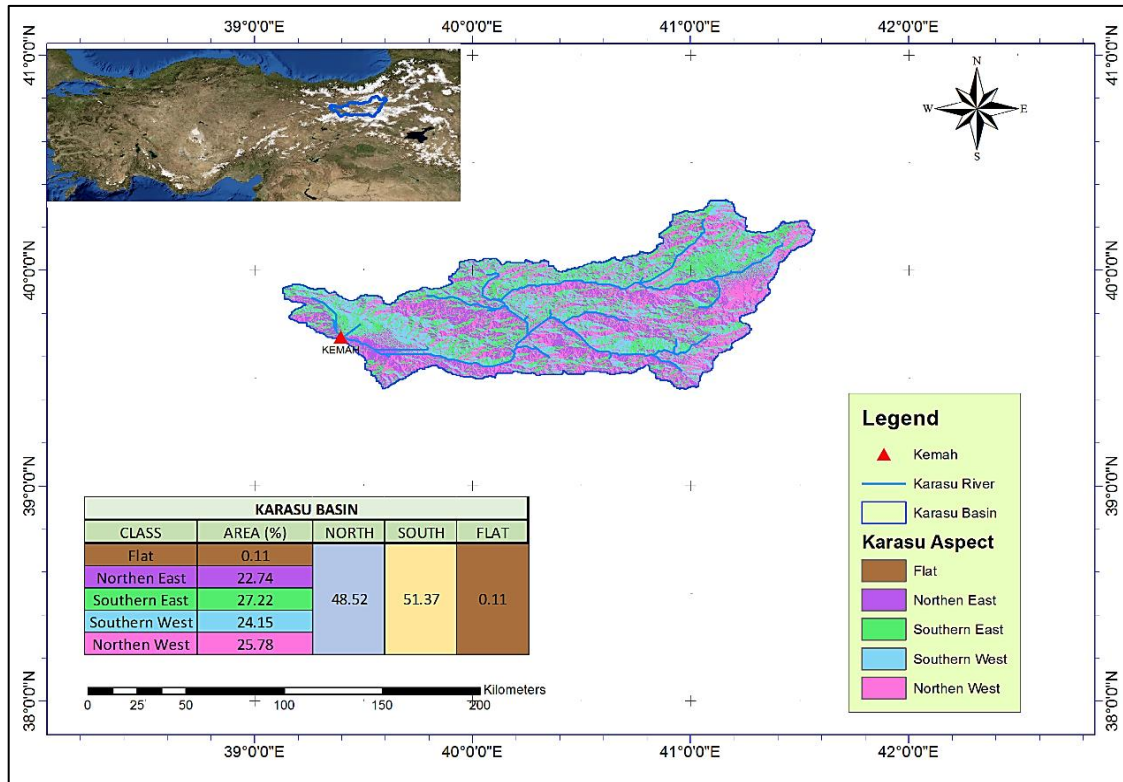


Figure 3.6. Aspect map of Karasu Basin.

When digital elevation map is analyzed, there is nearly on equal distribution in terms of aspect ratio within the basin (Figure 3.6). According to the Figure 3.6, north and south percentage of aspect is almost same. It could be inferred that the effect of aspect is almost equal for all of the edges in Karasu Basin.

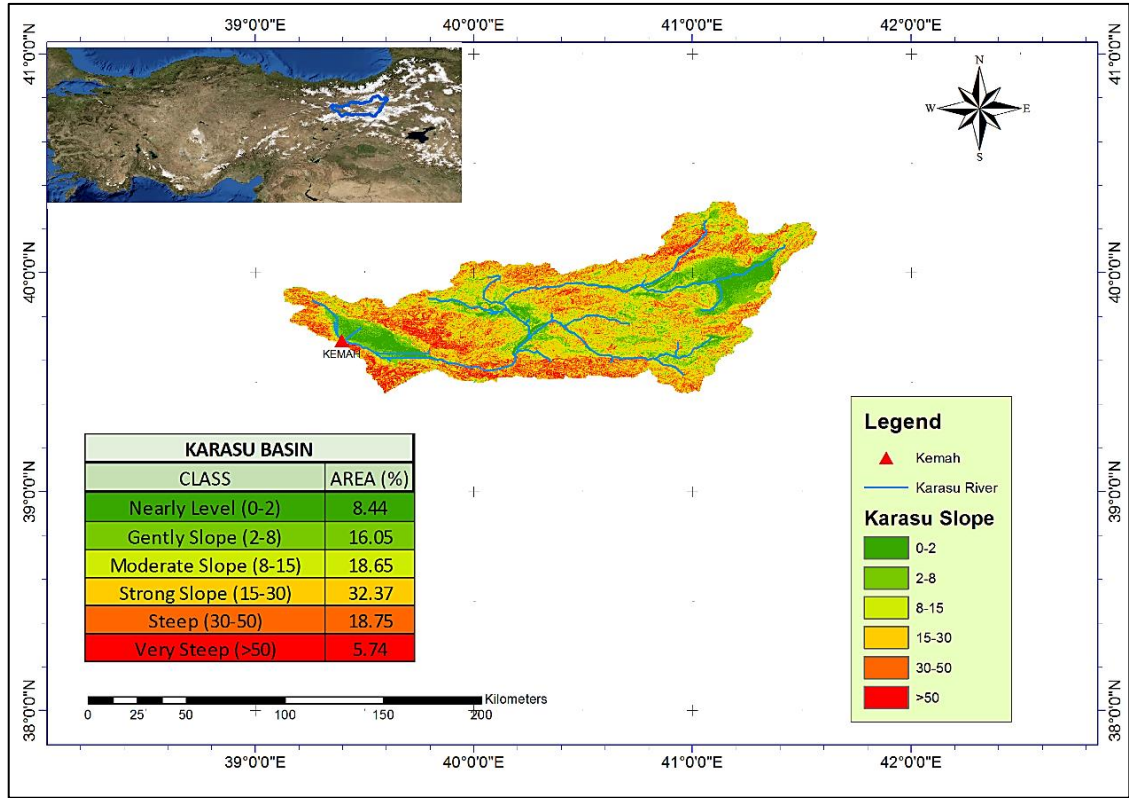


Figure 3.7. Slope map of Karasu Basin.

Slope map of Karasu Basin is created with meter/100 meter property of ArcGIS tool (Figure 3.7). The terrain includes nearly level area for cities of Erzurum and Erzurincan. On the other hand, the majority of the area could be classified as strong slope. According to the slope map, the average slope of Karasu Basin is calculated as 20%. As it is clear in Figure 3.7, the border of Karasu Basin is generally marked with very steep slope.

3.2. Hydro-meteorological Data

Hydrology science and applications consist of management, assessment and forecasting of water quality and quantity. Not only historical hydro-meteorological data but also real time data are collected, stored and analyzed. The records of data are used to prevent flood, drought and water pollution by management of water resources. Because of these vital tasks, collecting accurate, reliable and actual data is a very important prior condition (WMO, 1999). Data acquisition process is applied by responsible institutions and these data are uploaded and updated in a database to be used by researches in industrial countries. In addition, databases are capable of data access, reporting statistical analysis, model calibration and preparing model input. Turkish State Meteorological Service (TSMS) and General Directorate of State Hydraulic Works (DSI) are in charge

of data acquisition and data storage in Turkey. Since there is not any common database that is created by different institutions, transferring and accessing data is not an easy process in Turkey (Yamankurt, 2010). Collecting and transferring hydro-meteorological data that is especially related with snow is difficult and expensive due to harsh topographic and climate conditions at high altitudes. Furthermore, manual data collection at highly mountainous regions is very difficult on winter seasons. Consequently, knowledge of climate conditions at the region, which is mostly rippled, must be well-know.

Detailed climate observations are restricted at mountainous regions and generally most of the data are collected at low-elevations which are not that rippled (Marks et.al. 1992). Temperature and precipitation are the basic inputs for a hydrological model. Most of these data are measured at a point. To utilize these point observations, temporal and spatial distribution methods are needed.

Seventeen of meteorological stations are selected to be used in this study both inside or near outside of Karasu Basin (Figure 3.8). While fifteen stations from selected ones have both precipitation and temperature records, two of them have only temperature records.

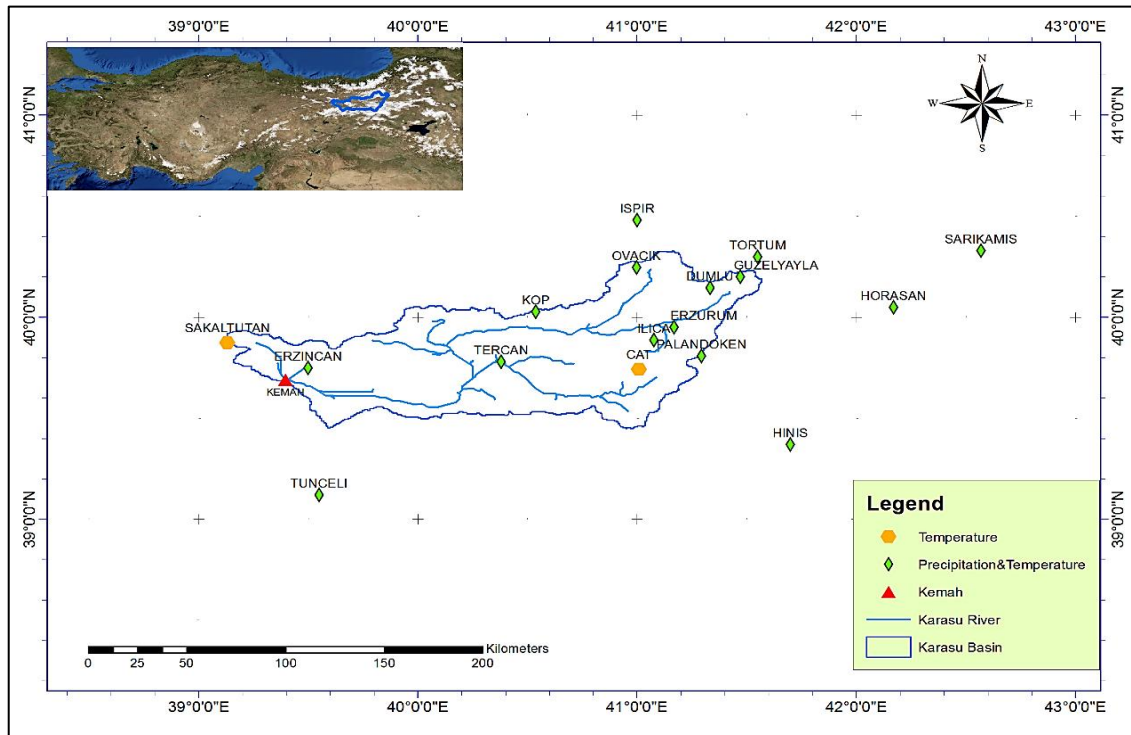


Figure 3.8. AWOS stations in and around Karasu Basin.

Figure 3.9 shows the total annual total precipitation over Turkey, besides Figure 3.10 demonstrates total annual precipitation for Erzurum (1860 m). The average precipitation values, between 1981 and 2015, are 574 mm and 579.6 mm for Turkey and Erzurum respectively. These data are provided by Turkish State Meteorological Service on <http://www.mgm.gov.tr/veridegerlendirme/yillik-toplam-yagis-verileri.aspx> website.

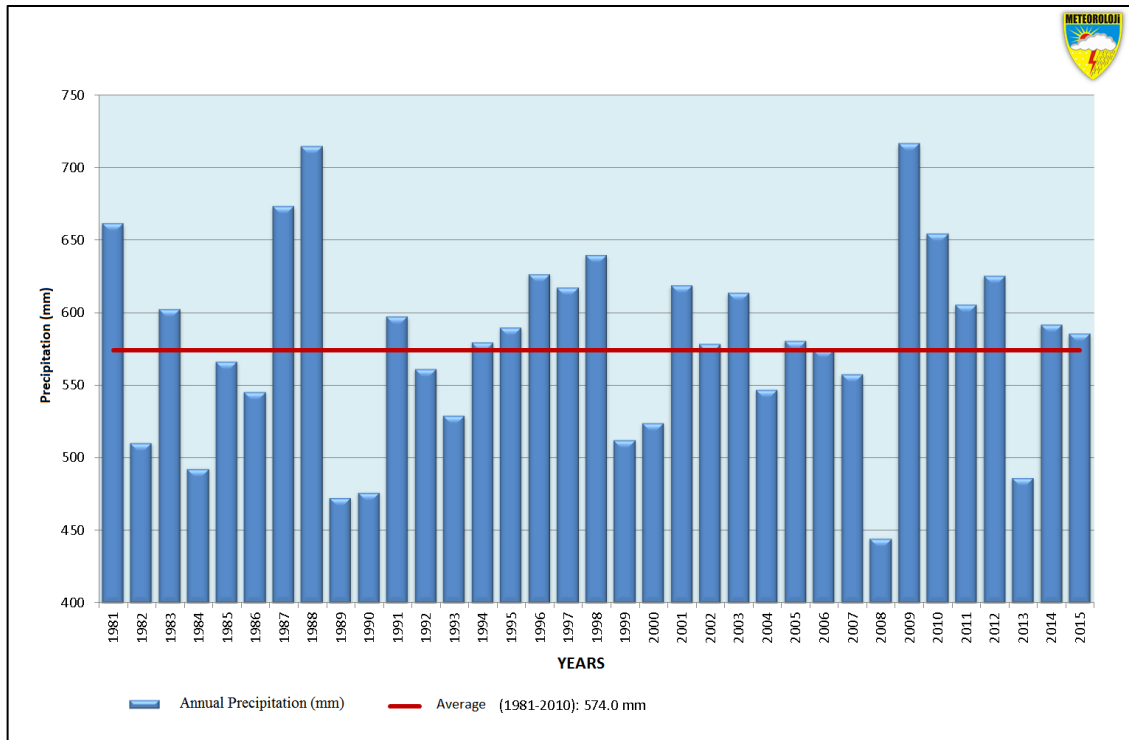


Figure 3.9. Total annual precipitation over Turkey.

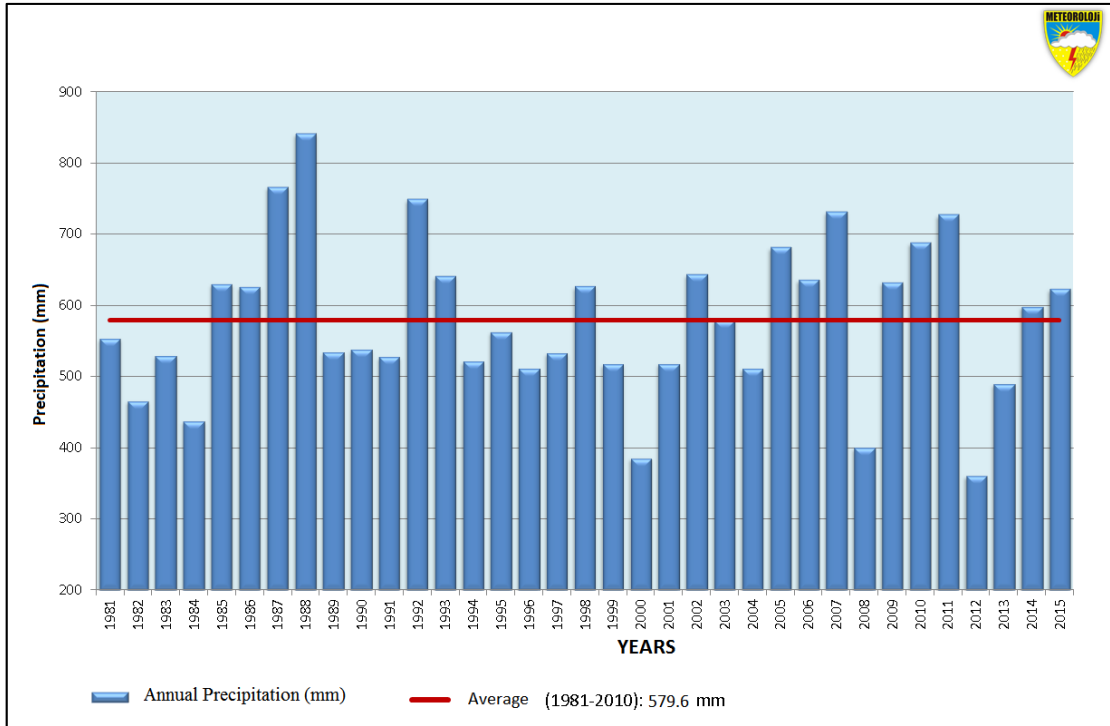


Figure 3.10. Total annual precipitation for Erzurum (1860 m).

For Karasu Basin, precipitation generally falls as snow between the months of December & March, whereas it falls as rain at the rest of the months. Monthly total precipitation values are shown in Figure 3.11 for Erzurum Automated Weather Observation Stations (AWOS) for the whole study years between 2001 and 2015. The years included in these statistics are 1981-2015, 1981-2015 and 2001-2015 for Turkey, Erzurum (1860 m) and Erzurum AWOS (1758 m) stations respectively.

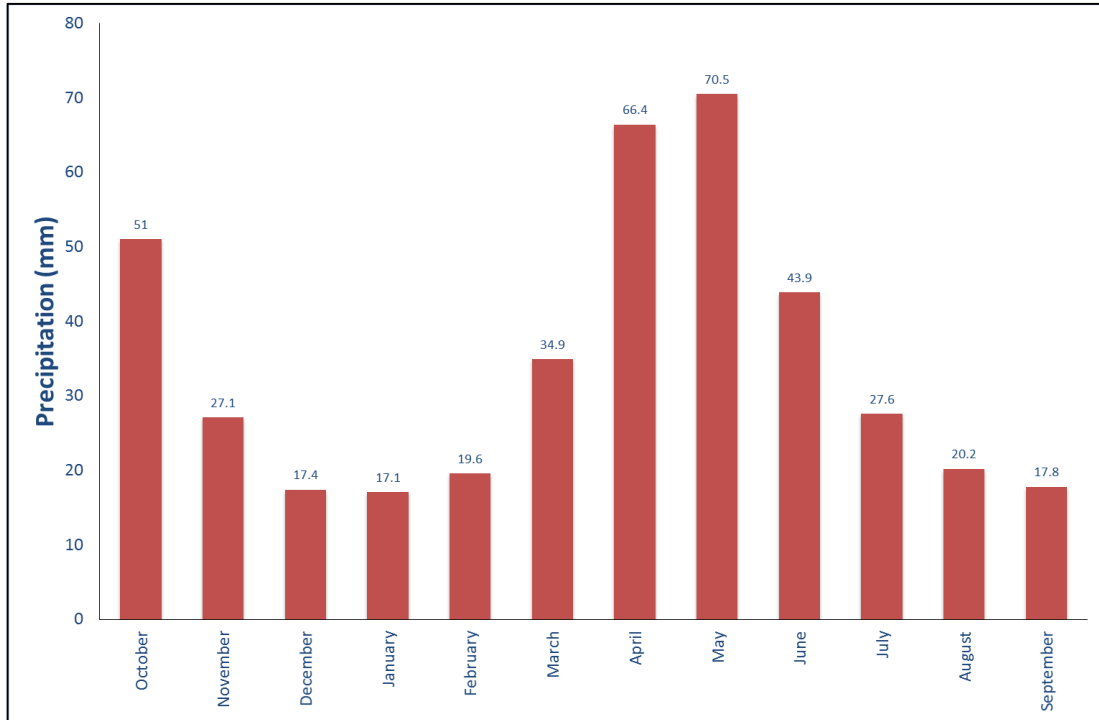


Figure 3.11. *Monthly mean precipitation for Erzurum AWOS (1758 m).*

Figure 3.12 indicates the comparison of temperature data for Turkey and Erzurum AWOS (1758 m) stations. Generally low temperature records are observed in the Eastern part of Turkey, especially in autumn and winter seasons. As it is clear from the Figure 3.12, the recorded monthly average temperature values for Turkey are higher than Erzurum.

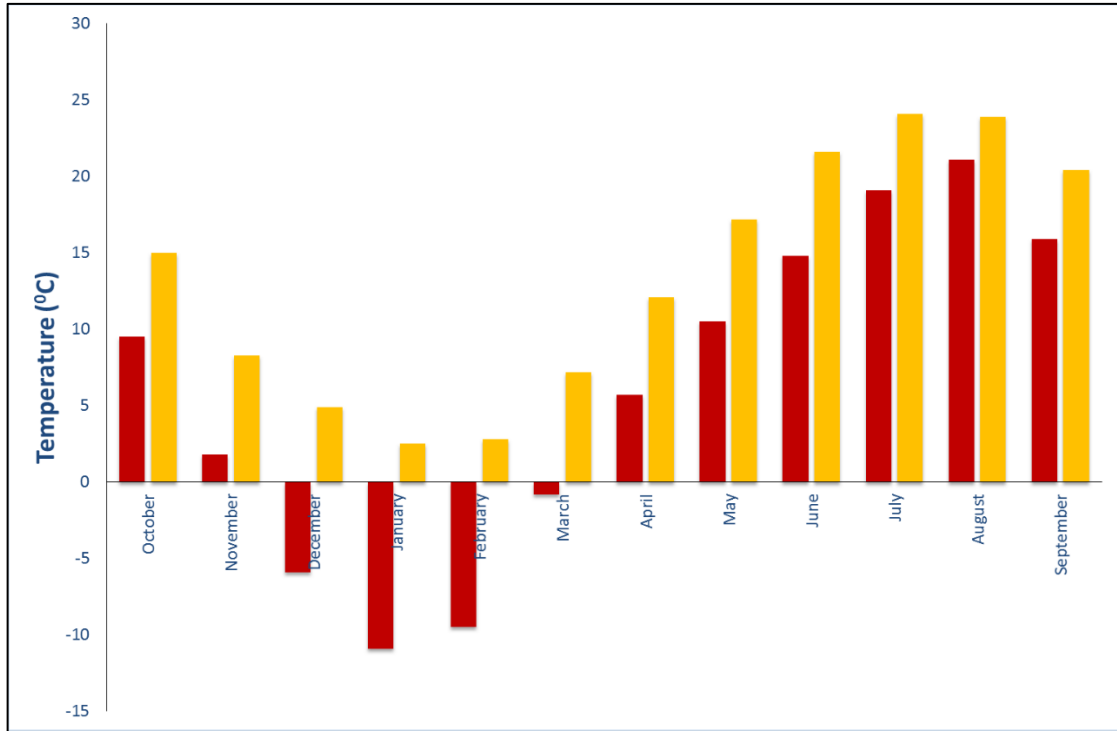


Figure 3.12. Comparison of monthly average temperature for Turkey and Erzurum AWOS

All meteorological data used in hydrologic modelling are point observations. These point measurements are distributed over the catchment to obtain areal average values and corresponding values for elevation zones. Several methods are being used for distribution of point observations to area. A few of them can be listed as; arithmetic mean, Thiessen polygon, isohyetal method, Inverse Distance Weighted (IDW), lapse rate and Kriging method. Detrended Kriging (DK) is selected in this study for the distribution of both precipitation and temperature measurements. The powerful side of this technique is that it can utilize topographical information of the given DEM (Garen et al., 1994). The main motivation of this algorithm is calculating mean areal inputs from point measurement especially in mountainous regions. The implicit assumption of this technique is that hydro-meteorological data and elevation have a homogenous relationship with ignoring the effect of slope, aspect and orographic regimes. The interface of the program is illustrated in Figure 3.13.

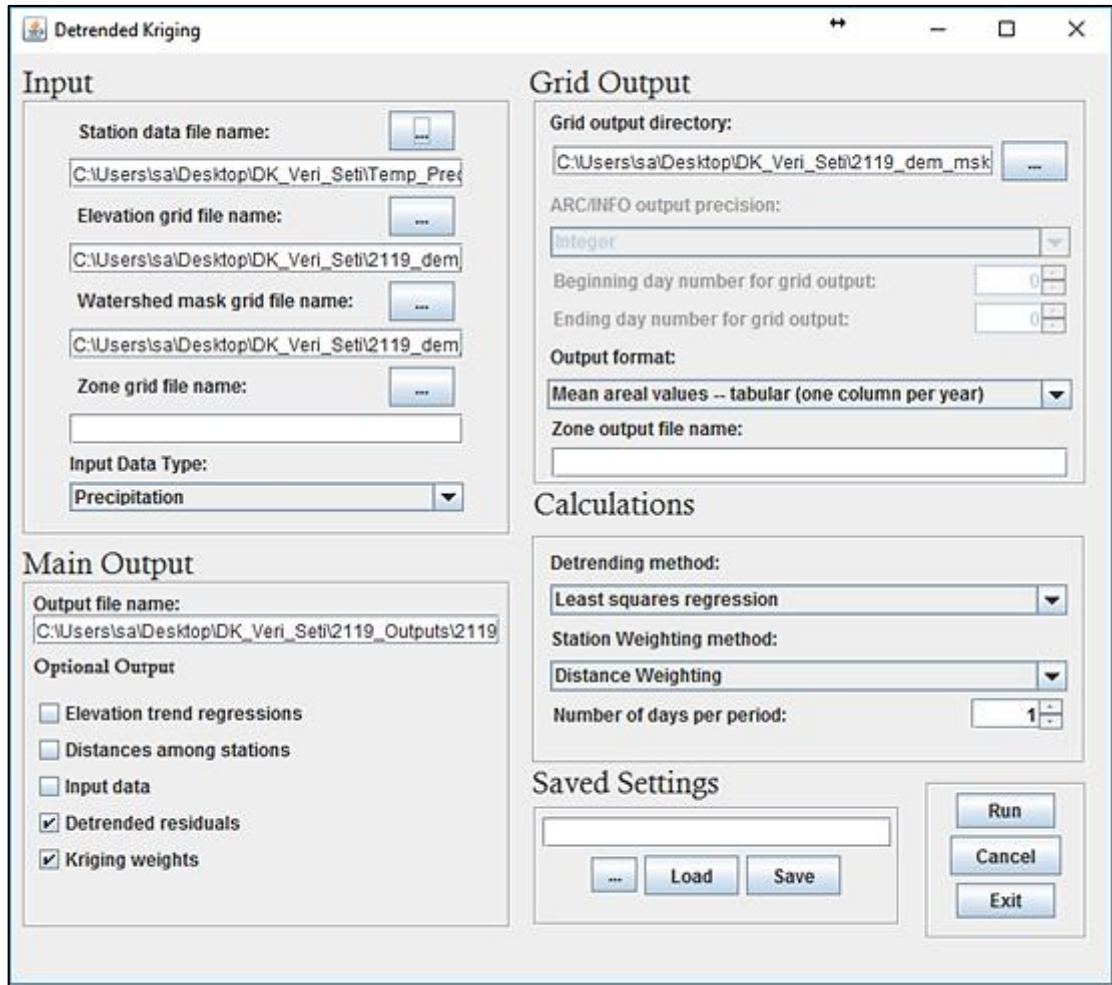


Figure 3.13. *The interface of DK program*

3.3. Satellite Snow Data

In order to increase the robustness of snowmelt forecasting, snow coverage and snow water equivalent are important variables for water resource management. While studying in a mountainous region, understanding variability of snow cover and melt could be prevented due to data limitations. In situ snowpack measurements are sparsely distributed relative to snowpack heterogeneity leaving much of the hydrologic cycle under sampled in both time and space (Bates et al., 2006). Nevertheless, accessibility constrains getting rainfall/snowfall and meteorological data especially in highest area of the basin in most mountainous regions (Boudhar, 2009). Hereat remote sensing observations are getting popular for monitoring snow properties.

When conventional in situ snow measurements and satellite data are compared, satellite data are especially well adapted to monitor snow covered surface over continuous

space-time scales. A wide range of instruments are available for measuring and observing snow cover; a variety of space borne sensors with various spectral, spatial and temporal resolutions meet the needs of climatologists and hydrologists.

In this study, snow products of H-SAF project, MSG-SEVIRI (H10) and SSMI/S (H13), and MODIS are used. MSG-SEVIRI (H10) and MODIS snow products are used to determine snow covered area (SCA) and SSMI/S (H13) product is dedicated to find snow water equivalent (SWE). They are provided as observed inputs to update the model states for data assimilation in this thesis.

The European Organization for the Exploitation of Meteorological Satellites (EUMETSAT) has several dedicated programs for processing satellite data. Each of these SAFs provides products and services on an operational basis. The main purpose of the “EUMETSAT Satellite Application Facility on Support to Operational Hydrology and Water Management”, H-SAF, is to provide new satellite derived products from existing and future satellites with sufficient time and space resolution to satisfy the needs of operational hydrology and to perform independent validation of the usefulness of the new products for fighting against floods, landslides, avalanches and evaluating water resources. The currently available and operational H-SAF products include information about precipitation, snow and soil moisture conditions (<http://hsaf.meteoam.it/>).

The H-SAF was established by the EUMETSAT Council on 3 July 2005 and its Development Phase was in between 2005-2010. The SAF is now in its second Continuous Development and Operations Phase (CDOP2) which started on 2012 and will end on 2017. In this phase, the vision is to develop or complement interface products for assimilating existing hydrological models, developing tools which will allow models to accept soil moisture and/or snow cover products that have been developed in the framework of H-SAF project. In this study, the use of these new satellite products in hydrological modeling with variational data assimilation approach is presented.

Snow recognition product (H10) by VIS/IR radiometry is based on multi-channel analysis of Spinning Enhanced Visible and Infrared Imager (SEVIRI) instrument on board the second generation of Meteosat (MSG) satellites. A key feature of this imaging instrument is its continuous imaging of the Earth in 12 spectral channels with a baseline repeat cycle of 15 min (Aminou, 2002). The observing cycle (15 min) enables continuous

monitoring of the cloud situation, in order to collect as many cloud free pixels as possible, multi-temporal analysis over the hours of illumination is performed. The imaging sampling is performed at 3 km intervals at the sub-satellite point for standard channels however; the output product is sampled at 0.05 degrees intervals (~ 5 km) over Europe (Figure 3.14). The product for mountainous areas and flat/forested have been operational from late 2007 and 2009, respectively (http://hsaf.meteoam.it/documents/PUM/SAF_HSAF_PUM-10_1_1.pdf).

The snow cover retrieval algorithms of flat and mountainous regions are different for the product. The products are merged by blending the information on flat/forest and mountainous areas at the end. The area is defined to be mountainous based on the mean altitude and standard deviation of the slope within $5 \text{ km} \times 5 \text{ km}$ pixels (Lahtinen et al., 2009). A detailed description of the MSG-SEVIRI snow algorithm is presented in the Algorithm Theoretical Basis Document (http://hsaf.meteoam.it/documents/ATDD/SAF_HSAF_ATBD-10_1_1.pdf).

Snow cover maps using MSG-SEVIRI data have been produced for each 15 minutes cycle between 8:00-15:45 UTC that makes 32 individual images a day. The product is an output of image classification processing. All individual 15 minute images acquired during a day are subjected to a series of thresholding tests based on spectral signatures and temporal stability criteria. Daily snow cover map is obtained from the snow cover maps of each individual 15 minutes image by accepting pixels having at least 4 snow hits among 32 images during a day. Finally, a daily thematic map has been produced which is consisting of 4 different classes: snow, land, cloud and unclassified.

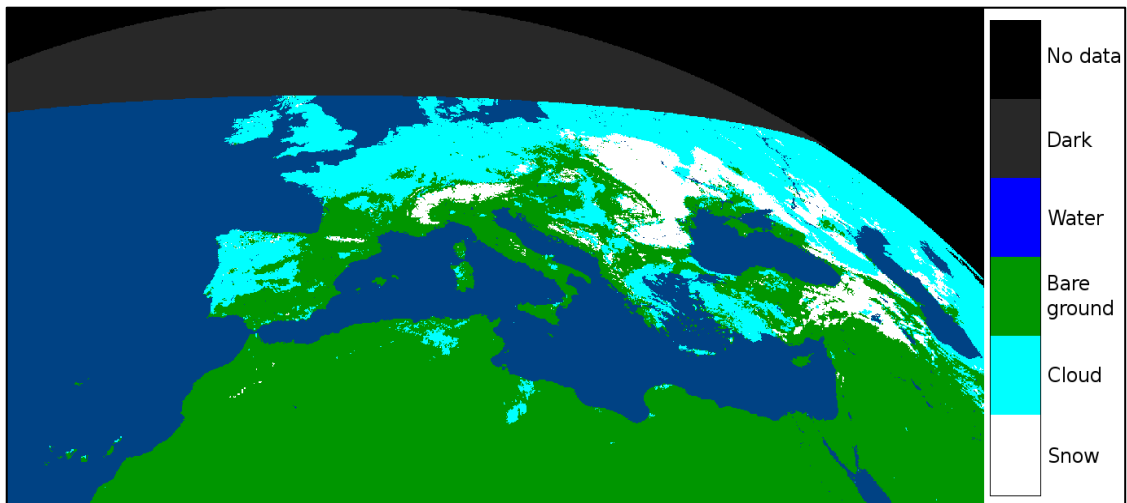


Figure 3.14. *View of MSG-SEVIRI (H10) product at 31-12-2012.*

Snow Water Equivalent product (H13) is generated from SSMI/S radiometer. Earlier version of the product by MW radiometry was fundamentally based on the AMSR-E microwave radiometer being flown on EOS-Aqua. Due to the failure of AMSR-E happened on October 2011, SSM/I and SSMIS flown on the DMSP satellites are used since that date. For mountainous areas SWE is derived using radiometer data only and for flat areas SWE is an assimilation of ground based snow depth observations and satellite data.

H-SAF product SSMI/S (H13) is delivered in a grid that has resolution of 0.25 degrees. At Earth's equator this corresponds roughly to 25 km. A detailed description of the model and its performance is given by Pulliainen et al. (1999). For more information, please refer to the Products User Manual, PUM-13 and Algorithm Theoretical Development Document, ATDD-13 (http://hsaf.meteoam.it/documents/PUM/SAF_HSAF_PUM-13_1_0.pdf).

The horizontal resolution descends from the instrument Instantaneous Field of View (IFOV), and other factors. For MW conical scanners the IFOV is constant, but depends on the frequency channels utilized for building the product. Thick snow requires lower frequencies with higher penetration that implies coarser resolution. In practice, the current algorithm utilizes the two frequencies 18.7 and 36.5 GHz, thus the resolution is that one of AMSR-E at 18.7 GHz, i.e. ~ 20 km. Sampling also is made at ~ 20 km intervals (0.25°). The global coverage is provided for observing cycle of every 24 h (Figure 3.15).

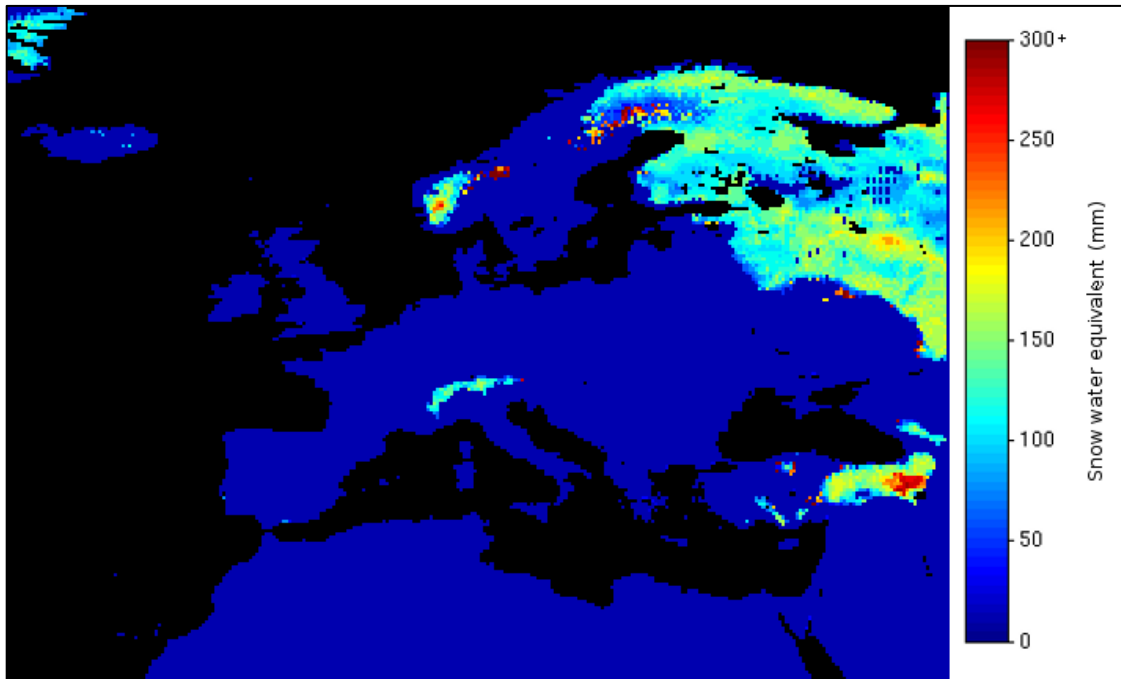


Figure 3.15. *View of SSMI/S (H13) product at 26-03-2012.*

The accuracy of satellite-derived products is provided by the convolution of several measurement features (random error, bias, sensitivity, precision, etc.) and it descends from the strength of the physical principle linking the satellite observation to the natural process determining the parameter. The validation activity is a continuous process for MSG-SEVIRI (H10) and SSMI/S (H13) products since 2009.

Moderate Resolution Imaging Spectroradiometer (MODIS) employs a cross-track scan mirror collecting optics and a set of individual detector elements to provide an imagery of the Earth's surface and clouds in 36 discrete, narrow spectral bands from approximately 0.4 to 14.4 μm (Barnes et al., 1998). There are two onboard satellites that Terra, which launched end of 1999, and Aqua, which deployed mid of 2002. Terra and Aqua image the Earth at 10:30 a.m. and 01:30 p.m. (local time) respectively. These two different overpass time allow satellites to obtain more clear views of the surface by increasing the chance to get rid of cloud coverage within 3 hours (Hall and Riggs, 2007).

The spatial resolution of MODIS is 500 m and the temporal resolution is daily. The data are ordered free of charge from the Earth Observation System Data and Information System (EOSDIS) located at the NASA (reverb.echo.nasa.gov). The raw data format is HDF (Hierarchical Data Format). Raw MODIS product is illustrated in Figure 3.16.

The accuracy of MODIS is tested with several different studies. The main disadvantage of MODIS is could coverage. Parajka and Blöschl (2008) applied spatial and temporal filter to reduce the cloud coverage on MODIS images. The results show that the average 63% cloud coverage reduces to 4% while the accuracies decrease 95.5% to 92.1%. Çoşkun (2016) uses the more sophisticated algorithm to reduce the cloud coverage with similar principles to Parajka and Blöschl (2008). The algorithm eliminates 70.77% cloud coverage for Terra satellite product, while the accuracy rate decreases from 98.42% to 93.56%.

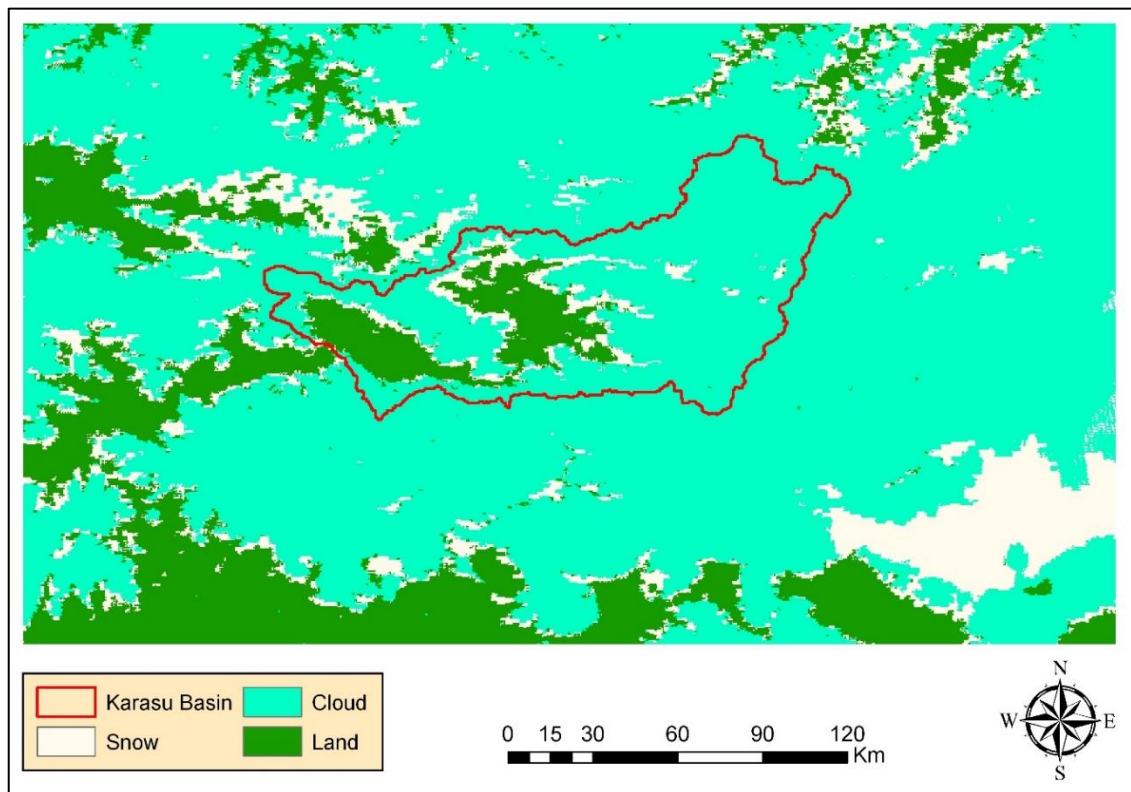


Figure 3.16. View of MODIS snow cover product at 31-12-2012.

4. METHODOLOGY

4.1. Hydrological Modelling

Complex natural dynamics are tried to be solved by human being from past to present. The positive science handles this complexity by converting this complicated nature to a more intelligible form. At that point, hydrological models that are part of modelling technology help to get through the problems.

Hydrological models vary by types as physically based, conceptual and deterministic models. In addition, lumped, semi-distributed and distributed models separate hydrological models with respect to spatial property. Lumped models take a river basin as a complete single component. In distributed models, a basin is divided grid by grid and calculations are done within a cell then summed up. Semi-distributed models take water catchments as sub-basins or subunits so these models are in between the lumped and distributed models. Each of them has several advantages and disadvantages, so it depends on data, basin, available software and purpose of the study to select a proper spatial distribution.

The HBV (Hydrologiska Byrans Vattenbalansavdelning) model, which is selected for this study, is a semi-distributed conceptual rainfall-runoff model designed in 1976 by Swedish Meteorological and Hydrological Institute (Bergström, 1976). The inputs for the HBV model consist of daily total precipitation, daily average temperature and estimates of daily total potential evaporation. In addition to the inputs, a parameter set is needed to represent the characteristics of a basin in runoff calculations (Figure 4.1).

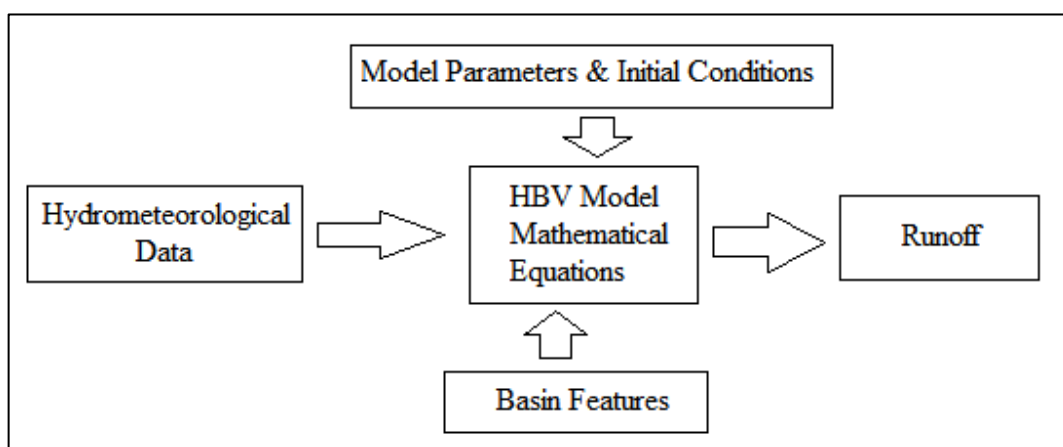


Figure 4.1. General flow chart of HBV model.

The essential properties of hydrological models are;

- It must be understandable by user
- It must be suitable with the data that are dealing with
- It must have parameters suitable with the scope of physical basis

HBV hydrological modelling is a well known conceptual model and it has been applied in more than 90 countries all around the world with different scales (Bergström and Lindström, 2015). HBV model could be described as semi-distributed (since it is capable to work with elevation zones) conceptual model. At this point, elevation-area distribution and land use of the basin gain importance. HBV model is introduced by routines in Figure 4.2

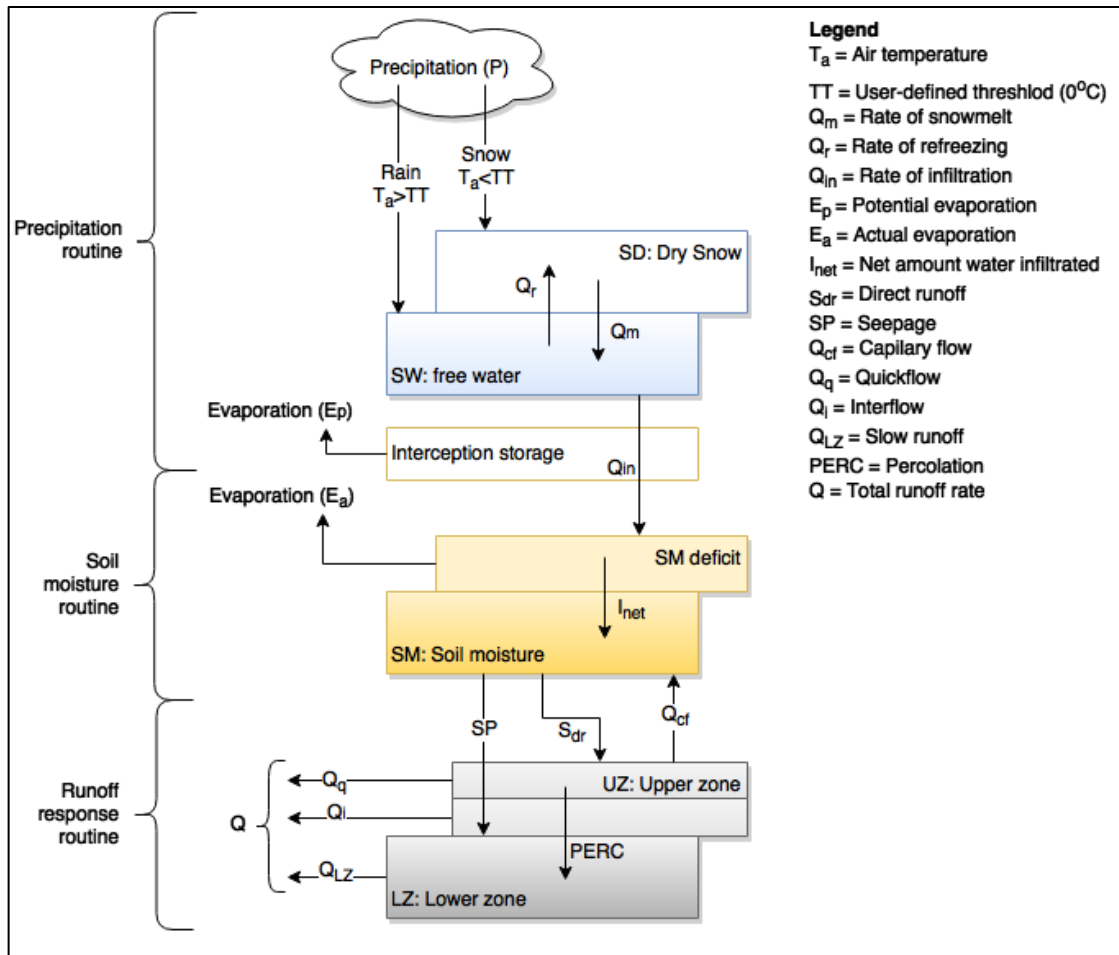


Figure 4.2. Schematization of HBV model
 Source: <http://schj.home.xs4all.nl/html/>

4.1.1. Precipitation routine

Daily total precipitation gets into HBV model through the snow routine. First comparison is tested by air temperature (T_a). if the average daily air temperature is below the user defined temperature threshold (TT), precipitation falls as snow, else it falls as rain. If it falls as rain, it directly ends up in the free water reservoir (SW); else it sums up with dry snow component (SD). In the box of dry snow (SD), the two components of it can interact as the free water can refreeze (Q_r) and snow can melt (Q_m) depend on the air temperature. This equation could be defined as:

$$Q_m = cfmax(T_a - TT); T_a > TT \quad (4.1)$$

$$Q_r = cfmax * cfr(TT - T_a); T_a < TT \quad (4.2)$$

Both degree-day factor ($cfmax$) and refreezing factor (cfr) are user-defined model parameters. Water holding capacity (WHC) limits SW and if SW exceeds WHC then excess SW is available as Q_{in} to infiltration. This can be described as follows:

$$Q_{in} = \max\{(SW - WHC * SD); 0.0\} \quad (4.3)$$

After all Q_{in} is calculated, it passes through the interception storage box. Maximum interception storage (LIC) controls this box. The available storage is filled with water coming from precipitation routine. if this box is not empty, evaporation occurs then the rest of the Q_{in} is convenient to get through soil routine.

4.1.2. Soil routine

Q_{in} is input of soil routine to determine the direct and infiltrated amount of water. Field capacity (FC) and soil moisture (SM) values take important role to calculate direct runoff (S_{dr}) in this box:

$$S_{dr} = \max\{(SM + Q_{in} - FC); 0.0\} \quad (4.4)$$

After calculating direct runoff, the amount of water that stuck in the soil is named as infiltrated water (I_{net}) and it describe as:

$$I_{net} = Q_{in} - S_{dr} \quad (4.5)$$

Part of the infiltrating water (I_{net}), will runoff through the soil layer through seepage (SP) into the lower zone. The amount of seepage is closely related to the amount

of soil moisture, SM: as the latter increases, the amount of seepage also increases. The power relation below describes this:

$$SP = (SM/FC)^\beta * I_{net} \quad (4.6)$$

β is an empirically based parameter, the value of which is higher than 1.0. If the β value is getting high, according to the equation, the absorption capacity of the soil is getting higher. Some of the SM will evaporate depending on the potential evaporation E_p and the amount of water available in the soil:

$$E_a = \left(\frac{SM}{T_m}\right) * E_p; SM < T_E \quad (4.7)$$

$$E_a = E_p; SM \geq T_E \quad (4.8)$$

The E_a is the actual evaporation; T_E is a user-defined threshold above which the actual evaporation is equal to the potential evaporation E_p . The T_E is defined as $LP * FC$.

4.1.3. Runoff response routine

Runoff response routine consist of two linear reservoir called as lower zone and upper zone. Lower zone represents slow runoff yet upper zone represents quick runoff and interflow.

This box is active when the direct runoff (S_{dr}) and seepage (SP) get in the response routine. If the direct runoff cannot exceed percolation value, which is percolation (PERC) from upper to lower response box, both direct runoff and seepage end up within lower zone box. The upper and lower zones equations are:

$$\Delta V_{lz} = \min\{PERC; (S_{dr} + SP)\} \quad (4.9)$$

$$\Delta V_{uz} = \max\{0.0; (S_{dr} + SP - PERC)\} \quad (4.10)$$

Where V_{lz} and V_{uz} is the content of the lower and upper zones respectively and Δ stands for increase of. Capillary flow (Q_{cf}) from the upper zone to the soil moisture reservoir is modeled according to:

$$Q_{cf} = cflux * ((Fc - SM)/Fc) \quad (4.11)$$

The lower zone is a linear reservoir, which means the rate of slow runoff, Q_{lz} , which leaves this zone during one time step equals:

$$Q_{lz} = K_{lz} * V_{lz} \quad (4.12)$$

Even though upper zone is a linear reservoir, it is more complicated than lower zone. Because of the fact that upper zone has two kind of inner zones which are interflow (Q_i) and quick flow (Q_q). If the total water content of the upper zone, V_{uz} , is lower than a threshold $UZ1$, the upper zone only generates interflow. On the other hand, if V_{uz} exceeds $UZ1$, part of the upper zone water will runoff as quick flow:

$$Q_i = K_i * \min\{UZ1; V_{uz}\} \quad (4.13)$$

$$Q_q = K * UZ^{(1+alpha)} \quad (4.14)$$

Total runoff rate Q consists of the three-runoff components:

$$Q = Q_q + Q_i + Q_{lz} \quad (4.15)$$

The runoff behavior in the runoff routine is controlled by two threshold values Tm and $UZ1$ and three reservoir parameters K_{lz} , K_i and K_q . In order for the differences in delay times of three runoff components to be represented, the parameters have to meet the following requirement:

$$K_{lz} < K_i < K_q \quad (4.16)$$

ECORR, RFCF and SFCF are the correction coefficients of evaporation, rainfall and snowfall, respectively. Moreover, ETF is a temperature correction that is used calculating actual evaporation. CFR is refreezing factor in the snow routine. TTI is the interval for smoothing the transition of rain and snow.

Table 4.1. Parameters of HBV model and default interval of their values.

| Parameter | Unit | Interval of the Values | Meaning of the Parameter |
|-----------|-----------|------------------------|--|
| ECORR | ---- | 0.8-2.0 | Evaporation Correction |
| ALPHA | ---- | 0.0-0.3 | Recession coefficient in $Q=k \cdot UZ^{(\alpha+1)}$ formula |
| BETA | ---- | 1.0-3.0 | Exponent in Formula for drainage from soil |
| CFLUX | mm/day °C | 0.2-0.8 | Maximum capillary flow from upper box to soil moisture routine |
| CFMAX | mm/day °C | 0.3-4.0 | Degree-day factor |
| CFR | ---- | 0.02-0.1 | Refreezing factor in the snow routine |
| FC | mm | 50-250 | Field capacity |
| LP | ---- | 0.2-0.9 | Limit for potential evaporation |
| PERC | mm/day | 0.4-6.0 | Percolation capacity from upper to lower box |
| RFCF | ---- | 0.8-1.3 | Rainfall correction factor |
| SFCF | ---- | 0.7-1.3 | Snowfall correction factor |
| TT | °C | -2.0-2.0 | Threshold temprature (rain or snow) |
| TTI | °C | 0.0-3.0 | Total lenght of a temprature interval |
| CWH | % | 0.01-0.1 | Water holding capacity of snow |
| TM | °C | -2.0-2.0 | Temperature for melting |
| ETF | ----- | 0.0-0.012 | Temperature correction factor |
| K | 1/day | 0.02-0.4 | Recession coefficient |
| K1 | 1/day | 0.001-0.1 | Recession coefficient for lower box |
| LIC | ----- | 0.0-2.0 | Maximum interception storage |

Source: Schwanenberg (2012).

4.2. Flood Early Warning System (Delft-FEWS)

Disasters, like floods and droughts, are natural events that human being can never totally avoid. Even investments to areas that are prone to floods and droughts are getting increasing, the potential loss of life and property do not decrease with the same acceleration.

Conventional measures are aiming to get rid of the risk and mainly focus on high capital investments in physical infrastructure, such as reservoirs, levees and other river engineering works. However, the risk is not fully eliminated. Hence, warning and event management are required to minimize the risk of damage caused by hydrological events.

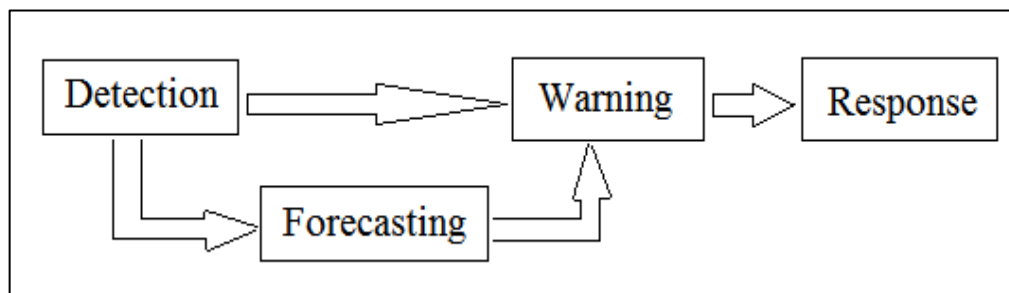


Figure 4.3. *Workflow of flood risk management.*

Hydrometeorological observation (detection) provides the information based on which warning can be issued. The warnings should be sufficiently reliable and be provided in time to allow a proper response by the responsible authorities. By the time, forecasting data can give additional information about the coming event. Responses can be evaluated with respect to the impact on the society. Thus, hydrological forecasting enables early warning. Figure 4.3 shows the workflow of flood risk management that the basic elements are clarified.

Within the scope of this information, one of the initiatives in Europe has been the development of the European Flood Forecasting System (EFFS), based upon WL | Delft Hydraulics' Delft-FEWS flood forecasting platform (Verwey, 2006). Its development took place over the period 2000-2003 with the objective of providing a flood forecasting platform that could be applied at European scale.

Following the completion of the EFFS in 2003, further developments were taken up in the Delft-FEWS flood forecasting platform as part of the assignments given by various forecasting agencies in Europe. Objective of this further investment with first UK Environment Agency (EA) contract was the development of the UK National Flood Forecasting System (NFFS) as a generic open platform for England and Wales. After with getting in contract with various country and communities, the scale of the project was extended and its application areas are now all around the world.

Mainly, the philosophy of the Delft-FEWS is to provide an open shell system for managing the forecasting process and encouraging participations with related topic of hydrometeorological data, meteorological forecasting and simulation models from all over the world (<https://publicwiki.deltares.nl/display/FEWSDOC/Home>). The Delft-FEWS programs abilities could be listed as:

- Handling with wide range of data to import into the system. These data could be in format of ASCII, XML, GRIB, CSV, etc.
- Data validation, serial and spatial interpolation of incoming data
- Data interpolation tools like regression function, Kriging, Thiessen Polygon and Inverse Distance Weighted (IDW)
- Options with gap-filling
- Data transformation to prepare the required inputs for forecasting or simulation module
- Using external hydrological and hydraulic forecasting models (with the capability of highly configurable nature)
- Updating the state of the models by using some embedded modules
- Well-organized visualization interface to create maps, graphs and images of the satellite data
- Dissemination of forecast through maps and HTML-formatted reports that allow broadcasting forecasting results to relevant authorities and public through channels such as intranet and internet (Verwey, 2006).

4.3. Integration of Delft-FEWS and HBV

As it is mentioned in Chapter 4.2, Delft-FEWS is a program that enables to integrate several model upon a platform. Flexibility advantage of FEWS accompanies complexity of integration scripts. For this reason, this part contains several sub-xml folders to describe and assign external files to FEWS.

Real-Time Control Tools (RTC-Tools) program is an open source, modular toolbox dedicated to the simulation of real-time control and decision support of hydraulic structure (https://oss.deltares.nl/documents/102774/467082/rtc-tools_UserManual.pdf). In addition to these features, RTC-Tools enable to build hydrological model. HBV hydrological model is programmed in RTC-Tools with all model equations by C++ Script Language (<https://oss.deltares.nl/web/rtc-tools>). Even executable files in RTC-Tools allow the users to run the model in a folder-based manner; the integration system is needed for long-time forecasting period to work in daily time step. DeltaShell software helps to integrate the external models (RTC-Tools program) into Delft-FEWS platform with its strong and flexible script features (<https://oss.deltares.nl/web/delta-shell>).

After this integration is completed, FEWS needs a general module adaptor tool to communicate data in FEWS and external module. Figure 4.4 shows the workflow of general module adaptor (<https://oss.deltares.nl/web/delft-fews/model-adapters>). According to the figure, stages of this process can be expressed in three steps.

1. Delft-FEWS feeds the external model by supplying data, which could be time series, parameter info or state information, in PI-XML.
2. Then the model runs without any user interaction.
3. The outputs of the model (States, stages, time series data, etc.) are converted back to the Delft-FEWS in a format of PI-XML.

In the first step of this process, FEWS allows manipulating data like interpolation. This interpolation property is used to fill the missing values that are not provided by user. After appropriate data are supplied to model, the outputs can easily be visualized in FEWS.

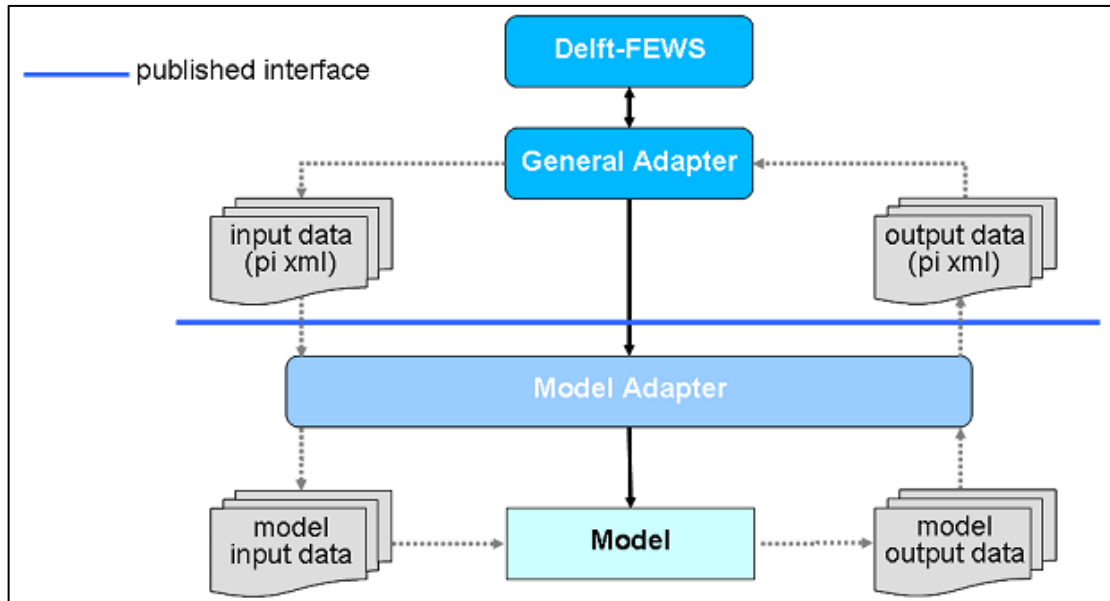


Figure 4.4. Schematic interaction between the General Adapter and an external module in FEWS.

Source: <https://oss.deltares.nl/web/delft-fews/model-adapters>.

4.4. Data Assimilation (DA)

Data Assimilation could be defined in papers and books on several ways. Couple of descriptions may be listed below.

DA is an analysis technique that observed information is gather into the model state by making use of consistency limits by taking into consideration of law of time evolution and physical attributes (Bouttier and Courtier, 1999).

DA is a technique, which enhance forecasting ability of a model. Model background states are blended with observed information in the DA process (Ren et al., 2014).

Therefore, (DA) is a technique that allows combined observation data into a model states to improve initial condition for forecasting period at the beginning of the forecast day.

Over the last couple of decades, improvement of data assimilation techniques expands the application area of DA. Some of them could be listed below.

Hydrology, meteorology and oceanography are the first area of using DA, since; the chaotic dynamics of these areas carry lots of uncertainty by themselves. To overcome

the uncertainties and improving initial condition for forecasting time, DA is a key procedure to concern (Ghil et al., 1991).

Chemical modelling could be challenging to estimating model parameters for a certain process. DA helps to eliminate uncertainty and give a best parameter set for it (<http://www.techbriefs.com/component/content/article/458>).

Space technology is another branch of DA applications. Recent development opens a gate to DA procedure that can be used in estimating climate at another planet for instance Mars (<http://badc.nerc.ac.uk/home/>).

Final area of application of DA is petroleum searches for uncertainty assessment of performance prediction of wells in oil reservoir (Shirangi, 2014). In addition, DA is a critical technique to improve decision parameters for oil recovery (Shirangi and Durlofsky, 2015).

4.4.1. Purpose of Data Assimilation

Even there are plenty of remote sensing observation, their spatial and temporal coverage are not adequate for many applications. Improvements for this area could be significant, but coverage could not be totally coherent for now and future. To overcome this problem, DA is needed to interpolate and extrapolate the data (McLaughlin, 2002).

Remote sensing instruments are capable of observing electromagnetic features of Earth system. This observation technique is limited, because of gathering information from Earth system that is monitored by penetrated electromagnetic radiation at microwave, infrared or visible frequencies. Generally, the thin layer of Earth can be observed because of the instrument properties. However, for accurate initialization, state of deeper mass and heat transfer must be known. DA can distribute remote sensing information to all model variables that are related with the observations.

The temporal and spatial resolution of remote sensing observations could be variable from application to application. For instance, Moderate Resolution Imaging Spectroradiometer (MODIS) has 500 m spatial resolution that is too fine for global climate change applications. On the other hand, Snow Water Equivalent (SSM/I (H13)) product of H-SAF project is produced at a resolution of around 25 km (<http://hsaf.meteoam.it/snow.php?tab=4>). This kind of a resolution is course for regional weather models for applications. DA technique is capable of aggregating and

downscaling the remote sensing observations that is combined with the product of the model.

Over the last couple of decades, availability of remote sensing data increased in terms of numerical weather predictions. Nonetheless, some products of satellite are almost same properties that consist of altitude, sensors, synchronous of satellite. This resemblance does not mean that the value of them is similar, due to the error factor of it. At that point, DA procedure helps to merge potentially redundant or conflicted satellite data and gives a single best estimation.

Geophysical models, whose basic principles are mass, momentum and energy conservation, are ranging from global atmosphere-ocean models to hydrological models. However, unaided remote sensing data are not so constrained. Additional information could arise while model is forced by physical boundaries at data assimilation procedure. These by-products are independent from remote sensing data (Reichle, 2008).

The need for effective data assimilation on hydrologic modelling is becoming important for flood forecasting purpose. DA improves the initial state condition at the beginning of forecasting by taking consideration of observation. The main idea behind is to achieve more consistency between the measurements and corresponding simulated results.

4.4.2. Methods of Data Assimilation

Including ongoing studies, several different kind of DA methods are used in meteorology, oceanography and hydrology. Most DA techniques that are used in hydrology can be classified as sequential DA or variational DA. Sequential technique, which is a general name of the various Kalman Filter, solves the system analytically. Kalman Filter estimates the best fit with including true state and model estimate, and between the true state and the observation. Linear Kalman gain matrix is the key component of equation of the optimal value that is explicitly determined by the measurement uncertainties and the description of model. Since these methods are easy to implement, there are several studies available and they are published in reviews, papers and books. In addition, Kalman Filter has modified versions to improve the solution as Extended Kalman Filter (EKF) and Ensemble Kalman Filter (EnKF). The former aims to solve the optimization problem by linearized equation for the error covariance

propagation. On the other hand, EKF requires a tangent-linear model that helps the system understand inner dynamics of nonlinear hydrologic model. The latter are designed to decrease the number of degrees of freedom to a controllable level. The EnKF is a Monte-Carlo approach with KF that considers an ensemble of model states to obtain the model uncertainties by perturbing the forcing variables. EnKF can handle the nonlinear problems by accounting for a wider range of model errors and relatively flexible for implementation, but computational efficiency depends on the ensemble size.

Variational DA depends on numerical approximation and optimization algorithm, which solve the matrix to find the best or optimal solution by a pre-defined objective function. Variational methods need to use an adjoint model to understand the sensitivity of variable that is used in model equations. Adjoint model could be described briefly as that it is a powerful tool for many studies that require an estimate on the sensitivity of model output with respect to input. Data assimilation, parameter estimation, stability analysis, and synoptic studies are some application fields then after sensitivity of model are produced directly and efficiently (Errico, 1997) Adjoint model links the variables and the output by derivational way of normal simulation. Defining the function of this method is the most challenging part of variational DA.

Variational approach, which is also called as representer-based approach, mainly tries to minimize objective function or cost function. The objective function penalizes the distance between model output and its corresponding observation value. On the contrary to sequential technique, variational technique does not rely on propagating the covariance matrix from one time step to next. The effects of simultaneously updating model states, forcing, and propagating in the model within the assimilation window is implicitly considered by variational approach. Flexibility of method is created with this feature of objective function, which allows using different variables at the same time with a long assimilation period (Seo et al., 2009). The challenging part of variational method can be overcome by an automatic adjoint code generated. With managing challenging part of variational methods by automatic adjoint code generator and its flexibility, this approach is robust and reliable.

The dimensions of variational DA are classified as 1D, 2D, 3D and 4D. With the increasing dimensions, the complexity of the DA structure is getting complicated. 4D-

VAR involves all dimensions with time element, so that it seeks the completely operating window while it runs objective functions.

4.4.3. Moving Horizon Estimation (MHE)

At operational forecasting systems, variational techniques are applied with batch-processing manner over the assimilation time window. Thus, state estimation does not rely on the previous assimilation run for the same window. Moving Horizon Estimation (MHE) can deal with this moving window by taking each windows separately (Rawlings, 2013).

It strictly follows an implementation according to:

$$x^k = f(x^{k-1}, d^k, u^k) \quad (4.17)$$

$$y^k = g(x^k, d^k, v^k) \quad (4.18)$$

where x, y, d are the state, output and external forcing vectors, respectively, u, v are noise terms, $f(), g()$ are functions representing arbitrary linear or nonlinear components of the HBV model and k is the time step index.

Based on equations (4.17)-(4.18) above, Moving Horizon Estimation (MHE) is formulated (Rawlings, 2013) for a forecast time $T_k = 0$ over an assimilation period $k = [-N + 1, 0]$ of $N \geq 1$ time steps by an optimization problem according to:

$$\min_{u,v} J(u, v) = \min_{u,v} \sum_{k=-N+1}^0 w_x \|\hat{x}^k - x^k(u)\| + w_y \|\hat{y}^k - y^k(u, v)\| + w_u \|u^k\| + w_v \|v^k\| \quad (4.19)$$

$$\text{subject to} \quad \begin{aligned} u_L &\leq u^k \leq u_U \\ v_L &\leq v^k \leq v_U \end{aligned} \quad (4.20)$$

where J is the objective function to be minimized, \hat{x}^k, \hat{y}^k are observations of the state and the dependent variable vectors, respectively, $\| \cdot \|$ is a suitable norm penalizing the deviation between observed and simulated quantities and the introduction of noise by the data assimilation procedure, $w_{u,v,x,y}$ are weighting coefficients to define the trade-off between different penalties. More detailed information about the formulation of cost function in MHE can be found in Rawlings (2013). Furthermore, the noise terms are

bounded by inequality constraints. For the sake of simplicity, our formulation considers constant lower and upper bounds only.

The key to the efficient solution of the optimization problems above, in particular in operational applications with runtime restrictions, is the computation of the derivatives of the objective function $dJ(u,v)/d(u,v)$ to enable the application of gradient-based optimizers such as IPOPT (Wächter and Biegler, 2005). Since numerical differentiation is a computational load for larger optimization problems and introduces truncation errors, we rely on adjoint modelling based on algorithmic differentiation in reverse mode (Griewank and Walther, 2008) to trace back first-order derivatives backwards in time through the simulation model.

The main purpose of selecting MHE is to enable a shifting window on data assimilation procedure. This helps to consider that each time step is independent from the next one. Moreover, since MHE is a variational method and using adjoint model, the inner changes directly affects the objective function by adding penalty value. Montero et al. (2016) tested this approach on HBV hydrologic model in forecasting by assimilating several inputs and states. Also, this approach can be compared by other well-known DA techniques like Kalman Filter, in the next phase of the study.

4.5. Ensemble Verification System (EVS)

After getting results from the hydrological model, the testing procedure is the key element to assess the performance of model whether it is consistent with ground observation or not. According to the calibration and validation of model, the forecasting period must be compatible with observation.

Ensemble Verification System (EVS) helps to evaluate systematic forecasting files with an observation file. In this study, EVS version 5.4 was selected to calculate the lead time performance criteria. This version and several different versions of EVS could be downloaded from the <http://amazon.nws.noaa.gov/ohd/evs/evs.html> web site.

EVS's background is written in JAVA code and its interface is shown in Figure 4.5. "ASCII", "XML" and "NetCDF4" are acceptable as input format. In each time step of forecasting period (Figure 4.6), FEWS gives the results of forecast in "XML" file format where date, location and parameter are already written for addressing in EVS (Figure 4.7). Firstly, EVS sorts data before generating the code for performance.

According to data pairs, which are created with matching the forecast and its corresponding observation, EVS calculates the lead time performance.

EVS have several different options to assess the performance tools; notwithstanding, only performance criteria of Root Mean Square Error was selected and used in this study.

Root Mean Square Error, shortly called RMSE, provides the square root of Mean Square Error (MSE), which measures the average square error of the forecasts. It gives the results in same units with measurements, thus comparing the outputs are likely more deductive. The equation is:

$$RMSE = \sqrt{\frac{1}{n} \sum_{k=0}^n [(x_i - y_i)^2]} \quad (4.21)$$

Where RMSE is Root Mean Square Error, n is the number of pairs and x_i and y_i are observation and forecast, respectively.

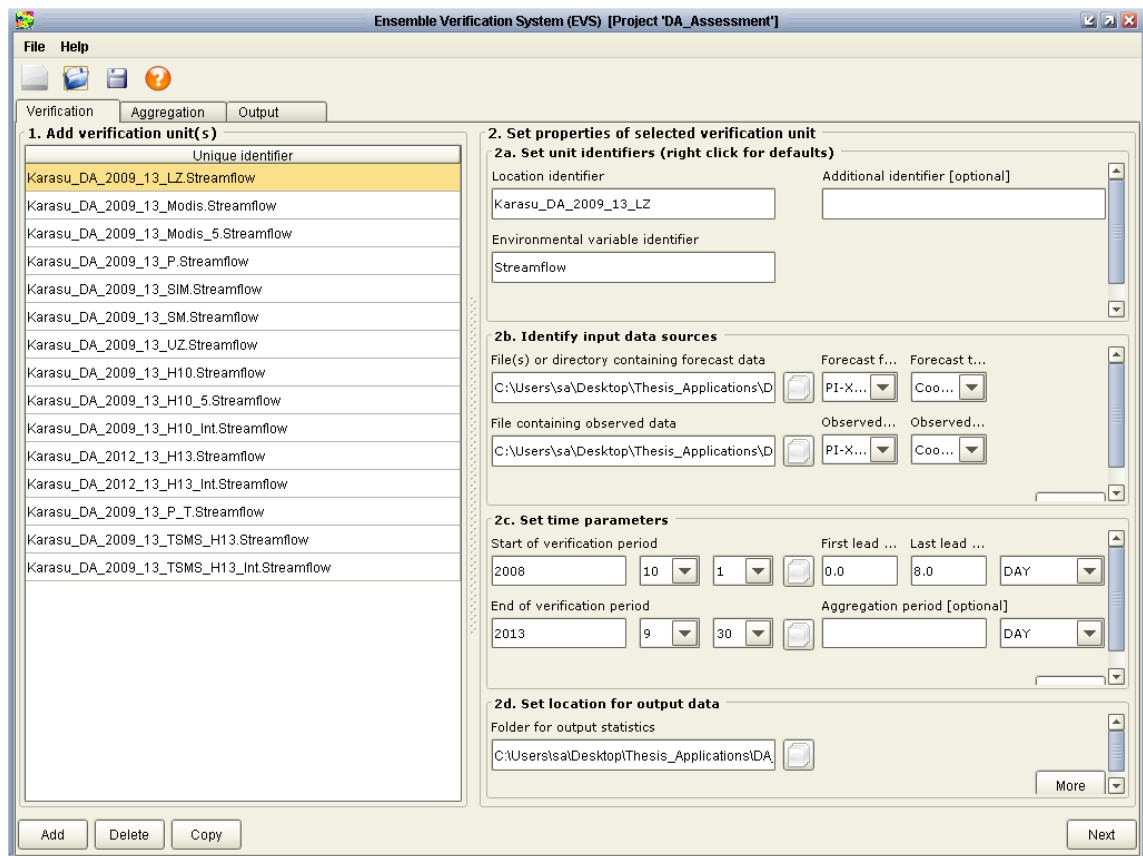


Figure 4.5. Interface of EVS program.

```

<series>
  <header>
    <type>instantaneous</type>
    <locationId>2119</locationId>
    <parameterId>Q.HBV.DA</parameterId>
    <timeStep unit="second" multiplier="86400"/>
    <startDate date="2008-10-01" time="00:00:00"/>
    <endDate date="2008-10-09" time="00:00:00"/>
    <forecastDate date="2008-10-01" time="00:00:00"/>
    <missVal>-999.0</missVal>
    <stationName>Kemah</stationName>
    <units>m3/s</units>
  </header>
  <event date="2008-10-01" time="00:00:00" value="33.05804" flag="0"/>
  <event date="2008-10-02" time="00:00:00" value="32.983837" flag="0"/>
  <event date="2008-10-03" time="00:00:00" value="32.90695" flag="0"/>
  <event date="2008-10-04" time="00:00:00" value="32.837788" flag="0"/>
  <event date="2008-10-05" time="00:00:00" value="32.777557" flag="0"/>
  <event date="2008-10-06" time="00:00:00" value="32.70659" flag="0"/>
  <event date="2008-10-07" time="00:00:00" value="32.629192" flag="0"/>
  <event date="2008-10-08" time="00:00:00" value="32.54979" flag="0"/>
  <event date="2008-10-09" time="00:00:00" value="32.4822" flag="0"/>
</series>

```

Figure 4.6. File format and order as EVS input format.














| Name | Date modified | Type | Size |
|--|-------------------|----------------------|------|
|  2008100100_Karasu_Q_DA.xml | 5/8/2016 11:35 PM | Extensible Markup... | 2 KB |
|  2008100200_Karasu_Q_DA.xml | 5/8/2016 11:35 PM | Extensible Markup... | 2 KB |
|  2008100300_Karasu_Q_DA.xml | 5/8/2016 11:36 PM | Extensible Markup... | 2 KB |
|  2008100400_Karasu_Q_DA.xml | 5/8/2016 11:36 PM | Extensible Markup... | 2 KB |
|  2008100500_Karasu_Q_DA.xml | 5/8/2016 11:36 PM | Extensible Markup... | 2 KB |
|  2008100600_Karasu_Q_DA.xml | 5/8/2016 11:37 PM | Extensible Markup... | 2 KB |
|  2008100700_Karasu_Q_DA.xml | 5/8/2016 11:37 PM | Extensible Markup... | 2 KB |
|  2008100800_Karasu_Q_DA.xml | 5/8/2016 11:37 PM | Extensible Markup... | 2 KB |
|  2008100900_Karasu_Q_DA.xml | 5/8/2016 11:37 PM | Extensible Markup... | 2 KB |
|  2008101000_Karasu_Q_DA.xml | 5/8/2016 11:38 PM | Extensible Markup... | 2 KB |
|  2008101100_Karasu_Q_DA.xml | 5/8/2016 11:38 PM | Extensible Markup... | 2 KB |
|  2008101200_Karasu_Q_DA.xml | 5/8/2016 11:38 PM | Extensible Markup... | 2 KB |
|  2008101300_Karasu_Q_DA.xml | 5/8/2016 11:39 PM | Extensible Markup... | 2 KB |

Figure 4.7. File view for importing values in EVS.

5. DATA ASSIMILATION & MODELLING

5.1. Pre-Processing of Snow Products

Even though the raw data are validated before being used in operational hydrology, pre-processing of satellite products is needed according to the purpose of usage. Pre-processing involves filling missing data, manual elimination of unreliable and/or doubtful data, combining two similar data, etc. In this chapter, several pre-processing techniques applied to raw H10, H13 and MODIS satellite products are explained briefly.

5.1.1. MSG-SEVIRI (H10) snow covered area

H10 is one of the new generation satellite products whose features are introduced in Chapter 3 in detail. Shortly, this product is giving snow covered area with a certain spatial and temporal resolution. H10 products are archived in a database platform at “hsaf.meteoam.it” as a HSAF data feeder. After accessing the platform, downloading option is available to get the data.

The file extension of H10 products is H5, which is a kind of Hierarchical Data Format (HDF). This type of format allows storing and organizing huge amount of data. Then, to convert the format of the data to a FEWS readable format, MATLAB code is generated. This code mainly converts H5 format to ASCII (American Standard Code for Information Interchange).

FEWS has import module to deal with variety of data type. ASCII format import module is one of the easiest and fastest import option in FEWS. Once the configuration of import module is done, FEWS is just transferring the external data into FEWS-database.

A sample of configuration files is illustrated in Figure 5.1 and Figure 5.2. Import module configuration is needed for assigning a folder to make imports. Moreover, it helps to introduce the data type, data format and its related location to the system. Later is the workflow, which is a trigger file to start the import module.

```

<import>
  <general>
    <importType>ArcInfoAsciiGrid</importType>
    <folder>%REGION_HOME%/Import/HSAF/h10</folder>
    <idMapId>ImportHSAF</idMapId>
    <unitConversionsId>ImportUnitConversions</unitConversionsId>
    <importTimeZone>
      <timeZoneOffset>+00:00</timeZoneOffset>
    </importTimeZone>
    <dataFeedId>HSAF</dataFeedId>
  </general>
  <timeSeriesSet>
    <moduleInstancId>ImportHSAF</moduleInstancId>
    <valueType>grid</valueType>
    <parameterId>SCA.H10</parameterId>
    <locationId>HSAF10</locationId>
    <timeSeriesType>external historical</timeSeriesType>
    <timeStep unit="day"/>
    <readWriteMode>add originals</readWriteMode>
    <synchLevel>6</synchLevel>
  </timeSeriesSet>
</import>

```

Figure 5.1. *Import module for H10.*

```

<activity>
  <runIndependent>true</runIndependent>
  <moduleInstancId>ImportHSAF</moduleInstancId>
</activity>

```

Figure 5.2. *Workflow to start H10 import module.*

When FEWS recognizes the H10 data, the rest of the process can be easily done. Initial step is to clip the product with reference to Karasu Basin. The original and clipped images are shown in Figure 5.3a and Figure 5.3b.

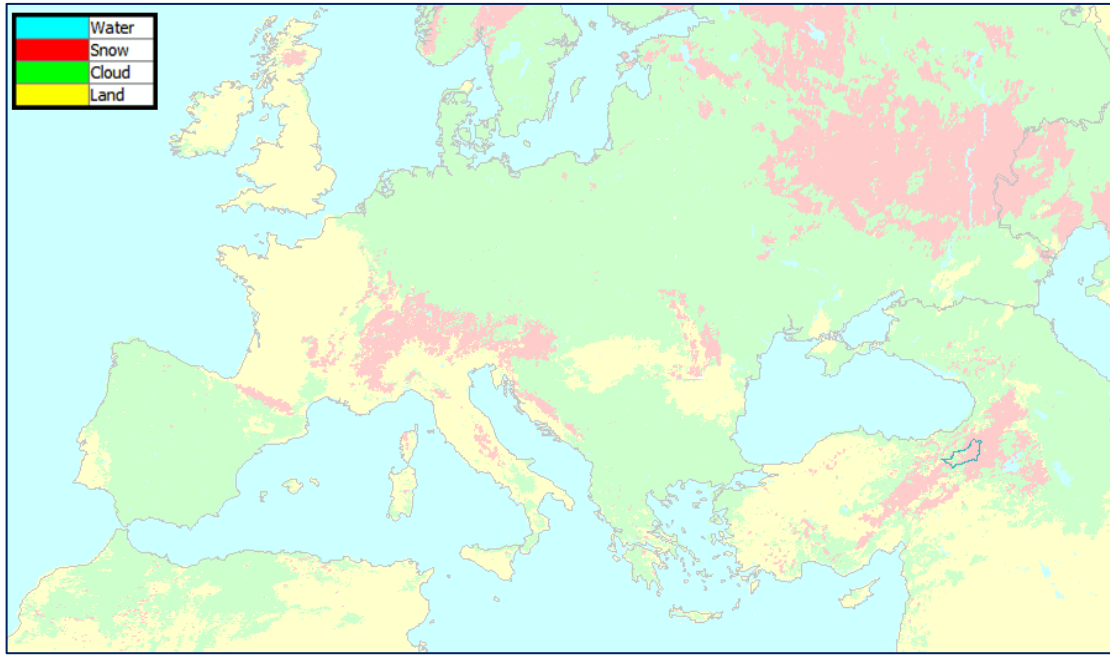


Figure 5.3 (a). *MSG-SEVIRI (H10) original image.*

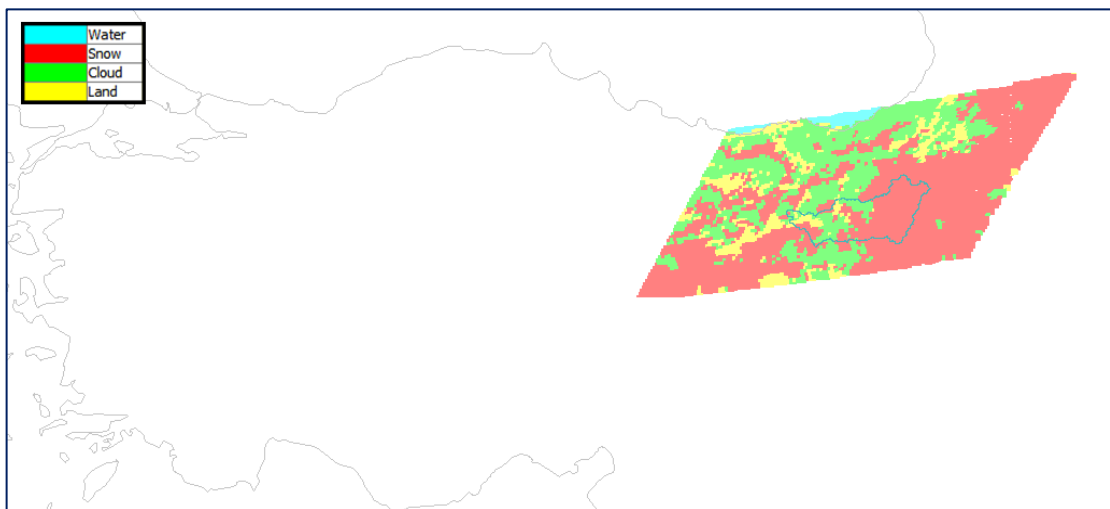


Figure 5.3 (b). *Clipped MSG-SEVIRI (H10) product with reference to Karasu Basin.*

The next step is to get the number of pixels of snow, land and cloud in Karasu Basin for each single day. If twenty-five percentage or more of Karasu Basin is covered by cloud, that day is omitted due to intense cloud coverage. This process is applied for each day and finally, the time-series of H10 product values over the whole catchment are handled. A discrete output time series is obtained due to cloudy days. Therefore, to make the time series in a continuous manner, the interpolation process, which is filling the gaps by linear interpolation, is used and shown in Figure 5.4.

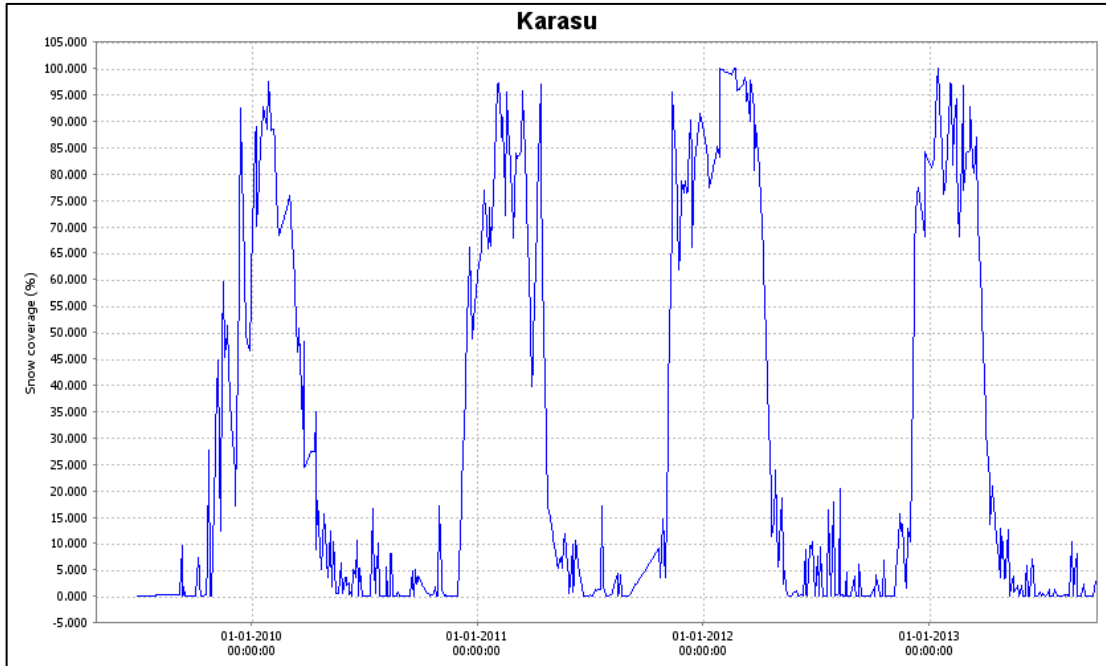


Figure 5.4. SCA values derived from H10.

5.1.2. SSMI/S (H13) snow water equivalent

Some of the steps for processing of H13 (Snow Water Equivalent (SWE) Product) are identical with H10. Data are acquired from “hsaf.meteoam.it”. After downloading the H13 products, they can be directly imported into FEWS. The format is grib2 and FEWS modules are compatible with this format. Therefore, it is simpler than H10 to transfer the data into FEWS and process them.

Processing part is relatively fast because the spatial resolution of H13 data is 25 km * 25 km which is a rather course resolution and easy to manipulate. Therefore, after data are visualized in FEWS they are clipped with regard to Karasu Basin. Then, the result of the process gives a daily time series data that involves average snow water equivalent (SWE) of Karasu Basin.

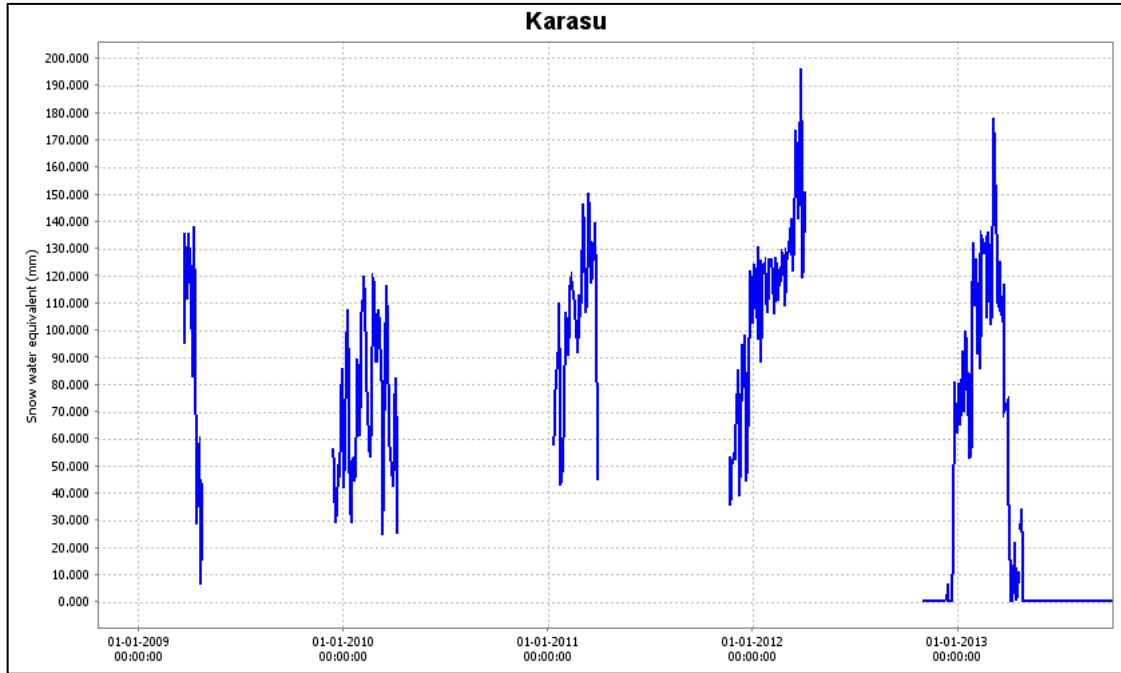


Figure 5.5. SWE values derived from H13.

After clipping the data, according to H13 time series for Karasu Basin, manual filtering process is applied. By this process, the date that contains no data, partial coverage or outlier values have been omitted to clear fluctuations in the time series. By the way, beginning and end of the snow period, H13 products could not clearly observe the SWE because of the shallow and wet snow conditions. Therefore, counting H13 products have to be considered carefully with respect to all these items (Figure 5.5).

5.1.3. MODIS snow covered area

Terra and Aqua daily images, which are handled from optical MODIS satellite, are affected from cloud, so the images do not recognize the land surface that is covered with cloud. In order to use the snow covered area product in hydrologic model applications, the products' cloud coverage must be low enough. Therefore, cloud filtering process on SCA products come into prominence throughout the water year (Yamankurt, 2010).

MODIS satellite data are acquired twice a day, MODIS/Terra in the morning and MODIS/Aqua 3 hours later in the afternoon. Combining Terra and Aqua images is the first step of filtering. This process gives more clear view due to cloud positions are changing in each time step. Then, the temporal filtering is applied to the combined imagery by going back in time of 3 (MODIS CM-3), 5 (MODIS CM-5) and 7 (MODIS

CM-7) days respectively. The cloudy grid cells are exchanged with land or snow if it is different from cloud at previous days. In elevation filter, it is assumed that there is a snow line, which is a threshold for snow and land according to the elevation (MODIS CM-7E). These elevations vary during the season and they are defined by the user. The range between snow and land line is called transition zone where cloudy cells may remain. Spatial filter changes the value of a cloud cell based on the situation of peripheral cells (MODIS CM-7ES). Finally, the seasonal filter clears all the remaining cloud uncertainty assuming the cloudy cells are snow in a snow season and land during the off-season (MODIS CM-7ESA) (Çoskun, 2016). All the process is illustrated as workflow in Figure 5.6.

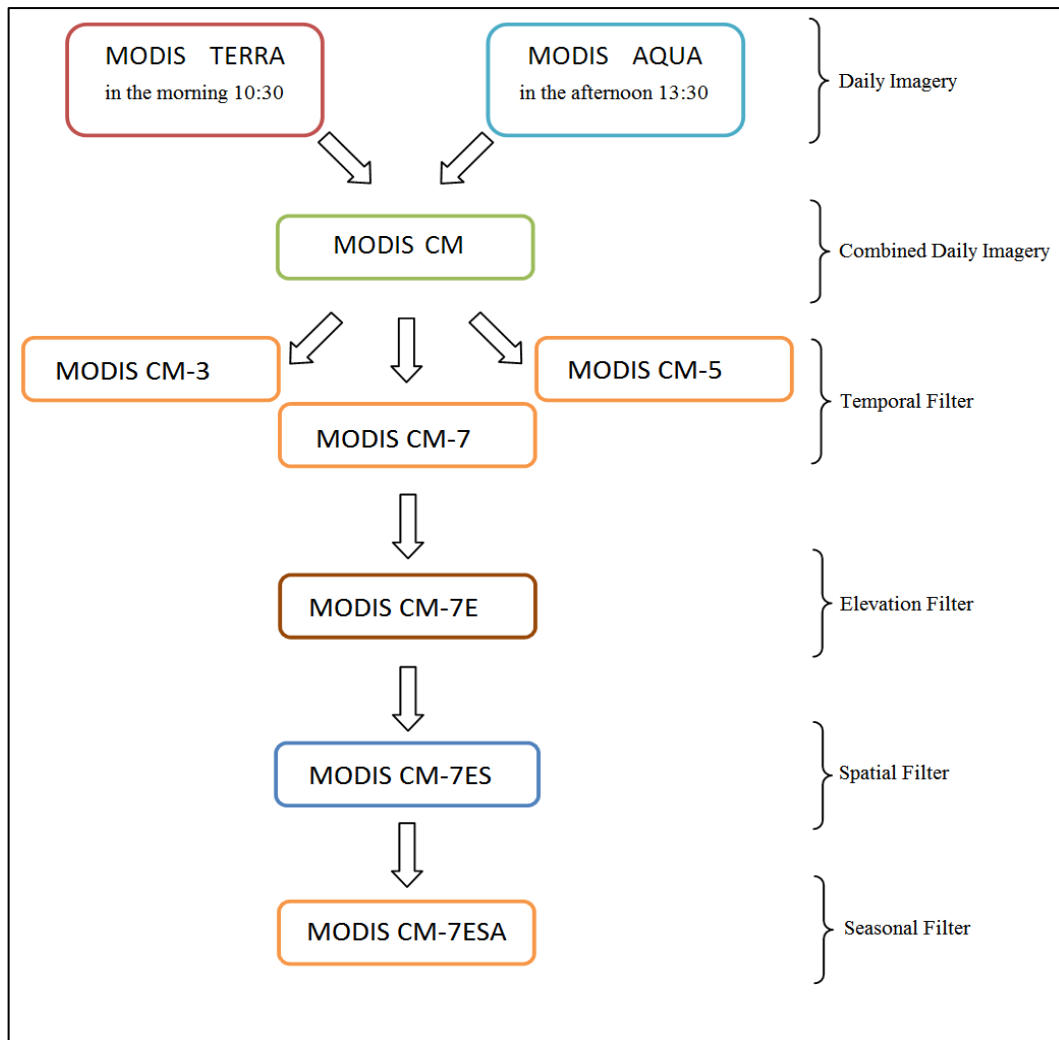


Figure 5.6. Flowchart of filtering daily MODIS data
Source: Çoskun (2016).

5.2. Calibration and Validation of HBV Model in Karasu Basin

Karasu Basin with elevations ranging between 1125 m to 3500 m is divided into ten equal area elevation zones of approximately 1025 km². The main purpose of this division is to model the basin with same areal contribution. To provide daily average temperature and daily total precipitation data into each zone, the output of DK values are used as areal averages.

Since HBV model is a conceptual model, parameter set, which lets to convert hydrological process to mathematical equations, needs to be adjusted. This process called as calibration. Then, another data set is used to make a validation of model parameters.

After the model is completely configured into FEWS, inputs for HBV model is supplied to MATLAB function for calibration. During this calibration process, *fmincon* (Find minimum of constrained nonlinear multivariable function) which is an optimization tool in MATLAB, is used (<http://www.mathworks.com/help/optim/ug/fmincon.html>). The requirements of this process are an integrated model with MATLAB and a proper optimization function for the model. Former requirement, integrated model with MATLAB, is already been solved by RTC-Tools program. On the other hand, later necessity, proper optimization, is selected and adjusted by user with respect to desired parameter to be optimized.

Performance criteria of Bias, Root Mean Square Error (RMSE), Volume Error (VE), correlation coefficient (R²) and Nash Sutcliffe Efficiency (NSE) are selected to evaluate the performance of the model. Formulation of Bias, RMSE, VE, R² and NSE are given in 5.1, 5.2, 5.3, 5.4 and 5.5, respectively. Table 5.1 shows the value range, unit and the assessment of performance indicators.

$$Bias = \sum_{t=1}^T (Q_o - Q_s) \quad (5.1)$$

$$RMSE = \sqrt{\frac{\sum_{t=1}^T (Q_o - Q_s)^2}{T}} \quad (5.2)$$

$$VE = 100 - \frac{\sum_{t=2}^T (Q_s^t + Q_s^{t-1})}{\sum_{t=2}^T (Q_o^t + Q_o^{t-1})} \quad (5.3)$$

$$R^2 = \frac{\sum_{t=1}^T (Q_o - \bar{Q}_o)(Q_s - \bar{Q}_s)}{\sqrt{\sum_{t=1}^T (Q_o - \bar{Q}_o)^2 (Q_s - \bar{Q}_s)^2}} \quad (5.4)$$

$$NSE = 1 - \frac{\sum_{t=1}^T (Q_o^t - Q_m^t)^2}{\sum_{t=1}^T (Q_o^t - \overline{Q_o})^2} \quad (5.5)$$

Table 5.1. Performance indicators and their assessment.

| | Value Range | | Assessment | | Unit |
|----------------------|-------------|-----------|------------|---|---------------------|
| | Minimum | Maximum | Best | Others | |
| BIAS | $-\infty$ | $+\infty$ | 0 | >0, overestimate <0, underestimate | (m ³ /s) |
| RMSE | 0 | $+\infty$ | 0 | | (m ³ /s) |
| VE | $-\infty$ | $+\infty$ | 100 | >100, overestimate <100, underestimate | - |
| R² | -1 | 1 | 1 | =0, not correlated = -1, negative correlated | - |
| NSE | $-\infty$ | 1 | 1 | | - |

The calibration period is selected as 2001-2008 water years. The parameter set is determined by optimization as given in Table 5.2. In addition, time series values of modelled runoff are sketched with respect to the streamflow observations during calibration period in Figure 5.7. Performance criterion of NSE is 0.85 for this period (Table 5.3). The rising and falling limbs of simulated hydrograph are generally coherent with observations during the calibration period. Moreover, the body of the observed hydrograph is comprehended by simulated hydrograph. Underestimation of relatively higher peak flows in years of 2008, 2009 and 2010 slightly reduces the performance of the model during the calibration period.

Table 5.2. Calibrated model parameters of HBV.

| PARAMETERS | VALUES |
|------------|--------|
| ECORR | 1.09 |
| RFCF | 1.1 |
| SFCF | 0.74 |
| TT | 2.255 |
| TTI | 1.47 |
| CFMAX | 1.874 |
| CFR | 0.098 |
| CWH | 0.0065 |
| TM | -0.101 |

| PARAMETERS | VALUES |
|------------|--------|
| BETA | 1.18 |
| CFLUX | 0.3 |
| ETF | 0.025 |
| FC | 131 |
| LP | 0.477 |
| ALPHA | 0.0367 |
| K | 0.0434 |
| K1 | 0.0024 |
| PERC | 1.125 |
| LIC | 0.379 |

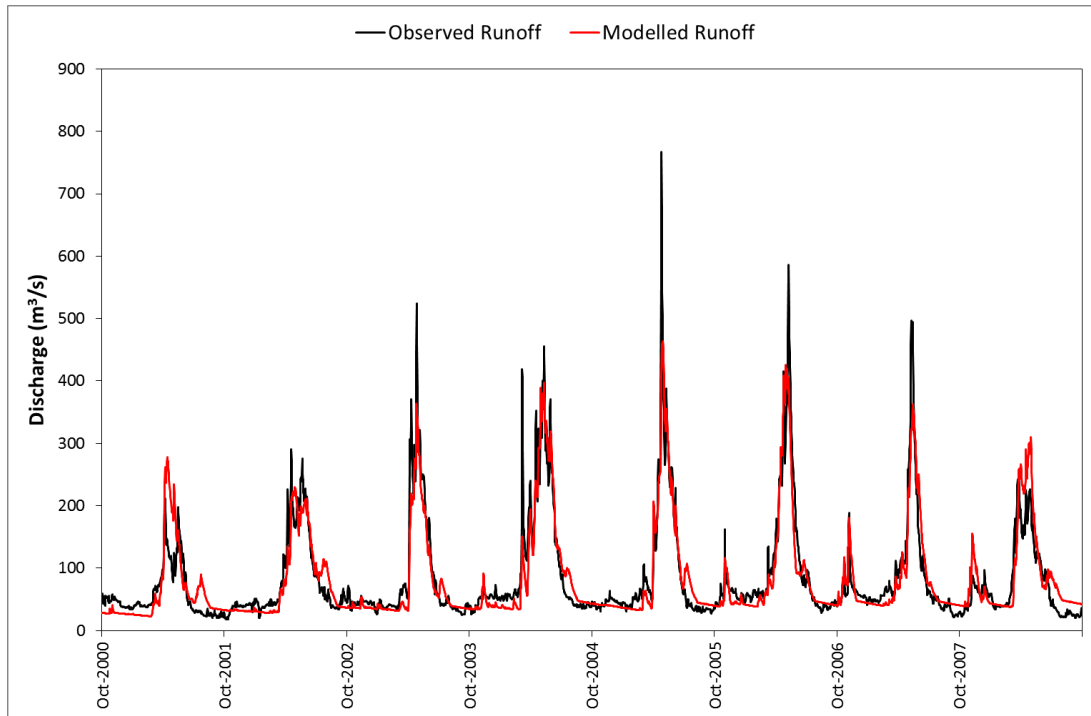


Figure 5.7. Observed and modelled runoff of Karasu Basin, calibration period.

Table 5.3. Performance statistics for the calibration period.

| KARASU-HBV | Calibration | | | | |
|------------|-----------------------------|-----------------------------|-----------|-----------------------|------------|
| | BIAS (m ³ /s) | RMSE (m ³ /s) | VE (%) | R ² (-) | NSE (-) |
| 2001-2008 | -1.45 | 32.46 | 98.29 | 0.85 | 0.85 |

Validation period is selected as 2009-2013 water years. Figure 5.8 shows the comparison of observed streamflow versus validated streamflows. NSE performance is 0.74 during the validation period, which is slightly lower than that of calibration period (Table 5.4). Even though relatively lower peak flows are observed during this period, the simulated hydrograph are not consistent with the streamflow observation in water years 2011-2013. VE performance of 86.85% shows underestimation in the model results due to the poor performance in recession part.

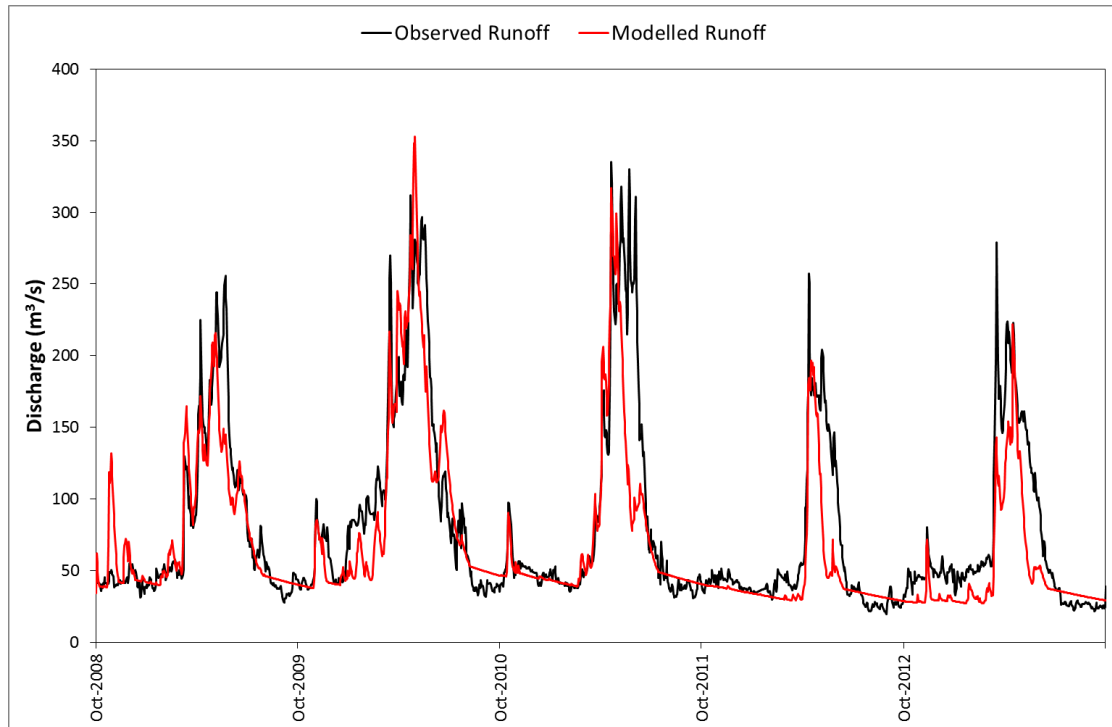


Figure 5.8. Observed and modelled runoff of Karasu Basin, validation period.

Table 5.4. Performance statistics for the validation period.

| KARASU-HBV | Validation | | | | |
|------------|------------------------------------|------------------------------------|------------------|-----------------------------|-------------------|
| 2009-2013 | BIAS (m ³ /s) | RMSE (m ³ /s) | VE (%) | R² (-) | NSE (-) |
| | -10.45 | 33.76 | 86.85 | 0.75 | 0.72 |

5.3. Data Assimilation Configuration

After the calibration and validation of the HBV hydrological model, the next step is DA application using both FEWS and RTC-Tools programs. Objective function and its corresponding forcing variables are changed for each different combination of DA process.

Understanding the objective function term is a key element in order to evaluate the results for this study. Thus, Table 5.5 shows each model inputs, states and outputs of HBV model contribution to the objective function.

Table 5.5. Terms in the objective function.

| Type | Variable | Objective Function Term | |
|---------------|-----------------------------|---------------------------------------|--|
| | | Noise | Observation |
| Model Inputs | Precipitation (P) | $w_p (P^k (1 - P_f^k))^2$ | |
| | Temperature (T) | $w_T (T^k - T_{up}^k)^2$ | |
| Model States | Soil Moisture (SM) | $w_{SM} (S_{SM}^k - S_{SM_{up}}^k)^2$ | |
| | Upper Zone Storage (UZ) | $w_{UZ} (S_{UZ}^k - S_{UZ_{up}}^k)^2$ | |
| | Lower Zone Storage (LZ) | $w_{LZ} (S_{LZ}^k - S_{LZ_{up}}^k)^2$ | |
| Model Outputs | Snow Water Equivalent (SWE) | | $w_{\Delta SWE} (\hat{S}_{SWE}^k - S_{SWE}^k)^2$ |
| | Snow Cover Area (SCA) | | $w_{\Delta SCA} (\hat{S}_{SCA}^k - S_{SCA}^k)^2$ |
| | Streamflow (Q) | | $w_{\Delta Q} (\hat{Q}^k - Q^k)^2$ |

In Table 5.5, “w” expresses the weighting factors, “k” is the time step, the values with “^” symbol represent observations whether ground or satellite, “Δ” indicates the difference between observation and simulated variable, P_f is precipitation factor, which gets in the equation as multiplier, deviations after changing the value to improve forecast (updating) are represented as T_{up} , SM_{up} , UZ_{up} and LZ_{up} which are temperature and model states of soil moisture, upper zone and lower zone respectively. As it is mentioned in Chapter 4.1.1, “u” and “v” variables, which are control variables for optimization, in equation 4.19 – 4.20 are substituted for noise factors of $P_f, T_{up}, SM_{up}, UZ_{up}$ and LZ_{up} .

In this study, temperature and precipitation, as model input, and soil moisture, upper zone and lower zone, as model states, are updated one by one or with combination to get a better agreement between observed and simulated streamflow, SCA and SWE. At this point, weighting factors are significant to determine which agreement is more vital for the user. This means that if the observation is reliable then the weighting factor could be higher which gives more penalty than the others do in an objective function.

In Table 5.5, SCA and SWE are displayed as an output of HBV model, not a model state. This is because these variables rely on model states indirectly. Namely, SWE

is sum of model states of Snow Pack (SP) and Water Holding Capacity (WHC) and SCA linearly related with SWE by using a transformation of lookup table inside the HBV model.

5.4. Number of Iteration in DA Procedure

Data assimilation procedure is one of the modules in RTC-Tools program. It has several options to be set by user even they can directly be taken as default values. Some of these options have significant impact on getting the optimal solution in DA procedure. In this section, the iteration number of DA is discussed.

The optimal solution is considered as the solution giving best results in a fast and reliable way. This test is run in the computer applying DA procedure, so the speed and corresponding time value could be change with properties of the computer. The role of the number of iteration to determine the optimal solution is tested by considering precipitation since precipitation is one of the major input variables in any hydrological modelling. To change the precipitation in each time step during DA, a multiplier in between 0.7 and 1.3 is used to minimize the penalty function according to the discharge agreement.

2015 water year is selected for this case study to determine optimum number of iterations. Four different iteration numbers have been assigned in RTC-Tools, which are 200, 400, 600 and 800. Performance criteria are defined as the speed and penalty function rate (robustness). The penalty function is shown in Equation 5.6. According to Equation 5.6 the unit of the penalty function is $(\text{m}^3/\text{s})^2$.

$$J = \min \sum_{k=-N+1}^0 w_{\Delta Q} (\hat{Q}^k - Q^k)^2 \quad (5.6)$$

According to Table 5.6, first elimination can be made with respect to the speed for each number of iteration. Therefore, iteration number of 800 is omitted since the objective function rate is almost same with 600 where the difference in speed is 20 second. The same reason can be used to omit 600 while comparing it to the 400. While the penalty values are almost close to each other, the speed is 50 percent more than 400.

Table 5.6. Number of iterations and their properties.

| Iteration Number | Penalty | Speed (millisecond) |
|------------------|----------|---------------------|
| 200 | 120436.1 | 20060.00 |
| 400 | 115840.4 | 39520.00 |
| 600 | 113795.5 | 57665.00 |
| 800 | 113769.2 | 73705.00 |

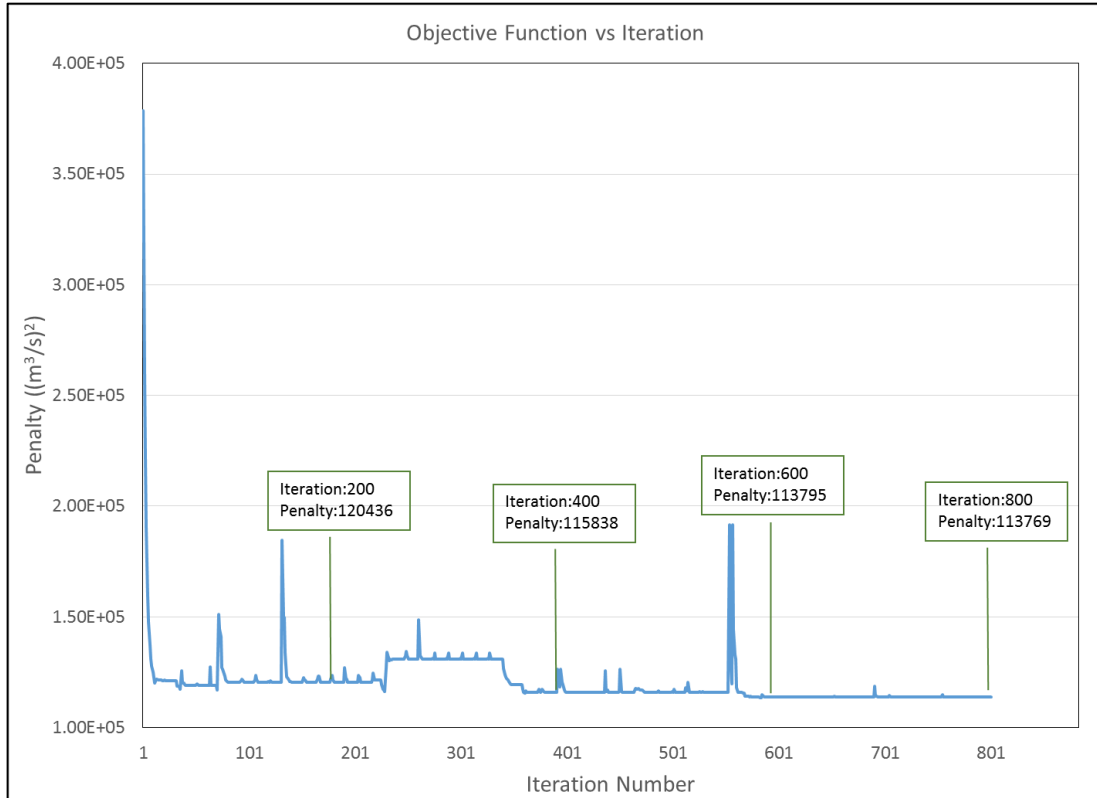


Figure 5.9. Objective function value versus iteration number.

The rest 200 and 400 number of iteration can be compared according to the Figure 5.9. After the DA procedure finding the result in 200th step, it tries to find more optimal solution with searching the whole period. After fitting in body of simulated discharge to streamflow observation by changing the precipitation, DA procedure makes some minor changes to get the best solution from DA. To make sure to select the number of iteration as 400, observation versus assimilation results are evaluated and it is observed that 400th step gives better results than 200th step for the peak and the recession part of the streamflow observation. Therefore, 400th iteration is selected for the rest of the study in terms of penalty value and in return for its computational speed.

5.5. Results and Assessments

According to the model structure, the results of the DA procedure are displayed, explained and interpreted in this section. To improve the streamflow forecasting, the model states, model inputs and external snow covered area and snow water equivalent data are used in DA procedure. In the first DA experiment mainly model states are evaluated, on the other hand, in the second DA experiment impact of satellite snow products (H10, MODIS and H13) are assessed both in terms of observed streamflow, SCA and SWE.

In this part of the study, not only DA application is categorized into two groups according to their data type, but also these two groups are divided into several sub-groups in itself. Since there are several common criteria in these model applications, they are described first.

In each of the DA experiment, an objective function is used to minimize the penalty of discharge. Namely, consistency in observed and simulated discharge is the main goal to get a better agreement. The lead time interval is selected as nine days considering a short and medium range forecasting. The DA application period is selected as the same with the validation period between the water years of 2009-2013. The assessment is based on this period and graphs of lead time performances comprise the dates specified.

Optimization variables and bound constraints are used to update the model by forcing precipitation, temperature as HBV model input and soil moisture, upper zone and lower zone as HBV model states. Table 5.7 shows the optimization variables with their corresponding range of constraints.

As it is mentioned earlier, precipitation factor contributes the updating procedure as a multiplier whereas all the other optimization variables are included as plus/minus addition.

Table 5.7. Optimization variables with their bound constraints.

| Optimization Variable | Bound Constraints |
|-----------------------|---|
| Precipitation Factor | $0.7 \leq P_f^k \leq 1.3$ |
| Temperature | $-2.0 \text{ }^\circ\text{C} \leq T_{up}^k \leq 2.0 \text{ }^\circ\text{C}$ |
| Soil Moisture Update | $-5.0 \text{ mm} \leq SM_{up}^k \leq 5.0 \text{ mm}$ |
| Upper Zone Update | $-5.0 \text{ mm} \leq UZ_{up}^k \leq 5.0 \text{ mm}$ |
| Lower Zone Update | $-5.0 \text{ mm} \leq LZ_{up}^k \leq 5.0 \text{ mm}$ |

5.5.1. First experiment

The first experiment in DA application includes model inputs and model states with a certain bound constraints (Table 5.7) by trying to get a better agreement on only discharge time series. Thus, all the optimization variables are allowed to be changed by the optimizer with a given range one by one, except “P_T” trial. P_T trial is created to optimize two variables, precipitation factor and temperature at the same time. The reason is that, Karasu River runoff is dominated by snowmelt runoff, which is strongly affected by both precipitation and temperature during the melting period. Even if temperature trial can be used in DA solely, it can only affect the model when the model starts to fill in and out the snowpack box. However, it would not increase or decrease the total volume of mass without a change in precipitation.

The lead time performance of DA application for model states and model inputs are illustrated with a performance indicator of RMSE in Figure 5.10. According to the figure, HBV model state of Upper Zone (UZ) causes a significant improvement in model performance with DA rather than the other input or state variables. This is because; state of UZ directly controls the quick flow in HBV. In this circumstance, the initial state of forecasting period is getting closer to observed discharge.

In addition, Lower Zone (LZ) has a good contribution to improve the results. The task for LZ box in HBV is related with low flows in simulation. Hereby, while the initial condition of forecasting is improved by LZ, it gives a better result in low flows.

Soil Moisture (SM), being another DA state, improves forecasting, but not as much as UZ and LZ. The reason is that, SM is indirectly linked with outflow in HBV. Hence it controls the soil box and the changes in SM responds slowly.

When the precipitation (P) and precipitation-temperature (P_T) trials are considered, P_T give reasonably higher performance than P. As it is mentioned before, temperature input has an important effect on snow in snow-accumulation and snow-depletion periods. Even if the changes in temperature are very small, it directly affects the amount of precipitation as rain or snow at that time. In addition, updating precipitation input has a benefit to catch the observed streamflow since the observed precipitation could be underestimated due to measurement errors. Hence, contribution of precipitation in DA as multiplier gives an extra benefit while a more precise initial condition is created.

All the DA applications showed that when the lead time increases the agreement between observation and modeled streamflow is diverging day by day. This is an expected result, due to the increased uncertainties in both model structure and model inputs.

Figure 5.11 displays the first lead time forecast results of updated states and inputs of HBV model in 2011 water year in Karasu Basin. This graph gives an idea on which updated states or inputs exposed the forecasting at which direction. It is clear that, all of the updated model states and model inputs are better than the simulation. Updating UZ provides more improvement on forecasting than the others. This is because; UZ can directly control the quick flow, which is effective on the high flow period of hydrograph. Furthermore, updating P_T gives a reasonable result according to the other component of experiments. This indicates that true water volume balance with the form of snow and/or rain improves the results positively.

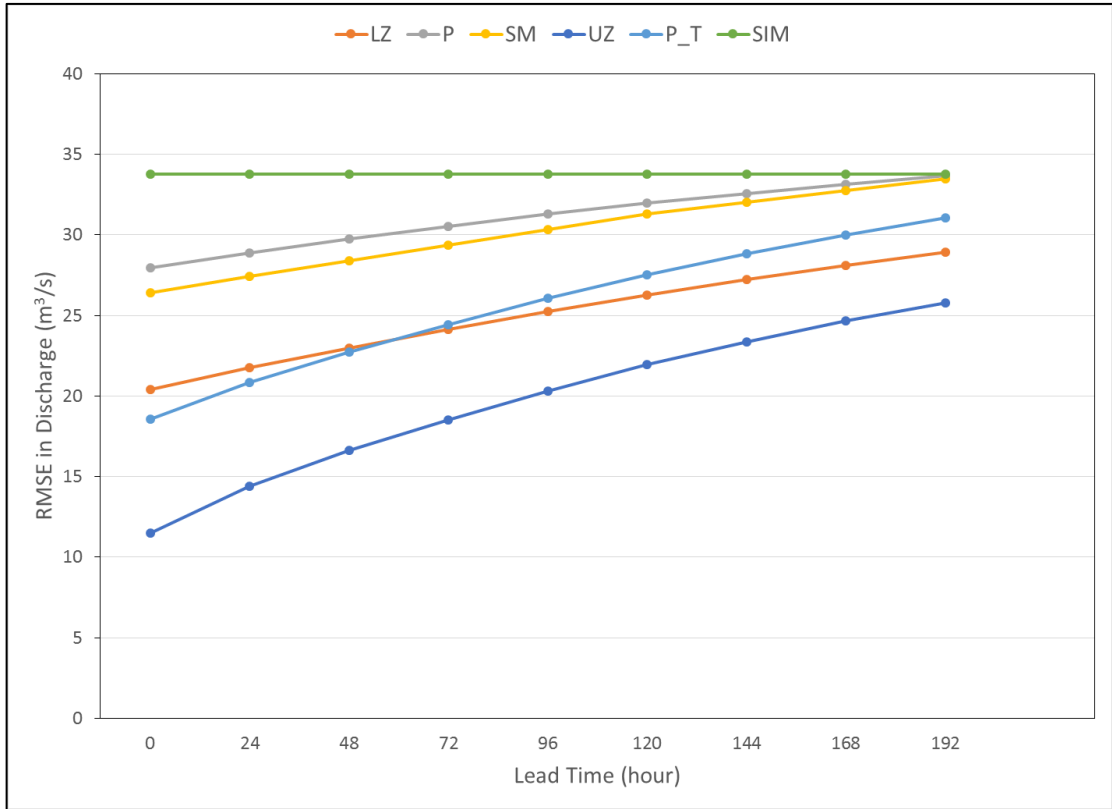


Figure 5.10. Lead time performance of DA on discharge using state variables.

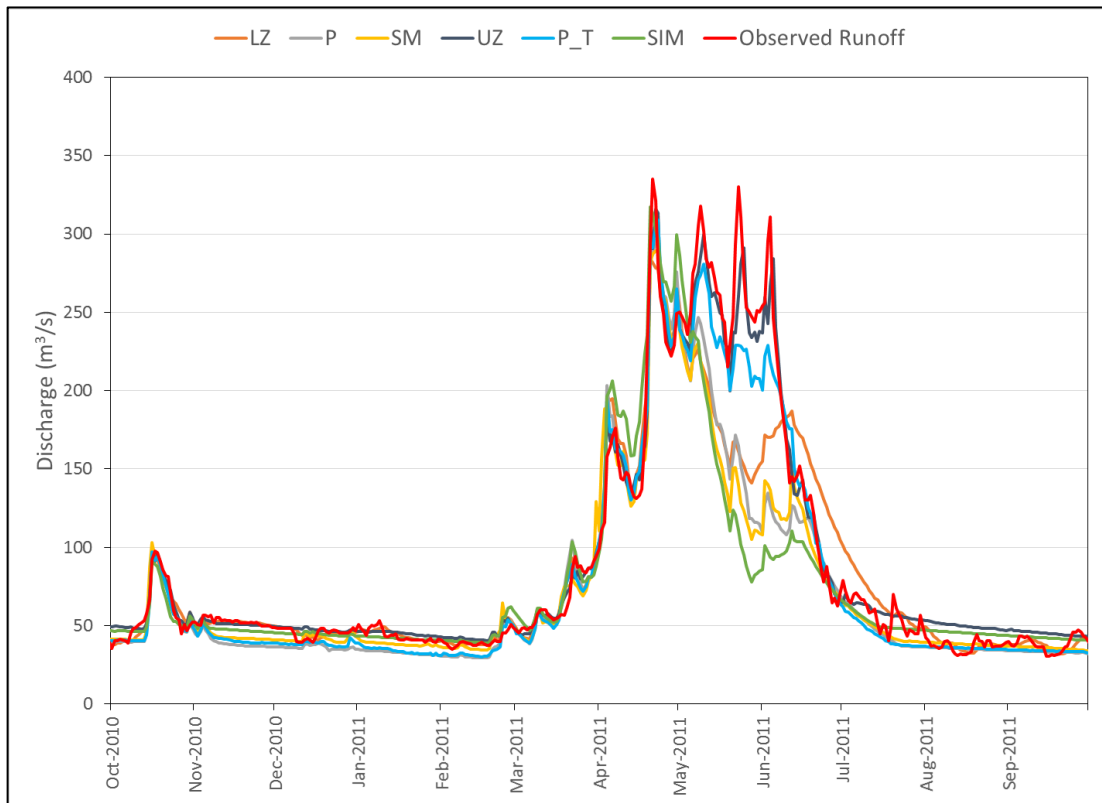


Figure 5.11. First lead time runoff values using DA, 2011 water year.

5.5.2. Second experiment

This test mainly focused on how the observed satellite snow products, which are H10, MODIS and H13, act on DA to improve the simulated discharge and corresponding internal variables. Since these snow data are not an input or states of HBV model, it is not possible to change SCA or SWE directly in the model. Therefore, these products would be a term in the objective function consisting of discharge, SCA and/or SWE. While objective function is searching the optimal solution, the optimization variables are selected as both precipitation factor and temperature. The reason for this decision is that SCA and SWE is linked with precipitation and temperature indirectly, so if one of them is chosen, even if the results are getting better, in terms of discharge agreement this would not mean that it would make the forecast better in sense of internal variables SCA and SWE.

The following two experiments are related with H10 and MODIS as Snow Covered Area and SWE as Snow Water Equivalent.

5.5.2.1. DA application including SCA (H10 and MODIS)

In this part of the study, the objective function was extended with observed SCA by comparing them with simulated SCA. Thus, the new objective function would become as Equation 5.7 and Equation 5.8, for MODIS and H10 respectively.

$$J = w_p \left(P^k (1 - P_f^k) \right)^2 + w_T (T^k - T_{up}^k)^2 + w_{\Delta MODIS} (\hat{S}_{MODIS}^k - S_{MODIS}^k)^2 + w_{\Delta Q} (\hat{Q}^k - Q^k)^2 \dots \quad (5.7)$$

$$J = w_p \left(P^k (1 - P_f^k) \right)^2 + w_T (T^k - T_{up}^k)^2 + w_{\Delta H10} (\hat{S}_{H10}^k - S_{MODIS}^k)^2 + w_{\Delta Q} (\hat{Q}^k - Q^k)^2 \quad (5.8)$$

MODIS snow product data are used after the cloud filtering process. In the first trials, different weighting factors ($w_{\Delta MODIS}$) are given to SCA in DA applications. The agreement in both the observed and modelled discharge and SCA is evaluated in the performance analysis concerning root mean square error (RMSE) (Figure 5.12 and Figure 5.13). The performance of weighting factor is opposite to each other in consistency of discharge and SCA, since an improvement in one of them causes a trade off in the other one. Taking discharge as the basis, the weighting factor of “1” is selected.

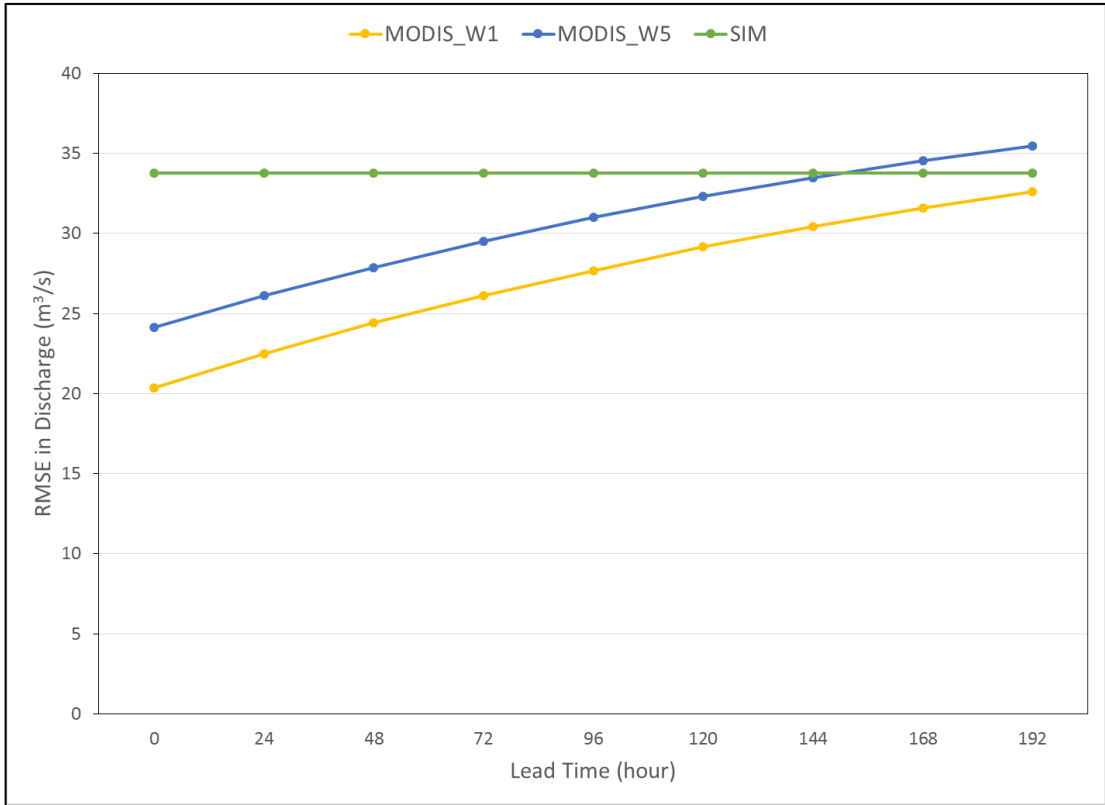


Figure 5.12. Lead time performance of DA on discharge using MODIS.

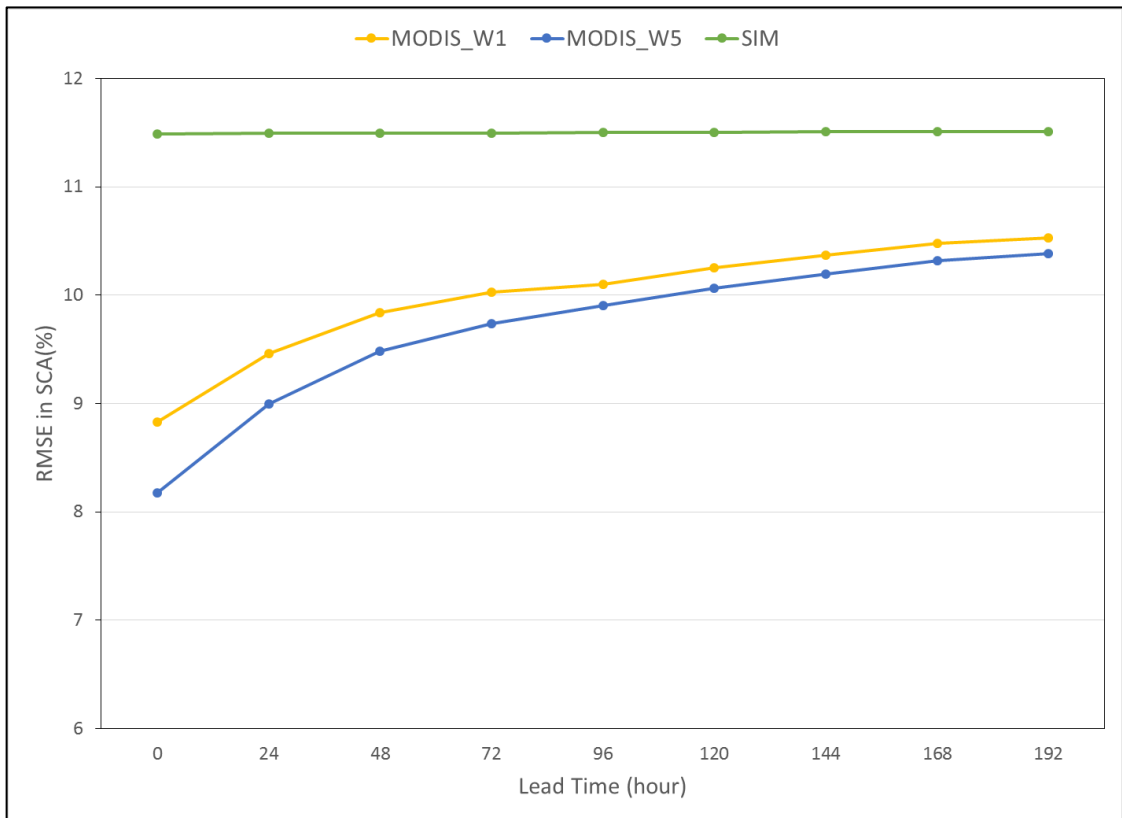


Figure 5.13. Lead time performance of DA on SCA using MODIS.

H10 snow product is assessed with two different options in this process. First, a discrete time series data is used by eliminating images having a cloud cover higher than 25%. Second, a continuous time series dataset is produced by interpolation. The discrete dataset is processed by using the transformation of interpolation. The interpolation is based on linear integration and weighting factor is applied on interpolated time series as one (W1). Figure 5.14 shows the results of these options in terms of both runoff and SCA. Besides, Figure 5.15 demonstrates the changes in SCA for the whole application period. The results in Figure 5.15 are evaluated by comparing the assimilated SCA with observed SCA of MODIS since its high accuracy rate is proven (Çoşkun, 2016).

According to the results that are illustrated in Figure 5.14 and Figure 5.15, H10_Int is selected to be used in the analysis. This is because, while the discharge output is almost the same, H10_Int gives a better result in terms of SCA agreement. In addition, H10_Int has a continuous dataset so there is a flexibility to compare results with MODIS products.

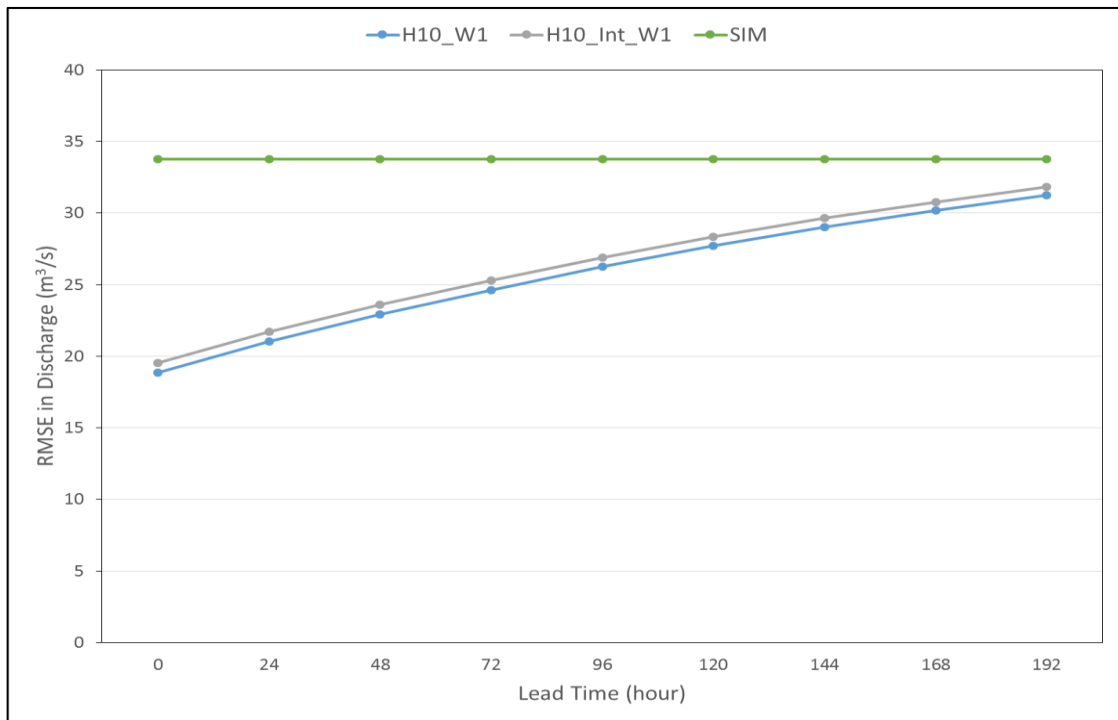


Figure 5.14. Lead time performance of DA on discharge using H10.

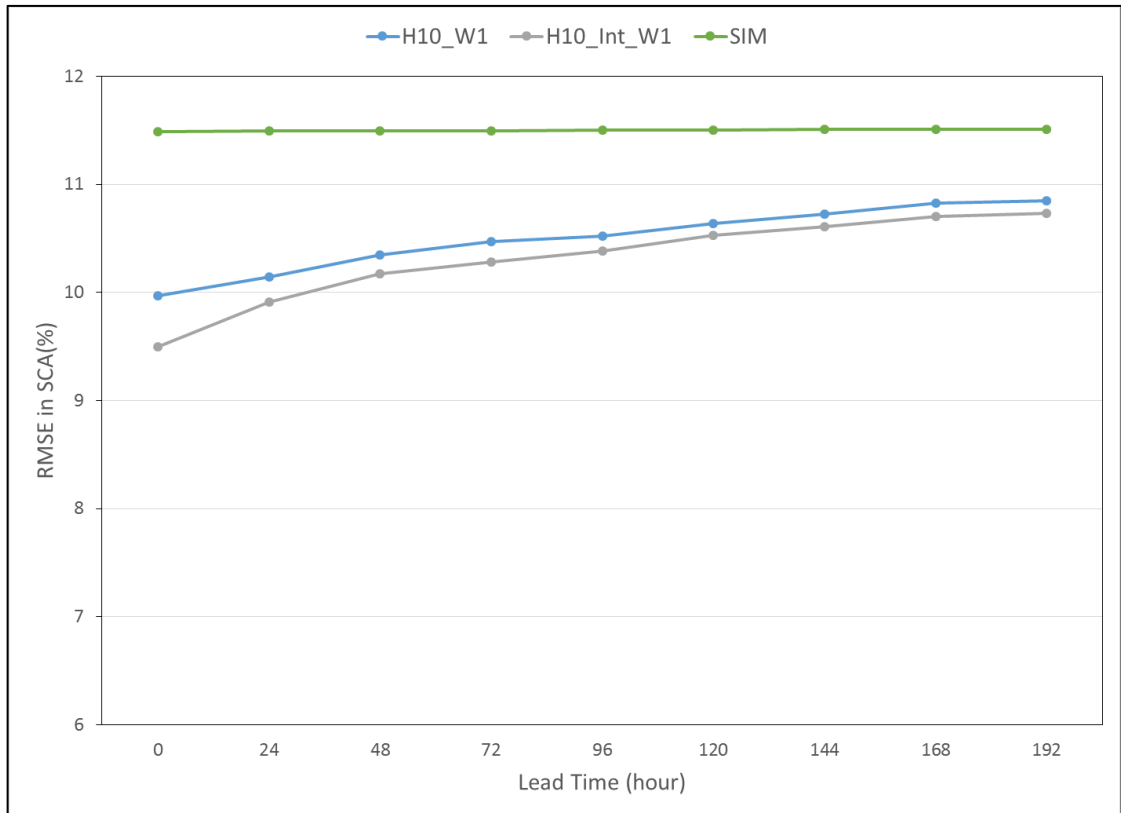


Figure 5.15. Lead time performance of DA on SCA using H10.

DA results with MODIS, H10_Int and P_T are illustrated in Figure 5.16 and Figure 5.17, together. As it is clear from graphs, all of them give relatively similar results on increasing error with the lead time. When MODIS and H10_Int are compared with P_T, DA with H10_Int provides slightly better results in sense of both observed discharge and snow covered area (Figure 5.16 and Figure 5.17). Table 5.8 and Table 5.9 indicate that H10_Int improves runoff forecasting by decreasing RMSE from 33.75 m³/s to 18.83 m³/s and SCA forecasting by decreasing RMSE from 11.49% to 9.5 % according to the first lead time. Even though P_T improves the runoff forecasting better than the others do since the variables directly affect the mass balance and states of the model, its performance is not good as the others in SCA forecasting. In addition, it is physically more meaningful to add independent observation of snow with satellites in the objective function through DA than perturbation of precipitation and temperature alone.

In addition, the time-series discharge forecasting with first lead-time value is sketched with streamflow observations (Figure 5.18). It could obviously be seen that all selected DA applications improve the runoff forecasting compared to simulation at low

and high flows in the whole period. Model performance is increasing at the recession period that starts from mid of May and extends until the end of June.

Figure 5.19 shows observed and modelled SCA as a result of DA application with MODIS, H10 and P_T for 2011 water year.

Table 5.8. RMSE according to discharge for forecasting period.

| RMSE in discharge (m ³ /s) for the 1 st lead time | | | |
|---|-------|---------|-------|
| P_T | MODIS | H10_Int | SIM |
| 18.58 | 20.34 | 18.83 | 33.75 |

Table 5.9. RMSE according to SCA for forecasting period.

| RMSE in SCA (%) for the 1 st lead time | | | |
|---|-------|---------|-------|
| P_T | MODIS | H10_Int | SIM |
| 10.67 | 8.83 | 9.50 | 11.49 |

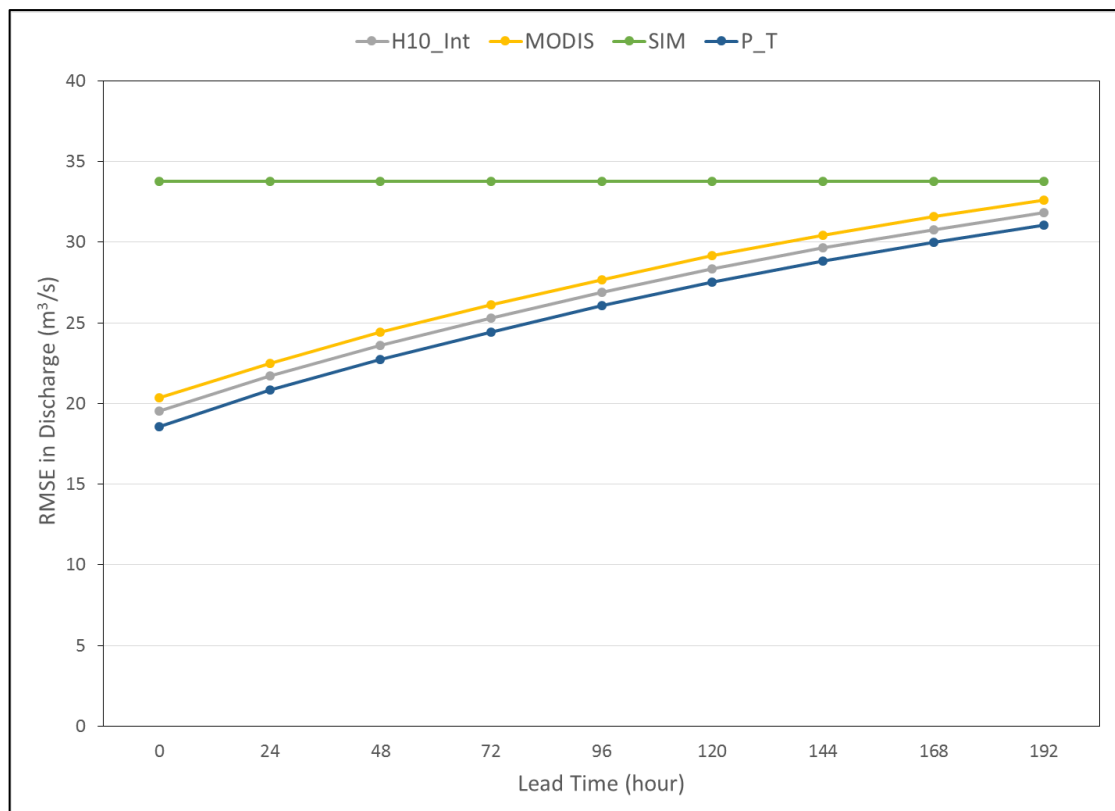


Figure 5.16. Lead time performance of DA on discharge using snow products and P_T.

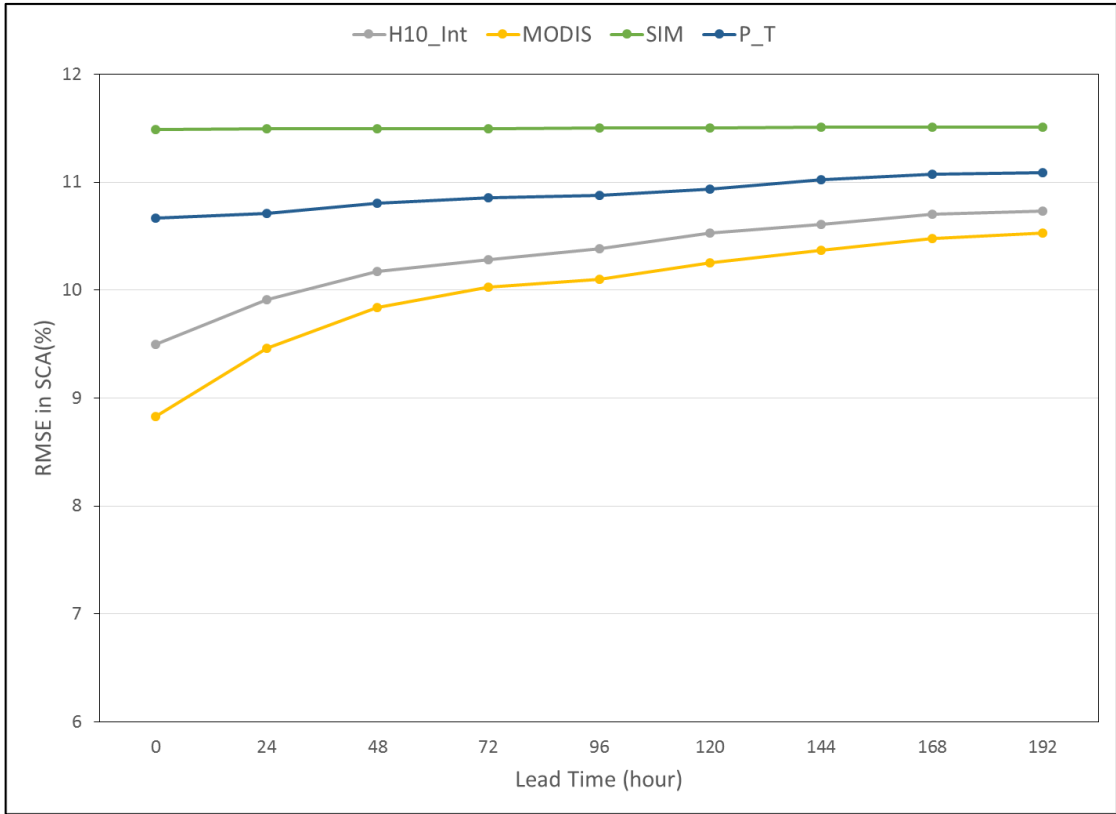


Figure 5.17. Lead time performance of DA on SCA using snow products and P_T.

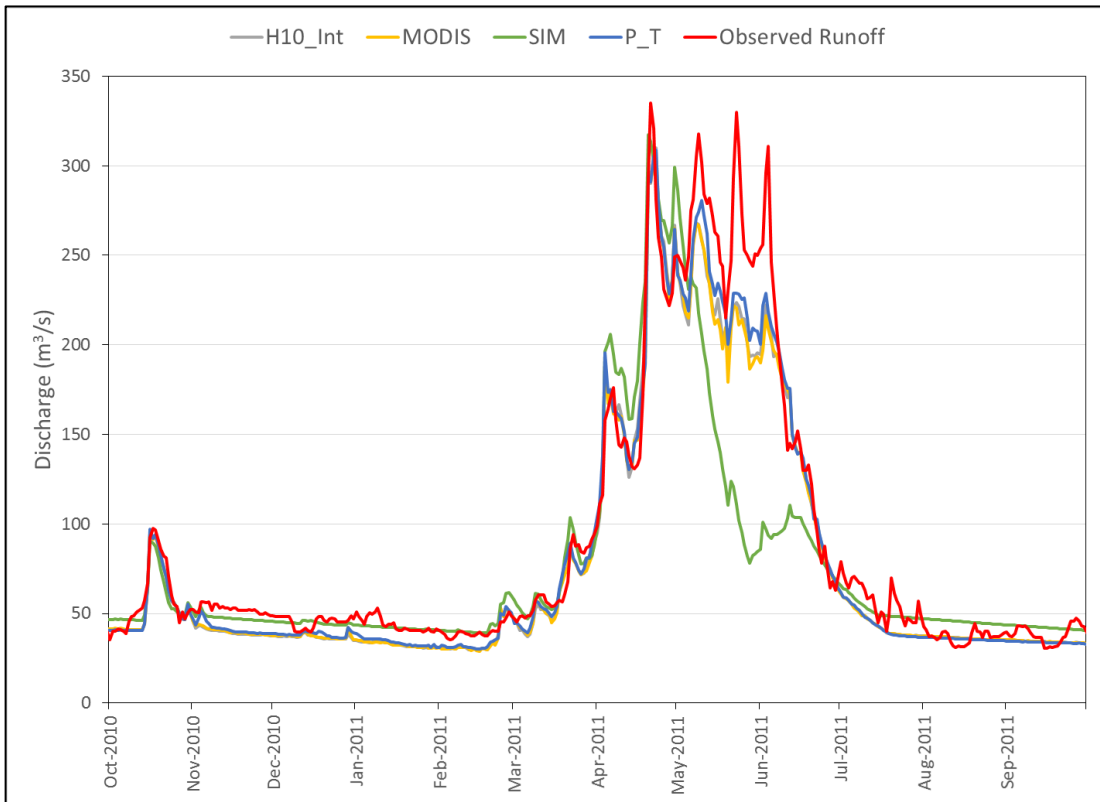


Figure 5.18. First lead time runoff values using DA based on SCA, 2011 water year.

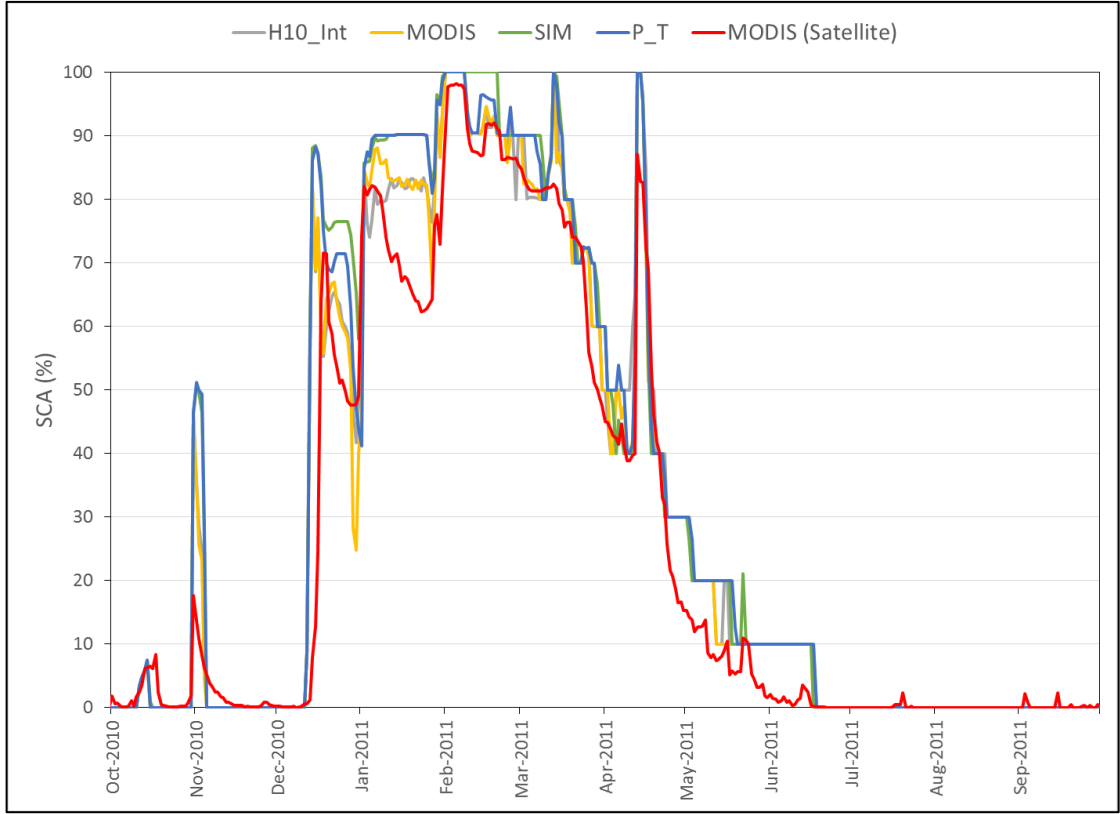


Figure 5.19. First lead time SCA values using DA based on SCA, 2011 water year.

5.5.2.2 DA application including SWE

Snow Water Equivalent (SWE) is an important variable in snow modelling studies and also it is one of the HBV model output which is a summation of snow pack (SP) and water content (WC). Therefore, it is allowed to perform DA procedure on this variable. The objective function to include SWE observation into DA could be written as Equation 5.9.

$$J = w_p \left(P^k (1 - P_f^k) \right)^2 + w_T \left(T^k - T_{up}^k \right)^2 + w_{\Delta SWE} \left(\hat{S}_{SWE}^k - S_{H13}^k \right)^2 + w_{\Delta Q} \left(\hat{Q}^k - Q^k \right)^2 \quad (5.9)$$

When Equation 5.9 is taken into account, depending on observed and simulated SWE and discharge, DA procedure would be run by using precipitation and temperature as optimization variables.

After pre-processing of H13 products, it is seen that a number of data is missing due to the physical limitations explained in section 5.1.3. Therefore, rather limited number of data is used in DA with both raw and interpolated time series of SWE in DA procedure. Figure 5.20 shows the lead time performance of SWE product in runoff forecasting with respect to DA of P_T and original simulation. The results of DA with

P_T and SWE clearly improve the forecasting performance by decreasing RMSE with 15-20 m³/s. Among the optimization scenarios, P_T gives slightly better results with a small difference. Moreover, H13 (not interpolated) and H13_Int (interpolated) give nearly identical results. The comparison of observed and simulated discharges for the first lead time for DA of H13_Int and P_T are illustrated in Figure 5.21. The graph indicates that the performance of H13_Int and P_T are better than the simulation, while result of P_T is slightly better than H13_Int.

On the other hand, Figure 5.22 demonstrates the time series of simulated and observed SWE as a result of DA by P_T and H13_Int. It could be inferred from Figure 5.22 that H13 observation is generally above simulation and optimized time series. The description of SWE product indicates average error of 40 mm (http://hsaf.meteoam.it/documents/ATDD/SAF_HSAF_ATBD-13_1_0.pdf), so while SWE products are included the DA procedure most of the time it increases the total amount of snow by using optimization variables. The tradeoff between discharge and SWE is founded to be reasonable.

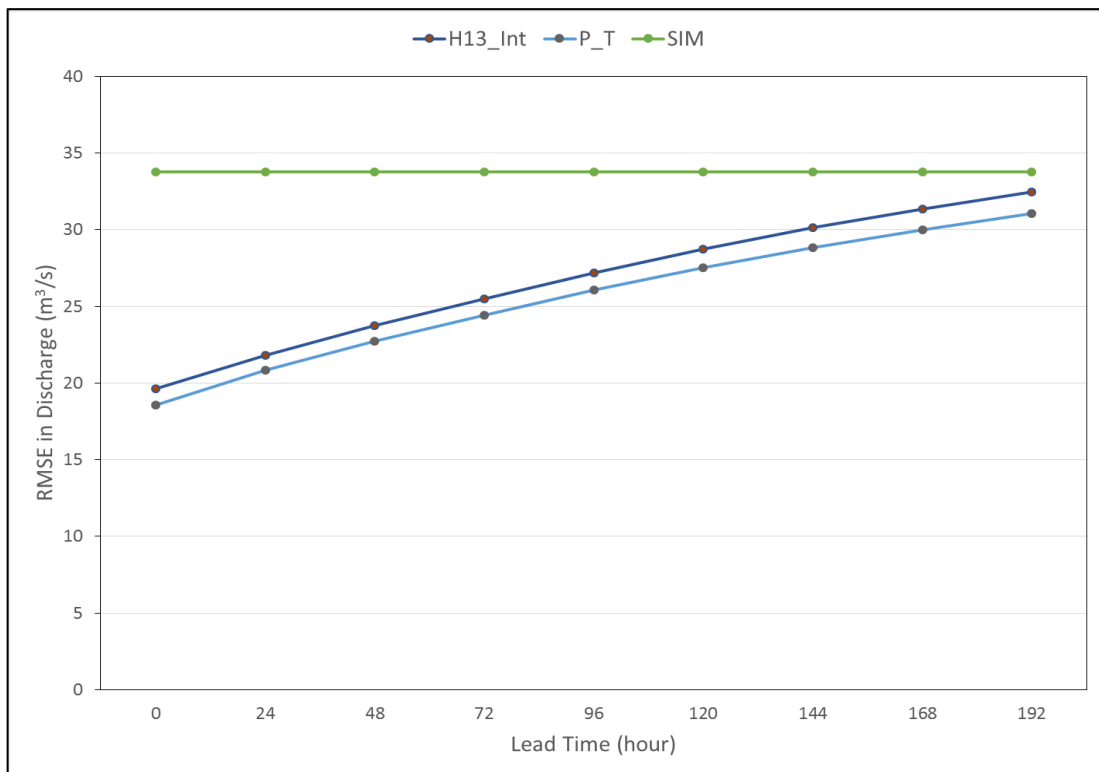


Figure 5.20. Lead time performance of DA on discharge using H13_Int and P_T.

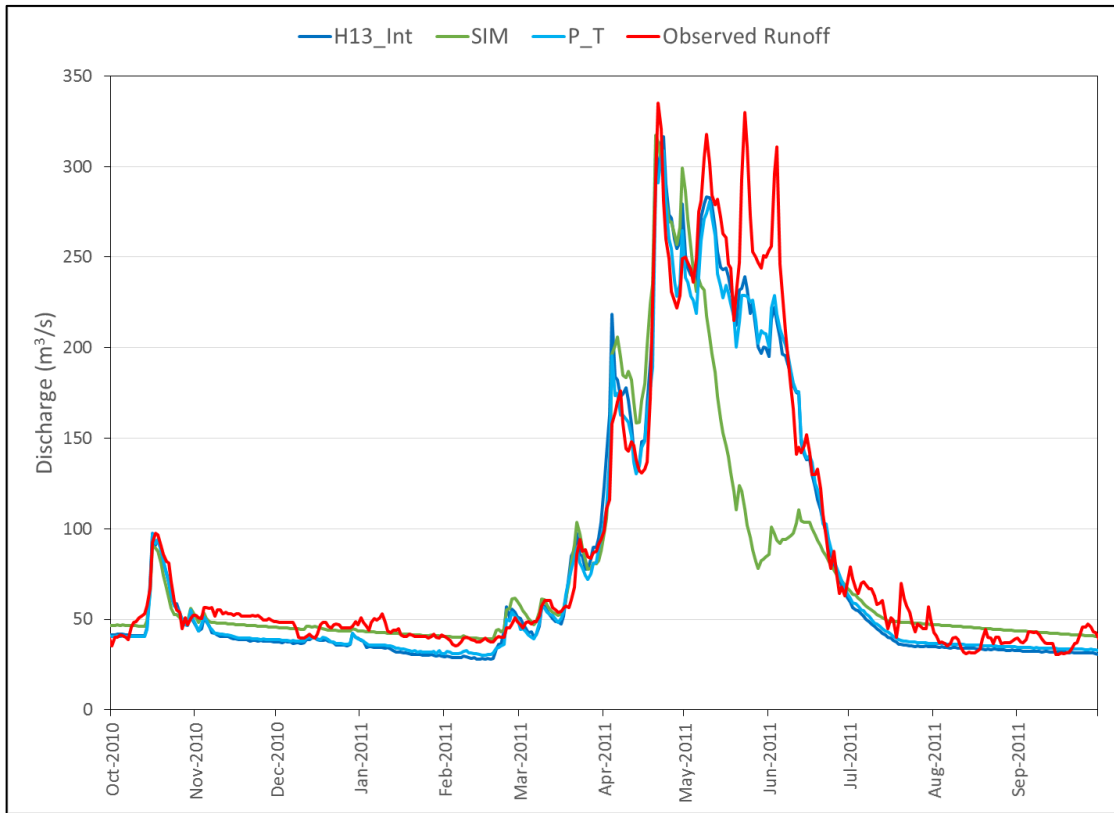


Figure 5.21. First lead time runoff values using DA based on SWE, 2011 water year

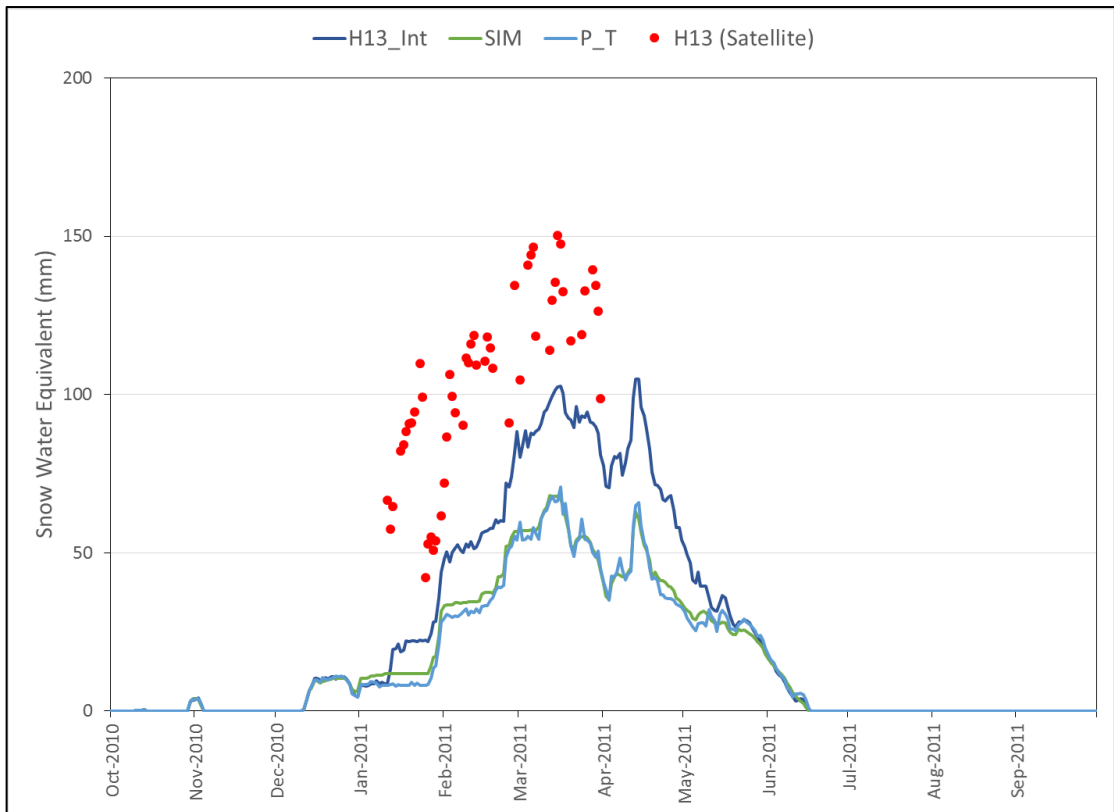


Figure 5.22. First lead time SWE values as a result of SWE based DA, 2011 water year.

5.5.3. Real-Time DA application

Real-time runoff forecasting is essential in the need to operate hydraulic structures such as reservoirs effectively. To achieve this aim a performance assessment is done for 2015 water year and runoffs are forecasted with HBV hydrologic model with and without DA application.

The availability of products plays a critical role on DA application for organizing the objective function in terms of penalty. Therefore, the selected SCA products of H10 and MODIS are taken into account in this part of the study, whereas H13 could not be used in this period due to unavailability of the product. By the time, two types of meteorological data are used in real time DA applications. The observed precipitation and temperature are used in the first part of the study as perfect forecast data. Then one of the numerical weather prediction models, Weather Research and Forecasting (WRF) model data is used with two day lead time total daily precipitation and daily average temperature data.

5.5.3.1. Real-Time DA application with observed data

Objective function is set as Equation 5.7 and Equation 5.8. In addition, P_T is also taken into account to compare the results (Figure 5.23). Runoff forecast performance is high in this year with low RMSE in the lead times. The results are slightly different from the previous ones, DA application improves the lead time accuracy for the first 5 days after on in 6th and 7th lead time, the error starts to increase. The reasons for this situation might be explained as; the updated initial conditions are changing the mass balance of forecasting period by model states values. Thus, even the initial conditions are well representing the observed streamflow at the beginning of the forecast, the interior model states are not good enough for medium range forecasting. Figure 5.24 shows the lead time accuracy of forecasted SCA with observed SCA of MODIS. According to the results, when H10 and MODIS data are taken into account in DA, objective function gives better agreement with the observed ones with respect to SIM and P_T. This shows that this situation is a trade off between discharge and snow covered area values. Generally, the performance of the lead time is increasing in one of them while the other one is decreasing. First lead time values of DA application results in terms of runoff are sketched in Figure 5.25. It is clear that all DA application results are better than that of SIM. In the accumulation period of snow, the agreement between observed SCA (by MODIS) and

simulated SCA with DA (MODIS and H10) are relatively consistent as shown in Figure 5.26. On the other hand, during the melting period an overestimation in SCA by the model is observed.

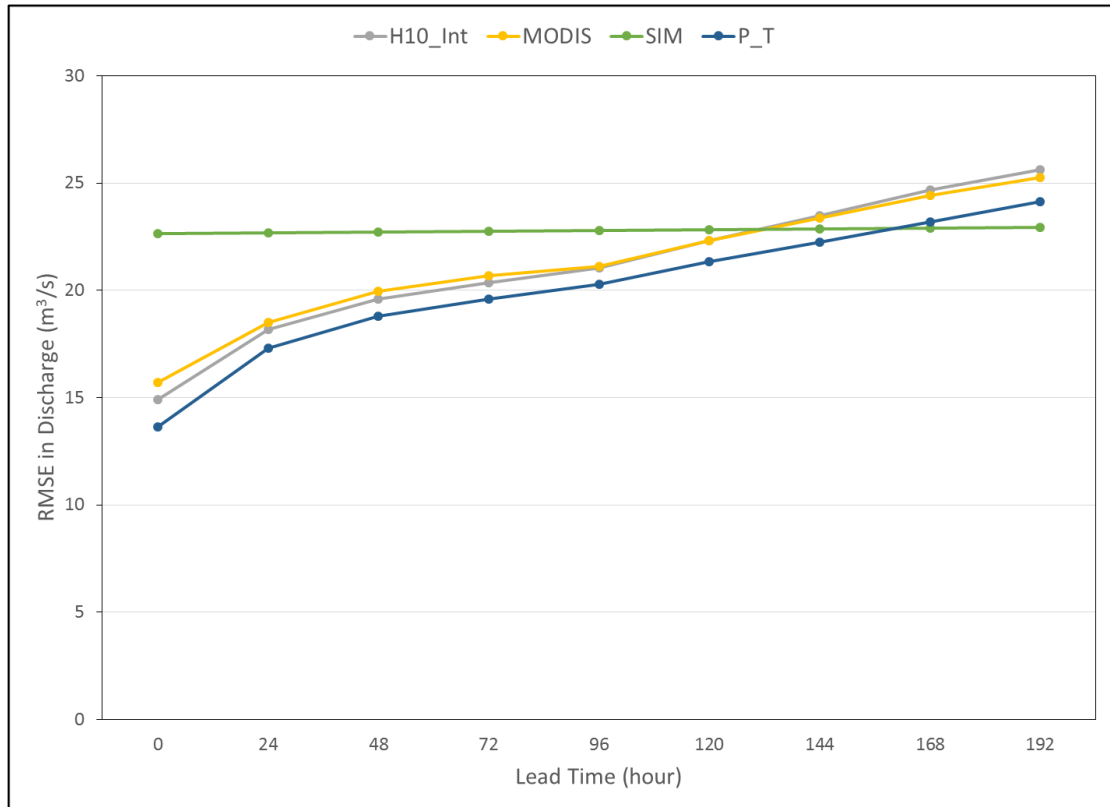


Figure 5.23. Performance analysis of DA on discharge, 2015 water year.

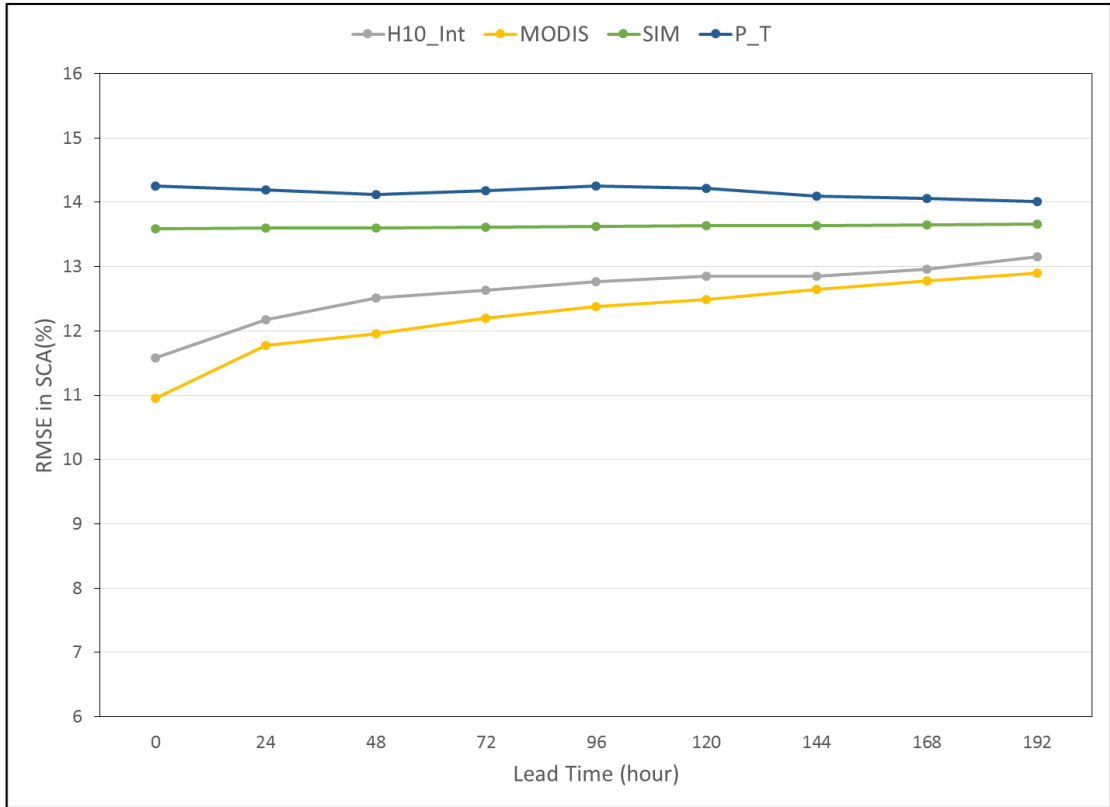


Figure 5.24. Performance analysis of DA on SCA, 2015 water year.

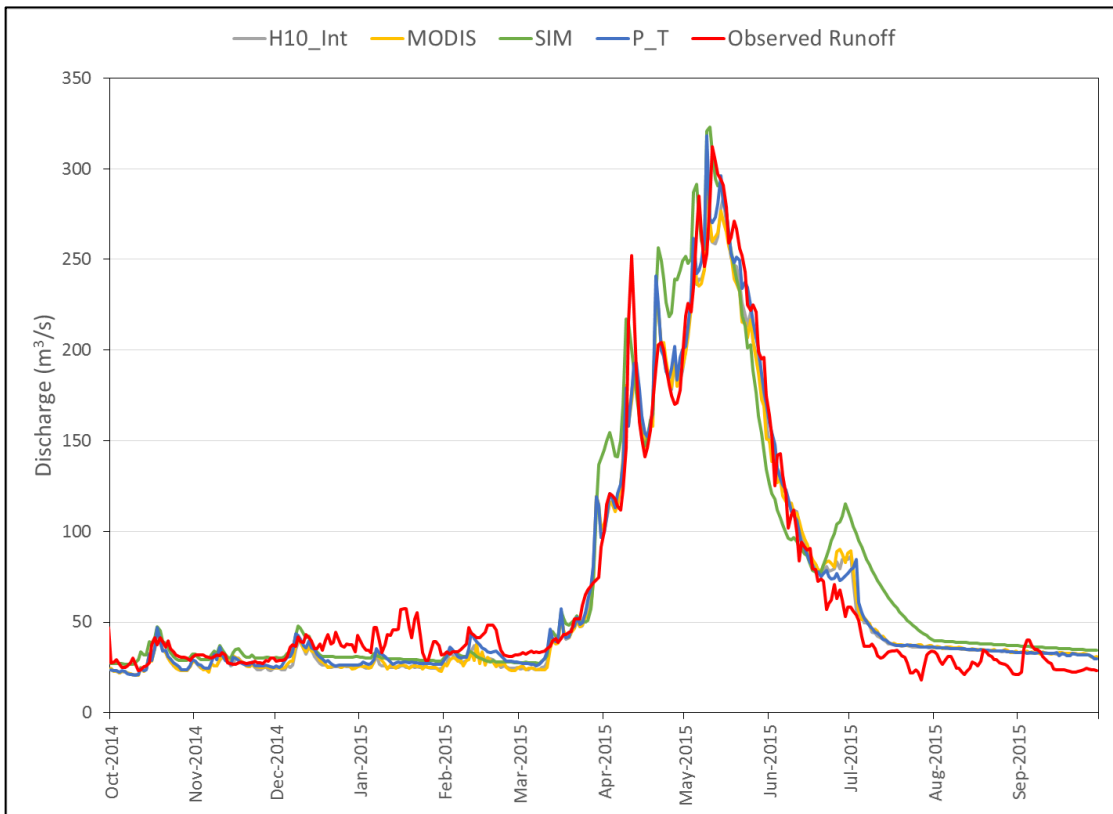


Figure 5.25. Comparison of discharge in Karasu Basin for 2015 water year.

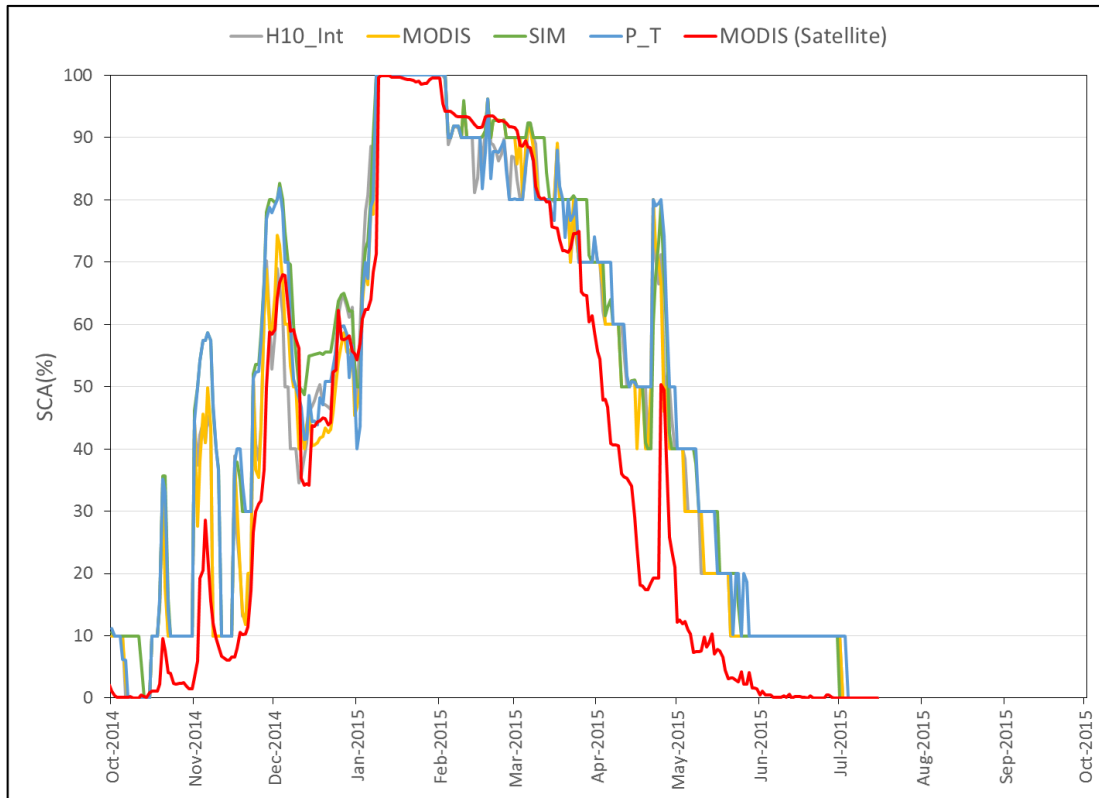


Figure 5.26. Comparison of SCA in Karasu Basin for 2015 water year.

5.5.3.2 Real-Time DA application with WRF

WRF Model, which is a Numerical Weather Prediction model, is designed for both operational forecasting and atmospheric research to meet the next generation needs on meteorology and operational hydrology. It has two dynamical cores, which are combined with data assimilation system and a software architecture facilitating parallel computational and system extensibility. The data could be retrieved from http://www2.mmm.ucar.edu/wrf/users/download/free_data.html website with registration.

In this study, daily total precipitation and daily average temperature data of WRF are used with two day lead times in a period from March to end of June in 2015 for operational forecasting. The daily retrieved data are processed with FEWS and prepared to be used in HBV hydrologic model. Updated initial states are created by not only with simulation itself, but also with DA applications then after forecasting are made with the data from WRF.

Figure 5.27 shows the time series of DA versus observed streamflow at first lead time only for the snowmelt period. The agreement between DA application results and

observed streamflow are relatively better than forecast of SIM. This improvement occurs at recession and after the second peak of the hydrograph.

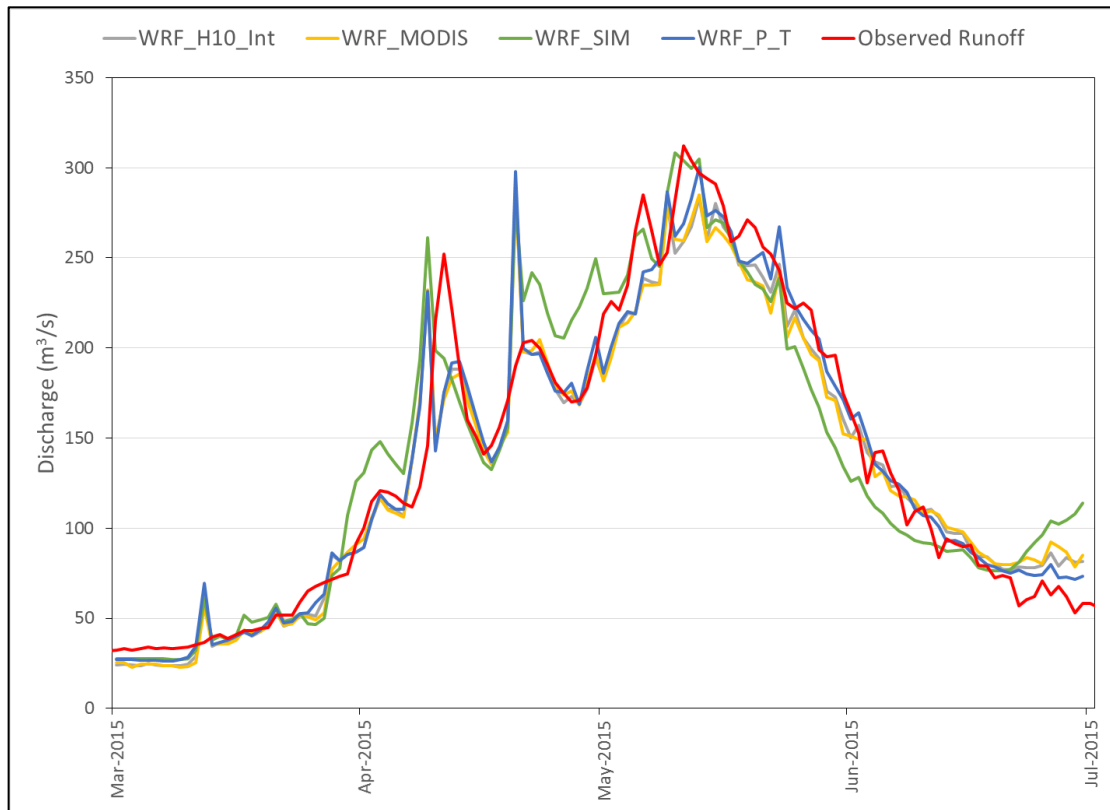


Figure 5.27. Comparison of discharge in Karasu Basin with WRF data for 2015 water year.

Since the forecasting period is only the snowmelt period, the comparison of SCA only shows the recession part of the SCA. In Figure 5.28, when snow products (H10 and MODIS) are taken into account, the time series is getting closer to the MODIS (Satellite).

Table 5.10 and Table 5.11 show the accuracy of forecasted SCA and discharge with respect to processed MODIS data and observed streamflow, respectively. DA applications force the P_T variable to improve initial states at the first lead time for streamflow prediction. On the other hand, only P_T based DA application affects the model slightly negative with respect to the SCA forecasts.



Figure 5.28. Comparison of SCA in Karasu Basin with WRF data for 2015 water year.

Table 5.10. Lead time performance of DA using WRF with respect to discharge.

| Lead Time (hour) | WRF_H10_Int (m ³ /s) | WRF_MODIS (m ³ /s) | WRF_P_T (m ³ /s) | SIM WRF (m ³ /s) | SIM observed data (m ³ /s) |
|------------------|---------------------------------|-------------------------------|-----------------------------|-----------------------------|---------------------------------------|
| 00 | 22.26 | 23.25 | 21.15 | 28.32 | 29.81 |

Table 5.11. Lead time performance of DA using WRF with respect to SCA.

| Lead Time (hour) | WRF_H10_Int (%) | WRF_MODIS (%) | WRF_P_T (%) | SIM WRF (%) | SIM observed data (%) |
|------------------|-----------------|---------------|-------------|-------------|-----------------------|
| 00 | 16.27 | 15.79 | 19.09 | 17.36 | 17.15 |

6. CONCLUSION

Accurate runoff forecasting especially at high flow period is crucial at mountainous regions, since it has strong effect on foreseeing future streamflow conditions and making decisions on reservoir operations. Runoff forecasting is enabled using hydrological models. A well-known hydrological model, HBV, is applied in this study, after calibration and validation processes. Initial conditions, which are the initial state variables before the start of forecasting, plays significant roll on the accurate runoff forecasting. To increase this accuracy, data assimilation approach, which is becoming more popular for hydrological applications in the last decade, is utilized to update and improve the initial states with and without the help of satellite snow products. To our knowledge, Data Assimilation using satellite products within HBV hydrological model is the first application in Turkey.

One of the 4D-variational algorithms, Moving Horizon Estimation, is selected for this study. The main advantage of the method is that it sees the whole forecasting window by rewriting the equations of the objective function separately, to get the optimal solution in each time step. In addition, since variational methods enable to take the gradient for each time step by the help of an adjoint model, satellite products are easily used with different weighting factors.

Satellite products are chosen in two categories as snow covered area (SCA) and snow water equivalent (SWE). Areal snow cover extent from both Moderate Resolution Imaging Spectroradiometer (MODIS) and Meteosat Second Generation-SEVIRI (H10) and snow water equivalent product of Special Sensor Microwave Imager/Sounder (SSMIS) (H13) is exploited for this study. Since SWE and SCA are outputs of HBV hydrologic model, the observed satellite products are used to evaluate the performance of data assimilation.

Karasu Basin, one of the headwaters of Euphrates Basin, is selected as a pilot area to apply hydrologic modeling and DA in order to increase the accuracy of forecasting. The mean elevation value of 1983 m indicates that the catchment is in the category of mountainous region. Approximately 2/3 of total annual flow comes during spring and early summer months due to both rain and snowmelt creating high flows.

The study period is selected as 2001-2015 water years; data of 2001-2008 water years are used to calibrate the model and that of 2009-2013 water years are used to

validate the model by performance indicators. Melting period of 2015 water year (March-June) is chosen for real time forecasting. According to the statistical analysis of mean annual runoff, 2014 water year is a low flow outlier year for Karasu Basin, so it is used neither in validation nor in forecasting.

After the HBV hydrologic model is set up in Delft-FEWS platform, first, calibration and validation analysis are performed. Promising results with Nash Sutcliffe Efficiency of 0.85 and 0.72 are obtained for the calibration and validation periods, respectively.

MHE method coupled with HBV hydrologic model is applied with a lead time of 192 hours (8 days) at 24 hour time steps for the validation period in Karasu Basin, after analyzing the optimum number of iterations. As a first step, DA is applied only for model states; results give better performance than that of simulation without DA and upper zone (UZ) states give the best result with a decreased RMSE from 34.5 m³/s to 12.4 m³/s at the first lead time. The main reason is that UZ controls the quick flow of HBV, and when DA is allowed to change this state, it increases the consistency of modelled and simulated runoff by improving the initial state especially in high flow period.

Second experiment is directly related with the usage of satellite products through DA. After processing the data and assigning proper weighting factors, SCA is selected as the first data set. MHE is applied with adding the difference between observed and modelled SCA into the objective function with a penalty term. DA procedure is run with disturbing precipitation and temperature according to the penalty function that is violated by two terms, observed streamflow and observed SCA. In all DA applications, the agreement between observed and simulated streamflow increases especially at the first lead time. As time progress, the lead time accuracy decreases and approaches to the accuracy of without DA application. The results show that when SCA products are used in the objective function, they help to increase the agreement between observed and simulated SCA with a rate of 2-3 %. Even though forecast accuracy between observed and simulated streamflow by disturbing only precipitation and temperature (P_T) variables give slightly better agreement in observed and simulated streamflow and SCA, the DA application with SCA increases the internal validity of the model with high consistency in observed and modelled SCA. In addition, since it uses an independent measure of snow data, it is physically more meaningful. In the second experiment, H13

snow water equivalent product is used with the same approach in DA. The results show that this helps the simulated SWE to approach to the observed SWE dramatically. Moreover, the effect on streamflow forecast is assumed to be reasonable according to without DA case.

The real time forecasting experiment is carried out with DA during 2015 water year using observed streamflow, H10 and MODIS data. DA is applied in two steps: firstly, observed precipitation and temperature data are used as perfect forecasts including SCA in the objective function. In the second step, Numerical Weather Prediction (NWP) data is utilized in real-time runoff forecasting again taking SCA into account within the objective function. The real time forecasting experiment is run with Numerical Weather Prediction (NWP) data of Weather Research and Forecast (WRF) model for two day lead time between March to June of 2015 water year. According to the results, DA application using observed SCA increases the accuracy of streamflow forecasts for the first lead time.

In this study, streamflow forecast is improved by the data assimilation technique when introducing the satellite products into the model. Even though the results of each experiment give a different aspect of DA, it is obvious that DA procedure is one of the significant techniques to improve forecasting. The flexibility of different DA techniques in modeling provides opportunities for integrating them with various models, data and algorithms. Therefore, this study could be a milestone for further operational studies in real time reservoir operations in Turkey.

This study can lead to usage of different DA applications in hydrologic modelling for improving the lead time forecast accuracy in Turkey. DA algorithms can be applied with various other satellite products and NWP data in the future studies. Moreover, other state variables like soil moisture besides snow data can be used in the objective function of DA to increase internal model validity with independent observation datasets.

REFERENCES

- Abebe, N. A., Ogden, F. L., & Pradhan, N. R. (2010). Sensitivity and uncertainty analysis of the conceptual HBV rainfall–runoff model: Implications for parameter estimation. *Journal of Hydrology*, 389(3), 301-310.
- Albergel, C., Rüdiger, C., Pellarin, T., Calvet, J. C., Fritz, N., Froissard, F., ... & Martin, E. (2008). From near-surface to root-zone soil moisture using an exponential filter: an assessment of the method based on in-situ observations and model simulations. *Hydrology and Earth System Sciences Discussions*, 12, 1323-1337.
- Albostan, A., Barutçu, B., & Bihrat, O. (2010). Data generation for murat river with artificial neural networks. In E. D. Schmitter, & N. Mastorkis (Eds.), *WSEAS International Conference. Proceedings. Mechanical Engineering Series (Vol. 5)*. World Scientific and Engineering Academy and Society.
- Allgöwer, F., Badgwell, T. A., Qin, J. S., Rawlings, J. B., & Wright, S. J. (1999). Nonlinear predictive control and moving horizon estimation—an introductory overview. In *Advances in control* (pp. 391-449). Springer London.
- Aminou, D. M. A. (2002). MSG's SEVIRI instrument. *ESA Bulletin(0376-4265)*, (111), 15-17.
- Andreadis, K. M., & Lettenmaier, D. P. (2006). Assimilating remotely sensed snow observations into a macroscale hydrology model. *Advances in water resources*, 29(6), 872-886.
- Arsenault, K. R., Houser, P. R., & De Lannoy, G. J. (2014). Evaluation of the MODIS snow cover fraction product. *Hydrological Processes*, 28(3), 980-998.
- Aubert, D., Loumagne, C., & Oudin, L. (2003). Sequential assimilation of soil moisture and streamflow data in a conceptual rainfall–runoff model. *Journal of Hydrology*, 280(1), 145-161.
- Aytemiz, L., & Kodaman, T. (2006). Sınıraşan Sular Kullanımı ve Türkiye-Suriye İlişkileri. *TMMOB Su Politikaları Kongresi*, 21-23.
- Barnes, W. L., Pagano, T. S., & Salomonson, V. V. (1998). Prelaunch characteristics of the moderate resolution imaging spectroradiometer (MODIS) on EOS-AM1. *IEEE Transactions on Geoscience and Remote Sensing*, 36(4), 1088-1100.

- Bavera, D., De Michele, C., Pepe, M., & Rampini, A. (2012). Melted snow volume control in the snowmelt runoff model using a snow water equivalent statistically based model. *Hydrological Processes*, 26(22), 3405-3415.
- Bennett, A. F., & Thorburn, M. A. (1992). The generalized inverse of a nonlinear quasigeostrophic ocean circulation model.
- Bergström, S. (1976). Development and application of a conceptual runoff model for Scandinavian catchments.
- Bergström, S., & Lindström, G. (2015). Interpretation of runoff processes in hydrological modelling—experience from the HBV approach. *Hydrological Processes*, 29(16), 3535-3545.
- Beşer, Ö. (2002). The use of SSM/I for snow mapping over the eastern part of Turkey. Master of Science Thesis, Middle East Technical University.
- Boudhar, A., Hanich, L., Boulet, G., Duchemin, B., Berjamy, B., & Chehbouni, A. (2009). Evaluation of the Snowmelt Runoff Model in the Moroccan High Atlas mountains using two snow-cover estimates. *Hydrological sciences journal*, 54(6), 1094-1113.
- Bouttier, F., Mahfouf, J. F., & Noilhan, J. (1993). Sequential assimilation of soil moisture from atmospheric low-level parameters. Part I: Sensitivity and calibration studies. *Journal of Applied Meteorology*, 32(8), 1335-1351.
- Bouttier, F., & Courtier, P. (1999). Data assimilation concepts and methods. Meteorological training course lecture series. ECMWF. Reading.
- Brocca, L., Melone, F., Moramarco, T., Wagner, W., Naeimi, V., Bartalis, Z., & Hasenauer, S. (2010). Improving runoff prediction through the assimilation of the ASCAT soil moisture product. *Hydrology and Earth System Sciences*, 14(10), 1881-1893.
- Brown, J. D., Demargne, J., Seo, D. J., & Liu, Y. (2010). The Ensemble Verification System (EVS): A software tool for verifying ensemble forecasts of hydrometeorological and hydrologic variables at discrete locations. *Environmental Modelling & Software*, 25(7), 854-872.

- Charney, J. G., Halem, M., & Jastrow, R. (1969). Use of incomplete historical data to infer the present state of the atmosphere. *Journal of the Atmospheric Sciences*, 26(5), 1160-1163.
- Clark, M. P., & Slater, A. G. (2006). Probabilistic quantitative precipitation estimation in complex terrain. *Journal of Hydrometeorology*, 7(1), 3-22.
- Clark, M. P., Slater, A. G., Barrett, A. P., Hay, L. E., McCabe, G. J., Rajagopalan, B., & Leavesley, G. H. (2006). Assimilation of snow covered area information into hydrologic and land-surface models. *Advances in water resources*, 29(8), 1209-1221.
- Clark, M. P., Rupp, D. E., Woods, R. A., Zheng, X., Ibbitt, R. P., Slater, A. G., ... & Uddstrom, M. J. (2008). Hydrological data assimilation with the ensemble Kalman filter: Use of streamflow observations to update states in a distributed hydrological model. *Advances in water resources*, 31(10), 1309-1324.
- Clark, M. P., Hendrikx, J., Slater, A. G., Kavetski, D., Anderson, B., Cullen, N. J., ... & Woods, R. A. (2011). Representing spatial variability of snow water equivalent in hydrologic and land-surface models: A review. *Water Resources Research*, 47(7).
- Corato, G., Matgen, P., Fenicia, F., Schlaffer, S., & Chini, M. (2014). Assimilating satellite-derived soil moisture products into a distributed hydrological model. In *2014 IEEE Geoscience and Remote Sensing Symposium* (pp. 3315-3318). IEEE.
- Cornwell, E., Molotch, N. P., & McPhee, J. (2016). Spatio-temporal variability of snow water equivalent in the extra-tropical Andes Cordillera from distributed energy balance modeling and remotely sensed snow cover. *Hydrology and Earth System Sciences*, 20(1), 411-430.
- Crawford, N. H., & Linsley, R. K. (1966). *Digital Simulation in Hydrology* Stanford Watershed Model 4.
- Crawford, C. J. (2015). MODIS Terra Collection 6 fractional snow cover validation in mountainous terrain during spring snowmelt using Landsat TM and ETM+. *Hydrological Processes*, 29(1), 128-138.

- Crow, W. T., & Ryu, D. (2009). A new data assimilation approach for improving runoff prediction using remotely-sensed soil moisture retrievals. *Hydrology and Earth System Sciences*, 13(1), 1-16.
- Çoskun, C., (2016). Comparative analysis of various satellite products through hydrological modeling, Master of Science Thesis, Eskişehir: Anadolu University.
- Da Ronco, P., & De Michele, C. (2013). On the use of MODIS Snow Cover Product for assessing snow extension and duration over the Po river basin. *CMCC Research Paper*, (182).
- Daley, R. (1991). *Atmospheric data analysis*, Cambridge atmospheric and space science series. Cambridge University Press, 6966, 25.
- Day, C. A. (2013). Satellite Data Utilization in Hydrological Research. *J Geol Geosci*, 2, e108.
- De Lannoy, G. J., Reichle, R. H., Houser, P. R., Pauwels, V., & Verhoest, N. E. (2007). Correcting for forecast bias in soil moisture assimilation with the ensemble Kalman filter. *Water Resources Research*, 43(9).
- De Lannoy, G. J., Reichle, R. H., Arsenault, K. R., Houser, P. R., Kumar, S., Verhoest, N. E., & Pauwels, V. (2012). Multiscale assimilation of Advanced Microwave Scanning Radiometer–EOS snow water equivalent and Moderate Resolution Imaging Spectroradiometer snow cover fraction observations in northern Colorado. *Water Resources Research*, 48(1).
- Dechant, C., & Moradkhani, H. (2011). Radiance data assimilation for operational snow and streamflow forecasting. *Advances in Water Resources*, 34(3), 351-364.
- Derksen, C., Walker, A., & Goodison, B. (2003). A comparison of 18 winter seasons of in situ and passive microwave-derived snow water equivalent estimates in Western Canada. *Remote Sensing of Environment*, 88(3), 271-282.
- Dong, J., Walker, J. P., Houser, P. R., & Sun, C. (2007). Scanning multichannel microwave radiometer snow water equivalent assimilation. *Journal of Geophysical Research: Atmospheres*, 112(D7).

- Dressler, K. A., Leavesley, G. H., Bales, R. C., & Fassnacht, S. R. (2006). Evaluation of gridded snow water equivalent and satellite snow cover products for mountain basins in a hydrologic model. *Hydrological Processes*, 20(4), 673-688.
- Duethmann, D., Peters, J., Blume, T., Vorogushyn, S., & Güntner, A. (2014). The value of satellite-derived snow cover images for calibrating a hydrological model in snow-dominated catchments in Central Asia. *Water Resources Research*, 50(3), 2002-2021.
- Durand, M., Andreadis, K. M., Alsdorf, D. E., Lettenmaier, D. P., Moller, D., & Wilson, M. (2008). Estimation of bathymetric depth and slope from data assimilation of swath altimetry into a hydrodynamic model. *Geophysical Research Letters*, 35(20).
- Dziubanski, D. J., & Franz, K. J. (2016). Assimilation of AMSR-E snow water equivalent data in a spatially-lumped snow model. *Journal of Hydrology*.
- Errico, R. M. (1997). What is an adjoint model?. *Bulletin of the American Meteorological Society*, 78(11), 2577.
- Finger, D., Vis, M., Huss, M., & Seibert, J. (2015). The value of multiple data set calibration versus model complexity for improving the performance of hydrological models in mountain catchments. *Water Resources Research*, 51(4), 1939-1958.
- Forsythe, N., Kilsby, C. G., Fowler, H. J., & Archer, D. R. (2012). Assessment of runoff sensitivity in the Upper Indus Basin to interannual climate variability and potential change using MODIS satellite data products. *Mountain Research and Development*, 32(1), 16-29.
- Franssen, H. J., & Kinzelbach, W. (2008). Real-time groundwater flow modeling with the ensemble Kalman filter: Joint estimation of states and parameters and the filter inbreeding problem. *Water Resources Research*, 44(9).
- Franz, K. J., & Karsten, L. R. (2013). Calibration of a distributed snow model using MODIS snow covered area data. *Journal of Hydrology*, 494, 160-175.
- Gafurov, A., & Bárdossy, A. (2009). Cloud removal methodology from MODIS snow cover product. *Hydrology and Earth System Sciences*, 13(7), 1361-1373.

- Gandin, L. S. (1963). *Applied Optimal Estimation*. Israel Program for Scientific Translations.
- Gao, Y., Xie, H., Yao, T., & Xue, C. (2010). Integrated assessment on multi-temporal and multi-sensor combinations for reducing cloud obscuration of MODIS snow cover products of the Pacific Northwest USA. *Remote Sensing of Environment*, 114(8), 1662-1675.
- Garen, D. C., Johnson, G. L., & Hanson, C. L. (1994). Mean areal precipitation for daily hydrologic modeling in mountainous regions1.
- Gascoin, S., Hagolle, O., Huc, M., Jarlan, L., Dejoux, J. F., Szczypta, C., ... & Sánchez, R. (2015). A snow cover climatology for the Pyrenees from MODIS snow products. *Hydrology and Earth System Sciences*.
- Ghil, M., & Malanotte-Rizzoli, P. (1991). Data assimilation in meteorology and oceanography. *Advances in geophysics*, 33, 141-266.
- Gözel, E., (2011). Yukari Firat Havzasında kar suyu potansiyelinin dönemsel ve akimların günlük modellenmesi, Master of Science Thesis, Eskişehir: Anadolu University.
- Griewank, A., & Walther, A. (2008). *Evaluating derivatives: principles and techniques of algorithmic differentiation*. Siam.
- Hall, D. K., & Riggs, G. A. (2007). Accuracy assessment of the MODIS snow products. *Hydrological Processes*, 21(12), 1534-1547.
- Haseltine, E. L., & Rawlings, J. B. (2005). Critical evaluation of extended Kalman filtering and moving-horizon estimation. *Industrial & engineering chemistry research*, 44(8), 2451-2460.
- He, Z. H., Parajka, J., Tian, F. Q., & Blöschl, G. (2014). Estimating degree-day factors from MODIS for snowmelt runoff modeling. *Hydrology and Earth System Sciences*, 18(12), 4773-4789.
- Huang, X., Liang, T., Zhang, X., & Guo, Z. (2011). Validation of MODIS snow cover products using Landsat and ground measurements during the 2001–2005 snow seasons over northern Xinjiang, China. *International Journal of Remote Sensing*, 32(1), 133-152.

- Immerzeel, W. W., Droogers, P., De Jong, S. M., & Bierkens, M. F. P. (2009). Large-scale monitoring of snow cover and runoff simulation in Himalayan river basins using remote sensing. *Remote sensing of Environment*, 113(1), 40-49.
- Jain, S. K., Goswami, A., & Saraf, A. K. (2010). Snowmelt runoff modelling in a Himalayan basin with the aid of satellite data. *International Journal of Remote Sensing*, 31(24), 6603-6618.
- Johansson, B., Caves, R., Ferguson, R., & Turpin, O. (2001). Using remote sensing data to update the simulated snow pack of the HBV runoff model. IAHS Publication, 595-597.
- Jónsdóttir, J. F., & Þórarinnsson, J. S. (2004). Comparison of HBV models, driven with weather station data and with MM5 meteorological model data. Reykjavík, National Energy Authority, Report ISBN 9979-68-147-0. OS-2004/017, 17pp.
- Kalnay, E. (2003). *Atmospheric modeling, data assimilation and predictability*. Cambridge university press.
- Kaya, I. (1999). Application of snowmelt runoff model using remote sensing and GIS. Master of Science Thesis. Ankara: Middle East Technical University.
- Kolberg, S. A., & Gottschalk, L. (2006). Updating of snow depletion curve with remote sensing data. *Hydrological Processes*, 20(11), 2363-2380.
- Kolberg, S., Rue, H., & Gottschalk, L. (2006). A Bayesian spatial assimilation scheme for snow coverage observations in a gridded snow model. *Hydrology and Earth System Sciences Discussions*, 10(3), 369-381.
- Kolberg, S., & Gottschalk, L. (2010). Interannual stability of grid cell snow depletion curves as estimated from MODIS images. *Water Resources Research*, 46(11).
- Komma, J., Blöschl, G., & Reszler, C. (2008). Soil moisture updating by Ensemble Kalman Filtering in real-time flood forecasting. *Journal of Hydrology*, 357(3), 228-242.
- Kostov, K. G., & Jackson, T. J. (1993, August). Estimating profile soil moisture from surface-layer measurements: A review. In *Optical Engineering and Photonics in Aerospace Sensing* (pp. 125-136). International Society for Optics and Photonics.

- Krajčí, P., Holko, L., Perdigão, R. A., & Parajka, J. (2014). Estimation of regional snowline elevation (RSLE) from MODIS images for seasonally snow covered mountain basins. *Journal of Hydrology*, 519, 1769-1777
- Kuchment, L. S., Romanov, P., Gelfan, A. N., & Demidov, V. N. (2010). Use of satellite-derived data for characterization of snow cover and simulation of snowmelt runoff through a distributed physically based model of runoff generation. *Hydrology and Earth System Sciences*, 14(2), 339-350.
- Kult, J., Choi, W., & Choi, J. (2014). Sensitivity of the Snowmelt Runoff Model to snow covered area and temperature inputs. *Applied Geography*, 55, 30-38.
- Kumar, S. V., Reichle, R. H., Koster, R. D., Crow, W. T., & Peters-Lidard, C. D. (2009). Role of subsurface physics in the assimilation of surface soil moisture observations. *Journal of Hydrometeorology*, 10(6), 1534-1547.
- Kunstmann, H., & Stadler, C. (2005). High resolution distributed atmospheric-hydrological modelling for Alpine catchments. *Journal of hydrology*, 314(1), 105-124.
- Lahtinen, P., Ertürk, A. G., Pulliainen, J., & Koskinen, J. (2009, July). Merging flat/forest and mountainous snow products for extended European area. In 2009 IEEE International Geoscience and Remote Sensing Symposium (Vol. 2, pp. II-563). IEEE. Chicago
- Lee, S., Klein, A. G., & Over, T. M. (2005). A comparison of MODIS and NOHRSC snow-cover products for simulating streamflow using the Snowmelt Runoff Model. *Hydrological Processes*, 19(15), 2951-2972.
- Leisenring, M., & Moradkhani, H. (2011). Snow water equivalent prediction using Bayesian data assimilation methods. *Stochastic Environmental Research and Risk Assessment*, 25(2), 253-270.
- Li, X., & Williams, M. W. (2008). Snowmelt runoff modelling in an arid mountain watershed, Tarim Basin, China. *Hydrological Processes*, 22(19), 3931-3940.
- Liu, Y. Y., Dorigo, W. A., Parinussa, R. M., de Jeu, R. A., Wagner, W., McCabe, M. F., ... & Van Dijk, A. I. J. M. (2012). Trend-preserving blending of passive and active

- microwave soil moisture retrievals. *Remote Sensing of Environment*, 123, 280-297.
- Lü, H., Yu, Z., Zhu, Y., Drake, S., Hao, Z., & Sudicky, E. A. (2011). Dual state-parameter estimation of root zone soil moisture by optimal parameter estimation and extended Kalman filter data assimilation. *Advances in Water Resources*, 34(3), 395-406.
- Marks, D., Dozier, J., Davis, R. (1992), Climate and energy exchange at the snow surface in the Alpine region of the Sierra Nevada 1. Meteorological measurements and monitoring, *Water Resources Research*, Vol.28, No. 11: 3029-3042.
- Martinec, J. (1975). Snowmelt-runoff model for stream flow forecasts. *Hydrology Research*, 6(3), 145-154.
- Martinec, J., Rango, A., & Roberts, R. (1998). Snowmelt runoff model (SRM) user's manual. M. F. Baumgartner, & G. M. Apfl (Eds.). University of Berne, Department of Geography. Chicago
- Matgen, P., Montanari, M., Hostache, R., Pfister, L., Hoffmann, L., Plaza, D., ... & Savenije, H. H. G. (2010). Towards the sequential assimilation of SAR-derived water stages into hydraulic models using the Particle Filter: proof of concept. *Hydrology and Earth System Sciences*, 14(9), 1773-1785.
- Maurer, E. P., Rhoads, J. D., Dubayah, R. O., & Lettenmaier, D. P. (2003). Evaluation of the snow-covered area data product from MODIS. *Hydrological Processes*, 17(1), 59-71.
- McLaughlin, D. (1995). Recent developments in hydrologic data assimilation. *Reviews of Geophysics*, 33(S2), 977-984.
- McLaughlin, D. (2002). An integrated approach to hydrologic data assimilation: interpolation, smoothing, and filtering. *Advances in Water Resources*, 25(8), 1275-1286.
- Molotch, N. P. (2009). Reconstructing snow water equivalent in the Rio Grande headwaters using remotely sensed snow cover data and a spatially distributed snowmelt model. *Hydrological processes*, 23(7), 1076-1089.

- Montero, R. A., Schwanenberg, D., Krahe, P., Lisniak, D., Şensoy, A., Şorman, A. A., & Akkol, B. (2016). Moving horizon estimation for assimilating H-SAF remote sensing data into the HBV hydrological model. *Advances in Water Resources*, 92, 248-257.
- Moradkhani, H., Hsu, K. L., Gupta, H., & Sorooshian, S. (2005a). Uncertainty assessment of hydrologic model states and parameters: Sequential data assimilation using the particle filter. *Water Resources Research*, 41(5).
- Moradkhani, H., Sorooshian, S., Gupta, H. V., & Houser, P. R. (2005b). Dual state–parameter estimation of hydrological models using ensemble Kalman filter. *Advances in Water Resources*, 28(2), 135-147.
- Moradkhani, H., & Sorooshian, S. (2009). General review of rainfall-runoff modeling: model calibration, data assimilation, and uncertainty analysis. In *Hydrological modelling and the water cycle* (pp. 1-24). Springer Berlin Heidelberg.
- Moradkhani, H., DeChant, C. M., & Sorooshian, S. (2012). Evolution of ensemble data assimilation for uncertainty quantification using the particle filter-Markov chain Monte Carlo method. *Water Resources Research*, 48(12).
- Nagarajan, K., Judge, J., Graham, W. D., & Monsivais-Huertero, A. (2011). Particle filter-based assimilation algorithms for improved estimation of root-zone soil moisture under dynamic vegetation conditions. *Advances in Water Resources*, 34(4), 433-447.
- NATO SfS 96-01-055 TU-REMOSENS (1996 – 2000), Establishment of satellite based observation and its applications in Turkey –NATO Consultant, NVE, Norway.
- Nester, T., Kirnbauer, R., Parajka, J., & Blöschl, G. (2012). Evaluating the snow component of a flood forecasting model. *Hydrology Research*, 43(6), 762-779.
- Nie, S., Zhu, J., & Luo, Y. (2011). Simultaneous estimation of land surface scheme states and parameters using the ensemble Kalman filter: identical twin experiments. *Hydrology and Earth System Sciences*, 15(8), 2437-2457.
- Ohara, N., Kavvas, M. L., Anderson, M. L., Richard Chen, Z. Q., & Yoon, J. (2011). Water balance study for the Tigris-Euphrates river basin. *Journal of Hydrologic Engineering*, 16(12), 1071-1082.

- Ottlé, C., & Vidal-Madjar, D. (1994). Assimilation of soil moisture inferred from infrared remote sensing in a hydrological model over the HAPEX-MOBILHY region. *Journal of Hydrology*, 158(3), 241-264.
- Parajka, J., & Blöschl, G. (2008). Spatio-temporal combination of MODIS images—potential for snow cover mapping. *Water Resources Research*, 44(3).
- Parajka, J., Pepe, M., Rampini, A., Rossi, S., & Blöschl, G. (2010). A regional snow-line method for estimating snow cover from MODIS during cloud cover. *Journal of Hydrology*, 381(3), 203-212.
- Pauwels, V. R., Hoeben, R., Verhoest, N. E., & De Troch, F. P. (2001). The importance of the spatial patterns of remotely sensed soil moisture in the improvement of discharge predictions for small-scale basins through data assimilation. *Journal of Hydrology*, 251(1), 88-102.
- Peters-Lidard, C. D., Kumar, S. V., Mocko, D. M., & Tian, Y. (2011). Estimating evapotranspiration with land data assimilation systems. *Hydrological Processes*, 25(26), 3979-3992.
- Pulliainen, J. T., Grandell, J., & Hallikainen, M. T. (1999). HUT snow emission model and its applicability to snow water equivalent retrieval. *IEEE Transactions on Geoscience and Remote Sensing*, 37(3), 1378-1390.
- Pulliainen, J. (2006). Mapping of snow water equivalent and snow depth in boreal and sub-arctic zones by assimilating space-borne microwave radiometer data and ground-based observations. *Remote sensing of Environment*, 101(2), 257-269.
- Rakovec, O., Weerts, A. H., Hazenberg, P., Torfs, P. J. J. F., & Uijlenhoet, R. (2012). State updating of a distributed hydrological model with Ensemble Kalman Filtering: effects of updating frequency and observation network density on forecast accuracy. *Hydrology and Earth System Sciences*, 16(9), 3435-3449.
- Raleigh, M. S., Rittger, K., Moore, C. E., Henn, B., Lutz, J. A., & Lundquist, J. D. (2013). Ground-based testing of MODIS fractional snow cover in subalpine meadows and forests of the Sierra Nevada. *Remote Sensing of Environment*, 128, 44-57.
- Rawlings, J. B., (2013). Moving Horizon Estimation. in: J Baillieul, T Samad, (Eds.). *Encyclopedia of Systems and Control*. Springer London, London. pp. 1-7.

- Reggiani, P., & Weerts, A. H. (2008). A Bayesian approach to decision-making under uncertainty: An application to real-time forecasting in the river Rhine. *Journal of Hydrology*, 356(1), 56-69.
- Reggiani, P., Renner, M., Weerts, A. H., & Van Gelder, P. A. H. J. M. (2009). Uncertainty assessment via Bayesian revision of ensemble streamflow predictions in the operational river Rhine forecasting system. *Water Resources Research*, 45(2).
- Reichle, R. H. (2008). Data assimilation methods in the Earth sciences. *Advances in Water Resources*, 31(11), 1411-1418.
- Ren, L., Hartnett, M., & Nash, S. (2014). Sensitivity tests of direct insertion data assimilation with pseudo measurements. *International Journal of Computer and Communication Engineering*, 3(6), 460.
- Riggs, G. A., Hall, D. K., & Salomonson, V. V. (2006). MODIS snow products user guide to collection 5. *Digital Media*, 80.
- Rodell, M., & Houser, P. R. (2004). Updating a land surface model with MODIS-derived snow cover. *Journal of Hydrometeorology*, 5(6), 1064-1075.
- Schumacher, M., Kusche, J., & Döll, P. (2016). A systematic impact assessment of GRACE error correlation on data assimilation in hydrological models. *Journal of Geodesy*, 1-23.
- Schwanenberg, D., (2012) A. H-SAF Associated/Visiting Scientist Activity ref. H-SAF_VSA_13_03 Generic Data Assimilation Test Bed for H-SAF Snow Products and a Conceptual Hydrological Model.
- Şen, O. L., Ünal, A., Bozkurt, D., & Kindap, T. (2011). Temporal changes in the Euphrates and Tigris discharges and teleconnections. *Environmental Research Letters*, 6(2), 024012.
- Şensoy, A. (2000). Spatially distributed hydrologic modeling approach using geographic information systems. Master of Science Thesis. Ankara:, Middle East Technical University.
- Şensoy, A. (2005). Physically based point snowmelt modeling and its distribution in Upper Euphrates Basin. Doctoral dissertation. Ankara: Middle East Technical University.

- Şensoy, A., & Uysal, G. (2012). The value of snow depletion forecasting methods towards operational snowmelt runoff estimation using MODIS and Numerical Weather Prediction Data. *Water resources management*, 26(12), 3415-3440.
- Şensoy, A., Schwanenberg, D., Şorman, A., Akkol, B., Alvarado Montero, R., & Uysal, G. (2014). Assimilating H-SAF and MODIS Snow Cover Data into the Conceptual Models HBV and SRM. In *EGU General Assembly Conference Abstracts* (Vol. 16, p. 10240).
- Seo, D. J., Koren, V., & Cajina, N. (2003). Real-time variational assimilation of hydrologic and hydrometeorological data into operational hydrologic forecasting. *Journal of Hydrometeorology*, 4(3), 627-641.
- Seo, D. J., Cajina, L., Corby, R., & Howieson, T. (2009). Automatic state updating for operational streamflow forecasting via variational data assimilation. *Journal of Hydrology*, 367(3), 255-275.
- Shamir, E., Lee, B. J., Bae, D. H., & Georgakakos, K. P. (2010). Flood forecasting in regulated basins using the ensemble extended Kalman filter with the storage function method. *Journal of Hydrologic Engineering*, 15(12), 1030-1044.
- Shirangi, M. G. (2014). History matching production data and uncertainty assessment with an efficient TSVD parameterization algorithm. *Journal of Petroleum Science and Engineering*, 113, 54-71.
- Shirangi, M. G., & Durlofsky, L. J. (2015). Closed-Loop Field Development Optimization Under Uncertainty. In *SPE Reservoir Simulation Symposium*. Society of Petroleum Engineers.
- Singh, P., Bengtsson, L., & Berndtsson, R. (2003). Relating air temperatures to the depletion of snow covered area in a Himalayan basin. *Hydrology Research*, 34(4), 267-280.
- SMHI (1996), *Integrated hydrological modeling system manual, Version 4.0*, IHMS, Swedish Meteorological and Hydrological Institute, Norrköping, Sweden.
- Şorman, A. A., (2005). Use of satellite observed seasonal snow cover in hydrological modeling and snowmelt runoff prediction in upper Euphrates basin, Turkey. *Doctoral Dissertation*. Ankara: Middle East Technical University.

- Şorman, A. A., Şensoy, A., Tekeli, A. E., Şorman, A. Ü., & Akyürek, Z. (2009). Modelling and forecasting snowmelt runoff process using the HBV model in the eastern part of Turkey. *Hydrological processes*, 23(7), 1031-1040.
- Şorman, A. U., & Beser, O. (2013). Determination of snow water equivalent over the eastern part of Turkey using passive microwave data. *Hydrological Processes*, 27(14), 1945-1958.
- Struzik, P. (2014). Japan Aerospace Exploration Agency GCOM-W1 satellite snow depth product: outcome of the first winter. *Journal of Applied Remote Sensing*, 8(1), 084686-084686.
- Sürer, S., & Akyürek, Z. (2012). Evaluating the utility of the EUMETSAT HSAF snow recognition product over mountainous areas of eastern Turkey. *Hydrological Sciences Journal*, 57(8), 1684-1694.
- Tahir, A. A., Chevallier, P., Arnaud, Y., Neppel, L., & Ahmad, B. (2011). Modeling snowmelt-runoff under climate scenarios in the Hunza River basin, Karakoram Range, Northern Pakistan. *Journal of Hydrology*, 409(1), 104-117.
- Tang, B. H., Shrestha, B., Li, Z. L., Liu, G., Ouyang, H., Gurung, D. R., ... & San Aung, K. (2013). Determination of snow cover from MODIS data for the Tibetan Plateau region. *International Journal of Applied Earth Observation and Geoinformation*, 21, 356-365.
- Tekeli, A. E. (2000). Integration of remote sensing and geographic information systems on snow hydrology modeling. Master of Science Thesis. Ankara: Middle East Technical University.
- Tekeli, A. E. (2005). Operational Hydrological Forecasting of Snowmelt Runoff by Remote Sensing and Geographic Information Systems Integration. Doctoral Dissertation. Ankara: Middle East Technical University.
- Tekeli, A. E., Akyürek, Z., Şorman, A. A., Şensoy, A., & Şorman, A. Ü. (2005a). Using MODIS snow cover maps in modeling snowmelt runoff process in the eastern part of Turkey. *Remote Sensing of Environment*, 97(2), 216-230.
- Tekeli, A. E., Akyürek, Z., Şensoy, A., Şorman, A. A., & Şorman, A. Ü. (2005b). Modelling the temporal variation in snow-covered area derived from satellite

- images for simulating/forecasting of snowmelt runoff in Turkey. *Hydrological Sciences Journal*, 50(4).
- Tekeli, A. E., Şensoy, A., Şorman, A., Akyürek, Z., & Şorman, Ü. (2006). Accuracy assessment of MODIS daily snow albedo retrievals with in situ measurements in Karasu basin, Turkey. *Hydrological Processes*, 20(4), 705-721.
- Thirel, G., Martin, E., Mahfouf, J. F., Massart, S., Ricci, S., & Habets, F. (2010). A past discharges assimilation system for ensemble streamflow forecasts over France—Part 1: Description and validation of the assimilation system. *Hydrology and Earth System Sciences*, 14, 1623-1637.
- Todini, E. (2008). A model conditional processor to assess predictive uncertainty in flood forecasting. *International Journal of River Basin Management*, 6(2), 123-137.
- Tong, J., Déry, S. J., & Jackson, P. L. (2009). Topographic control of snow distribution in an alpine watershed of western Canada inferred from spatially-filtered MODIS snow products. *Hydrology and Earth System Sciences*, 13(3), 319-326.
- TÜBİTAK (108Y161) (Kasım 2008 –Mayıs 2011), Yukarı Fırat Havzasında, arazi ölçümleri, uydu teknolojileri, hava tahmin verileri ve hidrolojik modeller kullanılarak, kar potansiyelinin dönemsel ve akımların günlük tahmini, Anadolu Üniversitesi, Eskişehir.
- TÜBİTAK (113Y075) (Eylül 2013 –Eylül 2015), Dağlık Fırat ve Seyhan Havzalarında EPS ve Uydu Verileri ile Operasyonel Hidrolojik Tahmin Sisteminin Geliştirilmesi, Anadolu Üniversitesi, Eskişehir.
- Udnæs, H. C., Alfnes, E., & Andreassen, L. M. (2007). Improving runoff modelling using satellite-derived snow covered area. *Hydrology Research*, 38(1), 21-32.
- Uzunoğlu, E. (1999). Application of the SLURP model using remote sensing and geographic information systems. Master of Science Thesis. Ankara: Middle East Technical University.
- Valstar, J. R., McLaughlin, D. B., Te Stroet, C., & van Geer, F. C. (2004). A representer-based inverse method for groundwater flow and transport applications. *Water Resources Research*, 40(5).

- Verwey, A., Heynert, K., Werner, M., Reggiani, P., Kappel, B. V., & Brinkman, J. (2006). The Potential of the Delft-FEWS Flood Forecasting Platform for Application in the Mekong Basin. In 4 th Annual Mekong Flood Forum, Siem Reap, Cambodia.
- Viterbo, P., & Beljaars, A. C. (1995). An improved land surface parameterization scheme in the ECMWF model and its validation. *Journal of Climate*, 8(11), 2716-2748.
- Vrugt, J. A., Diks, C. G., Gupta, H. V., Bouten, W., & Verstraten, J. M. (2005). Improved treatment of uncertainty in hydrologic modeling: Combining the strengths of global optimization and data assimilation. *Water Resources Research*, 41(1).
- Vrugt, J. A., ter Braak, C. J., Diks, C. G., & Schoups, G. (2013). Hydrologic data assimilation using particle Markov chain Monte Carlo simulation: Theory, concepts and applications. *Advances in Water Resources*, 51, 457-478.
- Wächter, A., & Biegler, L. T. (2006). On the implementation of an interior-point filter line-search algorithm for large-scale nonlinear programming. *Mathematical programming*, 106(1), 25-57.
- Wang, M., Son, S., & Shi, W. (2009). Evaluation of MODIS SWIR and NIR-SWIR atmospheric correction algorithms using SeaWiFS data. *Remote Sensing of Environment*, 113(3), 635-644.
- Wang, X., & Xie, H. (2009). New methods for studying the spatiotemporal variation of snow cover based on combination products of MODIS Terra and Aqua. *Journal of Hydrology*, 371(1), 192-200.
- Weerts, A. H., & El Serafy, G. Y. (2006). Particle filtering and ensemble Kalman filtering for state updating with hydrological conceptual rainfall-runoff models. *Water Resources Research*, 42(9).
- Weerts, A. H., El Serafy, G. Y., Hummel, S., Dhondia, J., & Gerritsen, H. (2010). Application of generic data assimilation tools (DATools) for flood forecasting purposes. *Computers & Geosciences*, 36(4), 453-463.
- WMO, 1975. Intercomparison of conceptual models used in operational hydrological forecasting Operational Hydrology Report 23 (WMO No. 646).
- WMO, 1986. Intercomparison of models for snowmelt runoff. Operational Hydrology Report 23 (WMO No. 646).

- WMO, 1992. Scientific Assessment of Stratospheric Ozone. Report 25.
- WMO, 1999. Scientific assessment of ozone depletion. Global Ozone Research and Monitoring Project- Report - 44, Geneva, Switzerland
- Yamankurt, E., (2010). Harmanlanan uydu görüntülerinin karla kaplı alanlar üzerindeki etkisi ve Türkiye'nin Yukarı Fırat Havzası'nda dönemsel kar potansiyelinin modellenmesi, Master of Science Thesis, Eskişehir: Anadolu University.
- Yirdaw, S. Z., Snelgrove, K. R., & Agboma, C. O. (2008). GRACE satellite observations of terrestrial moisture changes for drought characterization in the Canadian Prairie. *Journal of Hydrology*, 356(1), 84-92.
- Zaitchik, B. F., Rodell, M., & Reichle, R. H. (2008). Assimilation of GRACE terrestrial water storage data into a land surface model: Results for the Mississippi River basin. *Journal of Hydrometeorology*, 9(3), 535-548.
- Zeilew, M. B., & Alfredsen, K. (2013). Sensitivity-guided evaluation of the HBV hydrological model parameterization. *Journal of Hydroinformatics*, 15(3), 967-990.
- Zhang, F., Zhang, M., & Hansen, J. A. (2009). Coupling ensemble Kalman filter with four-dimensional variational data assimilation. *Advances in Atmospheric Sciences*, 26(1), 1-8.
- <http://srtm.csi.cgiar.org/SELECTION/inputCoord.asp> (Accessed: 20/07/2016)
- <http://www.esri.com/software/arcgis> (Accessed: 20/07/2016)
- <http://www.eea.europa.eu/data-and-maps/data/corine-land-cover-2006-raster-3>
(Accessed: 20/07/2016)
- <http://hsaf.meteoam.it/> (Accessed: 20/07/2016)
- http://hsaf.meteoam.it/documents/PUM/SAF_HSAF_PUM-10_1_1.pdf
(Accessed: 20/07/2016)
- http://hsaf.meteoam.it/documents/PUM/SAF_HSAF_PUM-13_1_0.pdf
(Accessed: 20/07/2016)
- <https://publicwiki.deltares.nl/display/FEWSDOC/Home> (Accessed: 20/07/2016)

https://oss.deltares.nl/documents/102774/467082/rtc-tools_UserManual.pdf
(Accessed: 20/07/2016)

<https://oss.deltares.nl/web/delta-shell> (Accessed: 20/07/2016)

<https://oss.deltares.nl/web/delft-fews/model-adapters> (Accessed: 20/07/2016)

<http://www.techbriefs.com/component/content/article/458> (Accessed: 20/07/2016)

<http://badc.nerc.ac.uk/home/> (Accessed: 20/07/2016)

<http://hsaf.meteoam.it/snow.php?tab=4> (Accessed: 20/07/2016)

<http://amazon.nws.noaa.gov/ohd/evs/evs.html> (Accessed: 20/07/2016)

<ftp://hsaf.meteoam.it> (Accessed: 20/07/2016)

<http://www.mathworks.com/help/optim/ug/fmincon.html> (Accessed: 20/07/2016)

<http://schj.home.xs4all.nl/html/>(Accessed: 20/07/2016)